REPORT 997

SUMMARY OF INFORMATION RELATING TO GUST LOADS ON AIRPLANES

By PHILIP DONELY

SUMMARY

Available information on gust structure, airplane reactions, and pertinent operating statistics has been examined. This report attempts to coordinate this information with reference to the prediction of gust loads on airplanes. The material covered represents research up to October 1947.

INTRODUCTION

The fact that all airplanes fly in rough air at some time poses a number of problems relative to safe flight. One of the most important of these problems is that of designing the airplane structure to withstand the loads imposed by gusts. The three principal phases of the gust-load problem are: (1) the determination of the gust structure (that is, the size, shape, intensity, and frequency of occurrence), (2) the reaction of any airplane to gusts of known structure, and (3) the determination of the operating statistics.

No order of importance can be given to the three phases of the problem since the final loads are a function of the gust, the airplane, and how the airplane is flown. The characteristics of gusts, where they occur, and the variation in their characteristics are of fundamental importance because the gust is the source of the problem. Analytical and experimental work on what happens to an airplane when it strikes a known gust is of importance since a knowledge of airplane reactions permits the load calculation for any airplane. Finally, operating statistics are of importance in setting the level of loading for operating airplanes since they define the gusts encountered under actual operating conditions and the speeds at which the gusts are encountered.

Although research on gust loads has been carried on for many years and many of the results have been incorporated in design rules (reference 1), these results have either been issued piecemeal or not published at all. Under these conditions, a compilation of available information within a logical framework is needed and, for this purpose, the present report has been prepared. The scope includes all NACA material available up to about October 1947 arranged according to the three principal phases previously mentioned.

Because airplanes are used to obtain gust data and the various phases of research are interdependent, the first section of the report is a presentation and discussion of the basic equations of the reactions of an airplane as used in gust-load calculations. This first section is followed by sections covering gust characteristics, airplane reactions, and operating statistics and by a short concluding section on the coordination of information and the calculation of applied loads. The material contained in this report is based mainly on past work of the NACA, much of which has been accomplished through the cooperation of the agencies and airlines listed in the appendix.

SYMBOLS

A	aspect ratio (b^2/S)
B	arbitrary constant
b	wing span, feet
C	arbitrary constant
$\bar{c}$	mean wing chord, feet
c	mean aerodynamic chord, feet
C_L	lift coefficient
C_{L_g}	variation of lift coefficient when penetrating a sharp-edge gust, expressed as a fraction of final lift (Küssner's function, reference 2)
C_{L_α}	variation of lift coefficient following a sudden change in angle of attack, expressed as a function of final lift (Wagner's function, reference 2)
$C_{m_{c.g.}}$	pitching-moment coefficient about center of gravity
D	differential operator $\left(\frac{d}{dt}\right)$
$dC_{m_{c.g.}}/dC_L$	static margin
f	frequency of occurrence
f_w	wing frequency, cycles per second
g	acceleration due to gravity, feet per second per second
H	gust-gradient distance (distance in which the vertical velocity of a gust rises linearly from zero to its maximum value), feet or chords
K	gust alleviation factor
L	lift, pounds
l	distance from trailing edge of wing to leading edge of tail, chords
M	Mach number
n	normal acceleration, g units

Δn acceleration increment due to a gust, g units ($n-1$ for most cases)

Δn_s acceleration increment, g units

$$\left(\text{computed according to formula } \frac{\rho SUV\frac{dC_L}{d\alpha}}{2W}\right)$$

Δn_r acceleration increment on rigid airplane, g units

P probability

q dynamic pressure, pounds per square foot $\left(\frac{1}{2}\rho V^2\right)$

S wing area, square feet

s distance airplane has penetrated gust at time t, chords

t time from start of gust penetration, seconds ($\bar{c}s/V$)

U gust velocity at peak of gust, feet per second

U_e effective gust velocity, feet per second

$$\left(\text{computed from recorded acceleration increment as } \frac{2\Delta n\, W/S}{\rho_0 V_e K\frac{dC_L}{d\alpha}}\right)$$

u vertical gust velocity at any point, feet per second

V true airspeed, feet per second

V_e equivalent airspeed, feet per second

V_p probable speed, miles per hour

V_L design level-flight speed, miles per hour

V_{max} maximum indicated airspeed, miles per hour

V_{ne} placard do-not-exceed speed, miles per hour

V_0 airspeed at maximum acceleration increment, miles per hour

W weight of airplane, pounds

z vertical displacement of airplane, feet

dp/dt angular acceleration in roll, radians per second per second

dq/dt angular acceleration in pitch, radians per second per second

$d\epsilon/d\alpha$ downwash factor

α angle of attack, degrees

β angle of gust to direction of flight of airplane, degrees

Δ incremental value

δ_f absolute displacement of equivalent fuselage, feet

δ_w absolute displacement of equivalent wing, feet

δ_{st} deflection of equivalent wing under conditions corresponding to normal static design procedure, feet

$\delta_{d_{max}}$ maximum value of $\delta_w-\delta_f$, feet

θ pitch angle, degrees

λ gust spacing (distance between gust peaks), chords

μ_g mass parameter (μ_g is twice the relative density (reference 24) divided by the lift-curve slope)

$$\left(\frac{2W}{\rho g S\bar{c}\frac{dC_L}{d\alpha}}\right)$$

ρ density of air, slugs per cubic foot

ρ_0 density of air at sea level, slugs per cubic foot

Subscripts:

av average

p probable; denotes the most probable value of a quantity as determined from experimental data

0 denotes value computed from local measurements

cg center of gravity

w wing

1 for extended equations denotes point at which solution applies

max maximum

Subscripts used with Δn:

0 acceleration increment due to a gust

m acceleration increment due to vertical motion of airplane

θ acceleration increment due to pitch of airplane

q acceleration increment due to angular velocity of airplane

ϵ acceleration increment due to downwash

w acceleration increment on wing

s acceleration increment on stabilizing surface

T total acceleration increment

Examples:

Δn_{0_w} acceleration increment on wing due to gust

Δn_{T_s} total acceleration increment due to tail

BACKGROUND AND BASIC EQUATIONS OF GUST-LOADS RESEARCH

In the earliest stages of research on gust loads, an immediate practical answer to the question of appropriate design loads was needed. The problem was approached by recourse to the obvious and necessary expedient of measuring the accelerations under actual operating conditions so that some data could be made available to designers pending a more complete understanding of gust-load phenomena.

Accelerometers were used in this work although it was evident that accelerations measured on one type of airplane would not be applicable to other types, or even to the same type operated at a different speed. The main effects of airplane characteristics and airspeed were taken into consideration in overcoming this difficulty by utilizing a formula based on the most elementary concepts of the nature and action of

gusts. This formula, called the "sharp-edge-gust formula," was applied in such a way that the accelerometer data were reduced to "effective" gust velocities, the term effective being employed to indicate the fictitious nature of these gust velocities.

Since that time, several advances have been made so that at present three concepts of evaluating airplane reactions are being utilized: (1) the very simple sharp-edge-gust formula, (2) extended equations taking into account the gust shape and additional airplane characteristics, and, finally, (3) the sharp-edge-gust formula modified by an alleviation factor. These relations and concepts are presented subsequently and form the basis of NACA research on gust loads.

SHARP-EDGE-GUST FORMULA

The simple sharp-edge-gust formula was derived on the basis of numerous simplifying assumptions which include the following:

1. The gust is sharp-edged in the direction of flight and represents an instantaneous change in wind direction or speed.
2. The gust velocity is uniform across the span of the airplane at any instant of time or position of the airplane in space.
3. The gust direction is normal to the lateral axis of the airplane.
4. The airplane is in steady level flight prior to entry into the gust, and the airplane flight path, attitude, and ground speed are not affected by the action of the gust on the airplane. (This assumption might be visualized by imagining the airplane to be driven along a fixed track through the gust so that the airplane has no resulting motions due to the action of the gust.)
5. The primary effect of encountering a gust is to change the lift on the airplane.
6. The lift increment of the horizontal tail due to the action of the gust is negligible as compared with the wing lift increment.
7. The lift coefficient of a wing is a unique function of angle of attack and is independent of time.

For the assumptions noted, the expression for lift or load factor for a gust of any angle is

$$\frac{L}{W}=n=1\pm\Delta n=\left[1+\left(\frac{U}{V}\right)^2+\frac{2U}{V}\cos\beta\right]\left(1+\frac{dC_L}{d\alpha}\frac{S}{W}\frac{\rho}{2}V^2\tan^{-1}\frac{\frac{U}{V}\sin\beta}{1+\frac{U}{V}\cos\beta}\right)$$

The term in brackets represents the effect of the increased resultant speed and the term in parentheses, the lift in steady level flight plus the lift increment due to the change in angle of attack. If the particular gust angles of 90°, 0°, and 180° are considered, then, for $\beta=90°$, the expression reduces to

$$\frac{L}{W}=1+\Delta n=1+\frac{dC_L}{d\alpha}\frac{S}{W}\frac{\rho}{2}UV$$

and, for $\beta=0°$ and 180°,

$$\frac{L}{W}=1\pm\Delta n=1\pm\frac{2U}{V}$$

The so-called sharp-edge-gust formula is the equation for $\beta=90°$ for sea-level density and is generally written

$$\Delta n=\frac{\rho_0 U_e V_e\frac{dC_L}{d\alpha}}{2\frac{W}{S}}$$

The effect of gust direction on the acceleration increment is shown in figure 1 for airplanes with wing loadings from 15 to 60 pounds per square foot flying at 200 miles per hour through a gust having a velocity of 15 feet per second. The ratio of the acceleration increment for given values of wing loading to the maximum value for each wing loading is plotted against the gust angle β. Figure 1 indicates, as do references 2 and 3, that the acceleration is a maximum for angles close to 90°; figure 1 also indicates that the vertical or near-vertical gust is 4 to 15 times as effective in producing acceleration as the horizontal gust. Therefore, in reducing acceleration data, the assumption is usually made that the significant accelerations caused by gusts result from vertical gusts; that is, $\beta=90°$.

The sharp-edge-gust formula, sometimes used with a correction factor, requires fairly rigid definition of the quantities to be substituted. The equation is used for general research studies, where masses of acceleration data are to be reduced and compared for evaluation of past airplane gust-load experience, and for the prediction of load experience. For research studies, the actual weight of the airplane is used to determine the wing loading since the data from different sources are to be compared. For load-evaluation studies of operating conditions, the gross weight is used because it yields conservative values of the effective gust velocity. In all cases the acceleration increment is defined as the acceleration minus one. The other quantities have been standardized as the result of instrumental limitations so that sea-level density is used with indicated airspeed (assumed to be equal to V_e) and gross wing area. The slope of the lift curve is generally obtained from the formula

$$\left(\frac{dC_L}{d\alpha}\right)_{airplane}=\left(\frac{dC_L}{d\alpha}\right)_{wing}=\frac{6A}{A+2}$$

For preliminary evaluation of acceleration data, sometimes a lift-curve slope must be assumed since the wing configuration

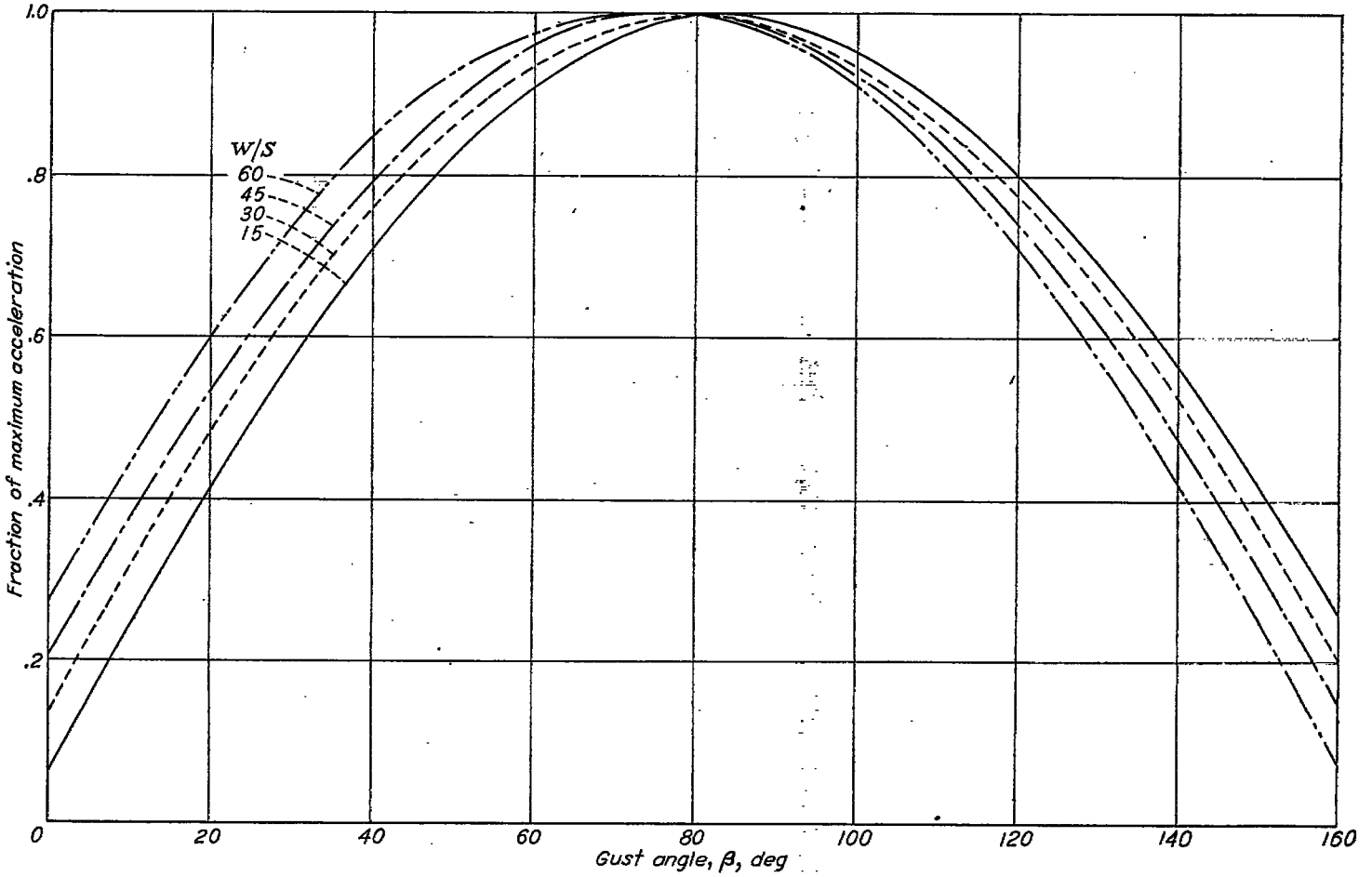

FIGURE 1.—Variation of normal acceleration with angle of gust for four values of wing loading. V=200 miles per hour; U=15 feet per second.

is not known. In these cases a value of 4.5 per radian has usually been selected.

In the case where loads are to be calculated by utilizing effective gust velocities in the sharp-edge-gust formula, the quantities used must be consistent with those described. If different procedures are followed, the answers obtained obviously are incorrect in proportion to the deviation. The simple formula with its simplifying assumptions limits the operations that can be performed on derived data.

EXTENDED GUST EQUATIONS

The restrictive assumptions of the sharp-edge-gust formula caused little concern until it was to be used for design calculations of gliders and airplanes whose wing loading and other characteristics differed widely from those of the airplanes that were initially used to establish the effective design gust velocities. The assumptions of infinite gust gradient, steady lift, and no vertical motion had to be eliminated in the derivation of the equations for airplane response to a gust. The basis for the final solutions was the work of Küssner reported in reference 2, which resulted in the analytical study presented in reference 4.

For the application of Küssner's work to the problem of gust loads, the assumptions already cited in the derivation of the sharp-edge-gust formula have been continued with the following exceptions: (1) the gust velocity has been assumed to be uniform across the span of the airplane at any instant and to increase linearly with distance in the direction of flight until the maximum gust velocity U is attained; (2) the airplane can rise but does not pitch under the action of the gust and is in steady level flight; (3) the unsteady-lift functions of Küssner and Wagner (reference 2), which were derived for the two-dimensional wing, are assumed to be made applicable to the finite wing by substituting the slope of the lift curve for the finite wing in place of the slope of the lift curve for the infinite-aspect-ratio or two-dimensional wing; and (4) except for the shorter gust-gradient distances, the acceleration peak was assumed to coincide in space with the position of the point of first attainment of maximum gust velocity.

The symbols used in the equation for the gradient gust are shown in figure 2, and the unsteady-lift functions used are shown in figure 3 (taken from reference 5). It is indicated that, while a sudden angle-of-attack change, such

as is obtained by rotating or pitching a wing, yields one variation of lift C_{L_α}, the gradual immersion of the wing into a gust yields a different curve C_{L_g}.

The equation of vertical motion can be written as

$$\frac{W}{g}\left(\frac{d^2z}{dt^2}\right)_1=\int_0^{t_1}\frac{\rho S V^2}{2}\frac{dC_L}{d\alpha}C_{L_g}(t_1-t)\frac{du}{V dt}dt-\int_0^{t_1}\frac{\rho S V^2}{2}\frac{dC_L}{d\alpha}C_{L_\alpha}(t_1-t)\frac{d^2z}{dt^2}\frac{dt}{V}$$

where the first integral is the force due to the gust and the second integral results from the vertical motion of the airplane. Since the unsteady-lift functions C_{L_α} and C_{L_g} depend on chord lengths from the start of a disturbance, the equation is generally transformed so that the distance traveled $s=\frac{V}{c}t$ rather than t is the independent variable. The equation becomes

$$\left(\frac{\Delta n}{\Delta n_s}\right)_1=\frac{\bar{c}}{H}\int_0^{s_1}C_{L_g}(s_1-s)ds-\frac{1}{\mu_g}\int_0^{s_1}C_{L_\alpha}(s_1-s)\frac{\Delta n(s)}{\Delta n_s}ds$$

from which the acceleration ratio $\left(\frac{\Delta n}{\Delta n_s}\right)_1$ is seen to be a function of the rate of development of transient lift, the mass parameter, and the shape of the acceleration curve.

The preceding equation has been solved by Fredholm's method (reference 6) and the solutions obtained are of the form

$$\left(\frac{\Delta n}{\Delta n_s}\right)_{max}=C-\frac{2B}{2\mu_g+H}$$

where C and B are constants representing solution of the integrals in the equation and whose values depend only on the distance penetrated into the gust. Figure 4 gives the solution for a range of gradient distance and mass parameter. Since the unsteady-lift functions C_{L_g} and C_{L_α} given in figure 3 were approximated for distances above about 8 chords, the curves for the larger gradient distances in figure 4 are also approximate. The dash line in the figure represents a rough limit of applicability of the gradient-gust solution obtained by this method. Above the dash line, the solutions for finite gradients are not valid, and the curve for $H=0$ is to be used. The dash line was determined on the assumption that no gradient gust has a peak acceleration occurring earlier than a gust with zero gradient distance.

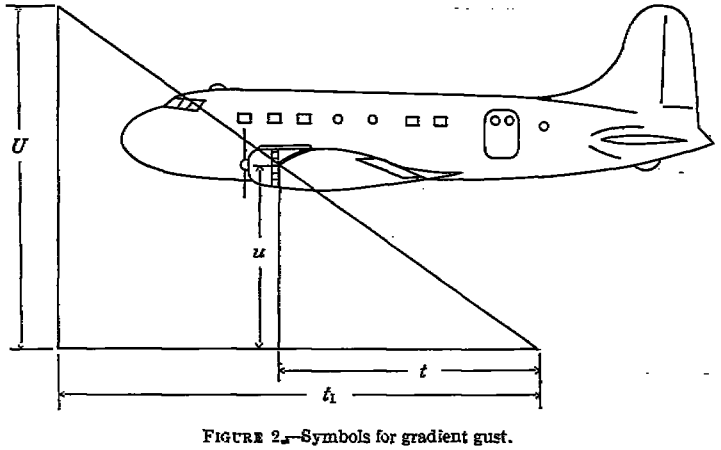

FIGURE 2.—Symbols for gradient gust.

Figure 4, together with the sharp-edge-gust formula, can be used to evaluate flight records to obtain the "true" gust intensity. The gradient distance $H=Vt_1$ and airplane mass parameter μ_g permit the determination of the acceleration ratio from figure 4. The substitution of pertinent values in the sharp-edge-gust formula yields an effective gust velocity which, when divided by the acceleration ratio, gives the true gust velocity. In this case, true airspeed and the actual air density are to be used in the sharp-edge-gust equation.

In the evaluation of time-history data of airspeed, altitude, and acceleration to obtain gust-gradient distance and true gust intensity, the following methods have been used: The acceleration increment is taken as the acceleration increment

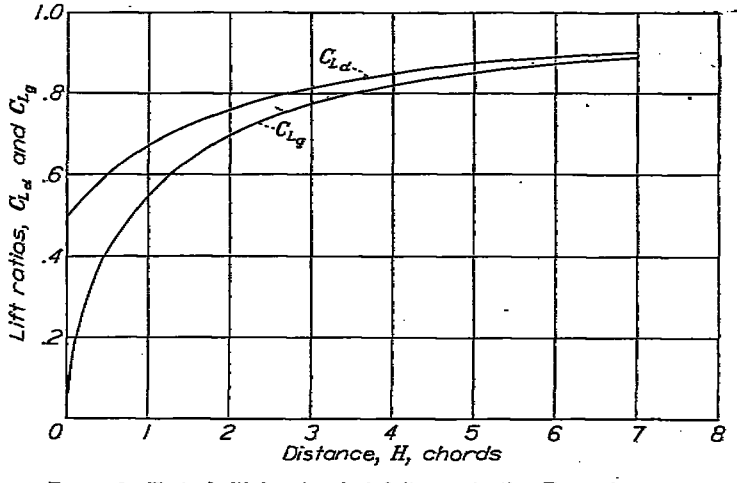

FIGURE 3.—Unsteady-lift functions for infinite aspect ratio. From reference 5.

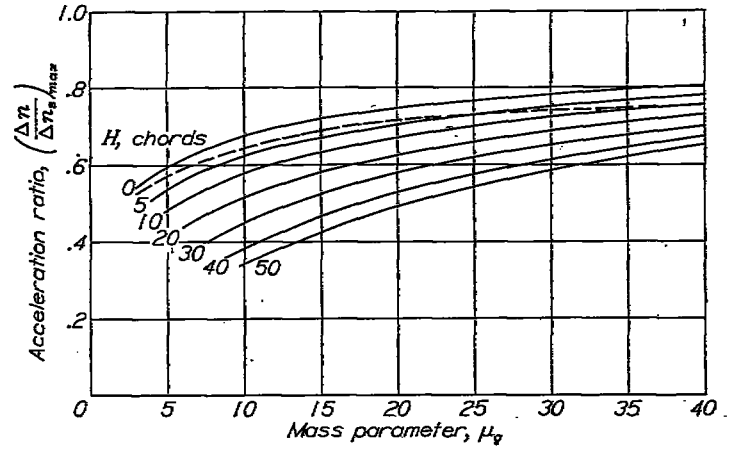

FIGURE 4.—Acceleration ratio as function of the mass parameter. Above dash line, finite gradient solution is not valid.

at the peak minus the steady value prior to the start of the gust. In the determination of the gradient distance, the time from zero to peak acceleration and the true airspeed are used. In expressing the gradient distance in chords, the mean geometric chord is generally used.

GUST ALLEVIATION FACTOR

Much of the data obtained from commercial operations with the NACA V–G recorder and some gust data from special investigations are not amendable to analysis by the extended equations of the previous section because of limited information or insufficiently defined acceleration peaks, and so means to account for the main effects of alleviations had to be established. Since, for much of the work, the level of gust intensity has been set by the airline data and special investigations, the results of the extended equations have been used mainly to adjust measurements of effective gust velocity for the effects of unsteady lift and vertical motion. The gust alleviation or correction factors so obtained were consequently based on a knowledge of the average gust characteristics and the response of the conventional airplanes on which considerable data had been accumulated.

The gust alleviation factor is defined as the relative response of two airplanes encountering the same gust with the gradient distance defined in chords. If a representative gust size is determined and a particular airplane selected as being representative of the airplanes used for gust measurements, then the effective gust velocities are related by the acceleration ratios. Thus, if all gust measurements were made on airplane 1 and the size of the average gust were known, then effective gust velocities from the accelerations experienced by airplane 2 are related to those for airplane 1 by the expression

$$\frac{U_{e_1}}{\left(\frac{\Delta n}{\Delta n_s}\right)_1}=\frac{U_{e_2}}{\left(\frac{\Delta n}{\Delta n_s}\right)_2}=U\sqrt{\frac{\rho}{\rho_0}}$$

The effective gust velocity representing the conditions is U_{e_1} or, if measured with airplane 2, is

$$\frac{\left(\frac{\Delta n}{\Delta n_s}\right)_1}{\left(\frac{\Delta n}{\Delta n_s}\right)_2}U_{e_2}$$

The ratio of acceleration ratios is the gust alleviation factor and may be determined by calculation or by experiment.

For load calculations, a specific alleviation factor K was derived and is shown in figure 5, as reproduced from reference 1. The factor K is calculated with the Boeing B–247 airplane as a reference and the assumptions were made that wing loading is proportional to mass parameter and that the effect of pitch on the gust load increment is the same for all airplanes. The curve is calculated as the acceleration ratio for any airplane to the acceleration ratio for the Boeing B–247 airplane $\left(\frac{W}{S}=16, C=11\right)$ when both airplanes traverse a gust with a gradient distance of 10 chords. The resulting curve is based on the assumption that all airplanes are similar to the Boeing B–247 airplane but have different wing loadings.

THE STRUCTURE OF ATMOSPHERIC GUSTS

The determination of the characteristics of atmospheric gusts pertinent to the airplane, their variations, and their frequency of occurrence in the atmosphere is of fundamental importance. Considerable research has been undertaken, therefore, to cover various aspects of the gust-structure problem. The research performed includes flight tests in the neighborhood of Langley Air Force Base over a period of about 10 years and special investigations made in conjunction with commercial airlines, the military services, and the Civil Aeronautics Administration.

METHODS OF GUST-STRUCTURE MEASUREMENTS

The general method followed in the investigation of gust structure has been to fly airplanes in rough air and to deduce the gust characteristics from the reactions of the airplane. Whenever possible, the airplane which was the primary instrument, as indicated in reference 7, has been calibrated by testing dynamically similar scaled models in the Langley gust tunnel in order to obtain the actual relation between acceleration and gust intensity for various gust shapes. Most of the data on over-all gust structure have been obtained from records of acceleration and airspeed as a function of time. These records have provided information on the gust velocities, the gradient distance, and the gust spacing. In the evaluation of the records, the pitching motion of the airplane is neglected except in those cases where it can be included through calibrations made in the gust tunnel.

In addition to measurements of over-all gust structure, some measurements have been made of the distribution of gust

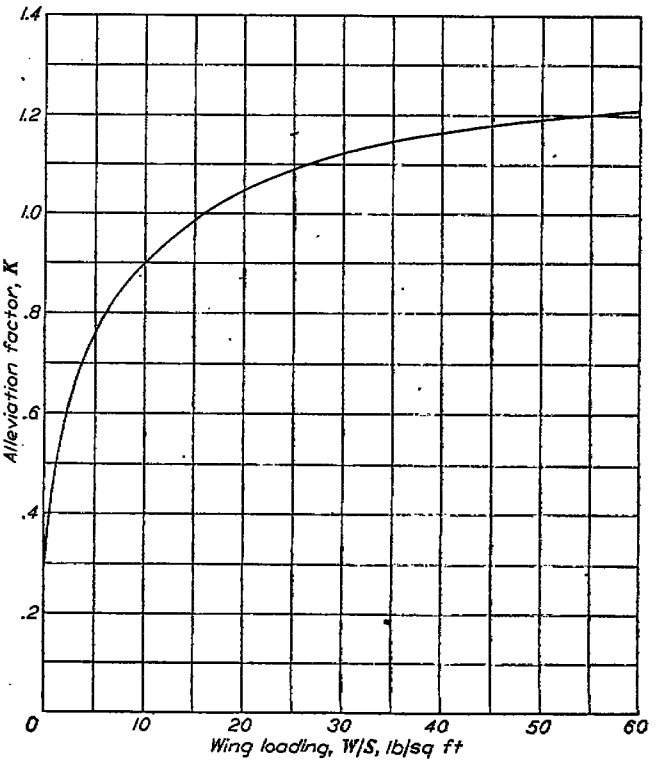

FIGURE 5.—Variation of alleviation factor with wing loading (from reference 1).

velocity along the airplane span by recording the airspeed and the local wing pressures at various stations along the span. From thin-airfoil theory, the change in pressure at any location on an airfoil divided by the dynamic pressure q is a function of the angle-of-attack change and that, in turn, is equal to the effective gust velocity divided by the equivalent airspeed of the airplane. Local values of true gust velocity cannot be measured because the motions of the airplane are somewhat involved and cannot be taken into account.

The intensity of horizontal gusts has been obtained from airspeed records on the assumption that the absolute velocity of the airplane remains constant in spite of rapid changes in wind speed which the airplane may experience. The apparent changes in airspeed are taken as the horizontal gust velocities when not associated with large normal accelerations.

APPARATUS AND TESTS

Five airplanes having the characteristics shown in table I and in figure 6 have been used to obtain gust-structure data. As may be noted from figure 6, all airplanes except the XBM–1 were monoplanes, and the F–61C airplane had twin tail booms instead of the usual fuselage. Table I shows that the weight of the airplanes varied from about 700 pounds to 55,000 pounds and the wing mean chord varied from about 4 feet for the Aeronca C–2 airplane to about 19 feet for the XB–15 airplane. The "sea-level" mass parameters of the various airplanes varied from about 6 to 23. In the case of the Aeronca C–2 and the XBM–1 airplanes, the response to

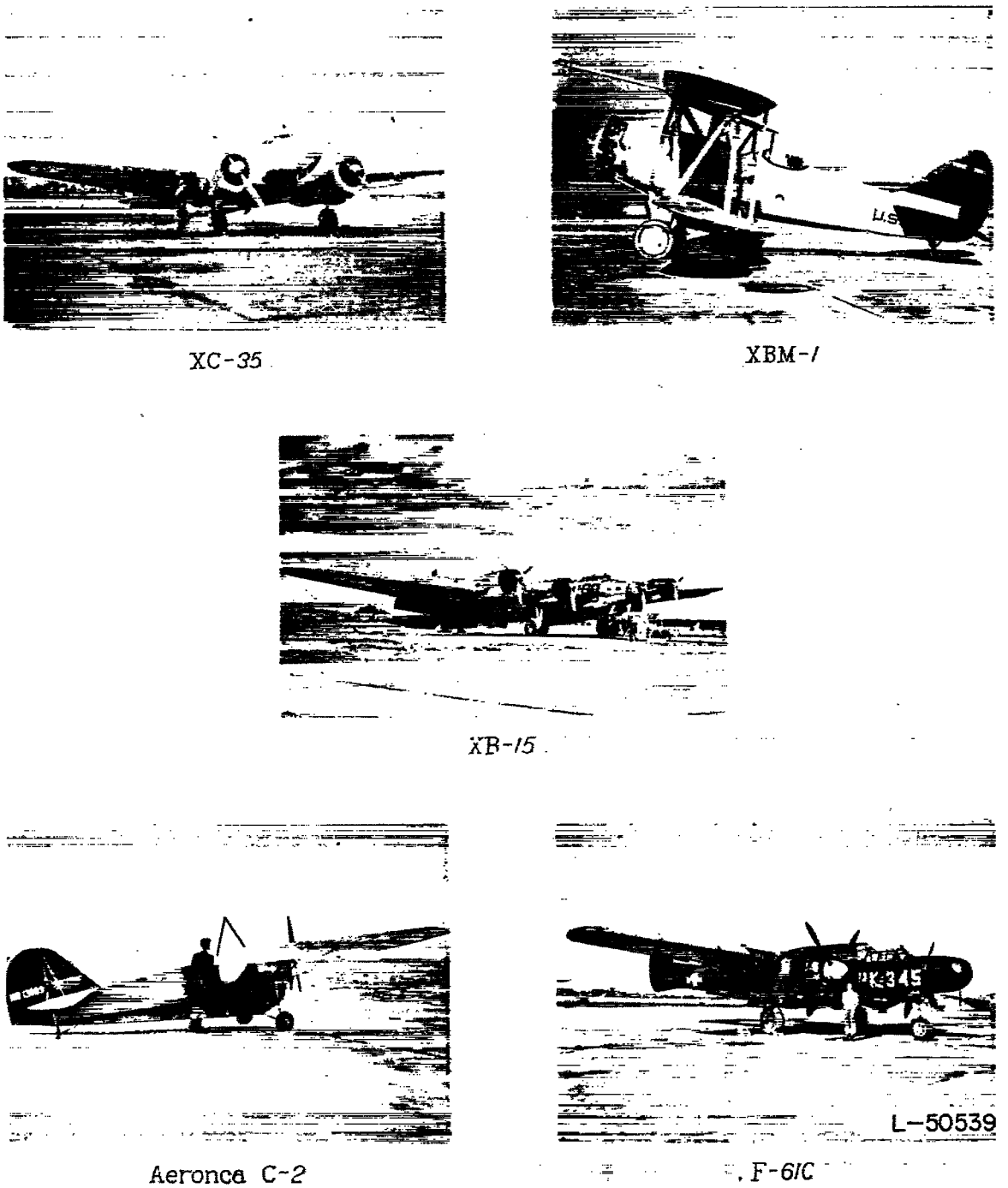

FIGURE 6.—Airplanes used in gust research.

known gusts had been obtained by tests in the Langley gust tunnel (references 7 and 8, respectively).

For the determination of the gust intensity, gradient distance, and gust spacing, all airplanes carried a standard set of instruments consisting of:

(1) Recording accelerometer located at the center of gravity
(2) Airspeed-altitude recorder
(3) Synchronizing timer

The instrument ranges were adjusted to suit the particular airplane. All instruments were equipped to give sufficient record time and were operated at film speeds to give adequate time resolution. A switch convenient to either the pilot or the observer enabled the instruments to be turned on or off at will.

All airplanes carried, in addition to the instruments mentioned, special instruments suited to the particular project. The XB–15 airplane, for example, was equipped with strain gages on wing beams, and optigraphs were provided to measure both wing and tail deflections. The XC–35 airplane carried four pressure recording units that were connected to orifices located on the wing of the airplane (fig. 7) to measure the differential pressure between the upper and lower surfaces. Radiosonde data, as well as temperature measurements, were also obtained during the tests of the XC–35, XBM–1, Aeronca C–2, and F–61C airplanes. Table II gives the scope of the flight tests. With the exception of the flight investigations with the XB–15 airplane, all tests had objectives associated with research on gust structure, and the flight tests were under the control of the test engineer as to the performance and the type of flying done. The stability of the various airplanes was adjusted whenever possible so that the airplanes showed stick-fixed stability.

RESULTS

The time histories of acceleration and airspeed obtained during these flight investigations were evaluated to obtain the effective gust velocity, the gradient distance, and the corresponding true velocity. As noted previously, every acceleration peak can be evaluated to obtain the effective gust velocity corresponding to the acceleration increment as measured from the 1 g datum, but only those acceleration peaks that are preceded by a smooth part of record can be evaluated to obtain the gust-gradient distance and the true gust velocity.

Gust intensity.—The available data on gust intensity, as measured by the effective gust velocities, have been examined in some detail in reference 9, and the frequency distributions given in figure 8 were derived therein. The results given in figure 8 are based on early German work, NACA flight tests, and V–G records from commercial transport operations. Curves A and B are the approximate limits of the frequency distributions of effective gust velocities for over-all operating conditions and show the probability that a gust will exceed any selected value of intensity.

In addition, a more detailed investigation of limited scope has been made (reference 10) of the XC–35 data to compare the frequency distributions of effective gust velocity in thunderstorms and line squalls for various altitude ranges. Table III summarizes the data obtained to a threshold of 4 feet per second for several ranges of altitude from the surface to 35,000 feet. Table III also lists the record time and the average spacing between gusts for each altitude range. Figure 9 shows the probability distributions of effective gust velocity for the several altitude ranges that are obtained by curves fitted to the data of table III. In this investigation, the data for altitudes below 5,000 feet were not used because the conditions investigated represented random record taking in both clear air and clouds at the end of the flights.

From the tests performed with the XC–35 and the F–61C airplanes, the variation of expected maximum effective gust velocity with altitude within convective clouds has been determined. These results are summarized in figure 10, in which the data for the XC–35 airplane correspond to 100 miles of rough-air flying, whereas those for the F–61C airplane correspond to 1,000 miles. The latter data were obtained during the 1946 operations of the U. S. Weather Bureau thunderstorm project at Orlando, Fla., and are based on the maximum values of effective gust velocity for each 3,000-foot interval; however, the XC–35 data utilized a complete count of all gusts.

Gust spacing.—Some information on gust spacing—that is, the distance from peak to peak—has also been obtained. In reference 11, an analysis was made of the XC–35 data to determine the average spacing between the large gusts (defined as U_e greater than 5 to 8 fps) in areas of continuous rough air. Continuous rough air was defined as a sequence of large gusts in which the spacing between gusts was less than 2.2 seconds. Table IV, reproduced from reference 11, summarizes some of the pertinent characteristics of the large isolated and repeated gusts. The table presents a comparison of the average and the range of intensities and the average and range of spacings for isolated single gusts and sets of two and three repeated gusts occurring with equal frequency.

More general information on gust spacing, contained in reference 9, indicates that the average spacing between gusts that were counted to an estimated threshold of 0.3 foot per second was a function of the airplane mean geometric chord. This count indicated an average spacing between successive peaks of 11 chords so that the number of gusts per mile of rough air is roughly equal to $500/\bar{c}$. The definition of the number of gusts per mile of rough air led to the concept of "path ratio" which provides a measure of the percent of rough air encountered under operating conditions.

Gust-gradient distance.—Figure 11 presents a typical plot of measurements of gradient distance and gust velocity. Inspection of the figure indicates that the scattered pattern of data is not amenable to detailed analysis and, for such purposes, the data on gust-gradient distance were sorted according to the variable under consideration. Figures 12(a), 12(b), and 12(c) present the data on the average gust-gradient distance as a function of the gust velocity (width of bracket, 4 fps). Figure 12(a) is a summary of

the data for all airplanes with H_{a_s} expressed as multiples of the mean wing chord; figure 12(b) presents the same data with H_{a_s} expressed in multiples of the airplane wing span; and figure 12(c), in feet. For comparison with other figures and for subsequent use, a faired curve was drawn through the data in figure 12(a) to agree best with the data from the XC–35 airplane.

The results presented in figures 12(a), 12(b), and 12(c) do not include the complete data for every airplane since some brackets, particularly below about 8 feet per second, are not complete. The magnitude of the acceleration increments for values of U less than 8 feet per second was about the same order as the resolution of the accelerometer. For the larger gust velocities some "average" values were not plotted since the number of points represented was less than three.

In some cases, sufficient data were available to obtain the probable values of the gust-gradient distance. The probable value was determined by fitting a theoretical frequency distribution to the data and determining the point with the highest frequency. The results are plotted against the corresponding average gust-gradient distance H_{a_s} in figure 13. Figure 13 includes two solid lines: a 45° line representing the equality of the quantities and a line through the data offset by 2 chords.

Data for the gust-gradient distance for the XC–35 and F–61C airplanes have been utilized to determine the variations of the average gradient distance expressed in chords as a function of altitude. (See fig. 14.) In the case of the XC–35 airplane where no fixed altitudes were flown, altitude brackets were selected and the average gradient distance was plotted against the center value for the pertinent bracket. The F–61C airplane tests were made at fixed altitudes, and the data have been plotted at the appropriate altitude level.

Spanwise gust distribution.—Records of local wing pressures and airspeeds obtained during the flight investigation with the XC–35 airplane (reference 12) were evaluated to obtain the local values of effective gust velocity at each of four spanwise stations. The general method followed was to plot the data for each gust as a function of the spanwise location and connect the points by straight lines. The individual spanwise distributions were later identified with the corresponding values of the gust velocity U and the effective gust velocity U_e obtained from the other flight records.

Data on the spanwise distribution were sorted according to the shape of the distribution as indicated in figure 15. Six shapes ranging from the uniform or rectangular distribution to the double triangular distribution are shown, and for each shape is noted the total number of gusts classified in that category. Figure 15 also indicates possible variations included under each heading.

The spanwise gust distributions represented in figure 15 were, in turn, evaluated graphically to obtain values of the lateral gust-gradient distance H. The results are shown in figure 16 where the average values of the gradient distance in chords are given for a range of values of gust velocity. The associated gust velocity U was obtained from the synchronized acceleration data, and the faired curve shown in figure 16 corresponds to that given in figure 12 (a).

The significance of the values of U_e obtained from pressure measurements as compared with those determined from acceleration measurements has been examined in reference 12. Figure 17, reproduced from that reference, shows the average value of the local effective gust velocity as a function of the effective gust velocity for a given gust as determined from acceleration records. The average value of U_e from the pressure measurements is the average value weighted according to the amount of wing area represented by the particular orifice or measuring station. Also shown in the figure is the line for equality of the two measures of U_e and the error band.

Since, in some cases, it is convenient to divide the lateral gust distribution into symmetrical and unsymmetrical components, the gust shapes listed in figure 15 were classified according to whether they were symmetrical or unsymmetrical and then represented as having a linear variation of gust velocity across the span of the airplane. The results are shown in figure 18. The inset in figure 18 indicates the type of variation assumed and the two quantities obtained from the evaluation. The average gust velocity $U_{e_{a_s}}$ and the increment in gust velocity at each wing tip ΔU_e were taken as the symmetrical and unsymmetrical components, respectively. Many small values have been omitted from the figure.

As in the case of the gust-gradient distance, the data have been further analyzed to find an average unsymmetrical gust increment. Figure 19 has been prepared from the summary of data for the different gust shapes to show the average gust velocity for a gust of the unsymmetrical shape as a function of the average gust velocity of a triangular gust for equal frequencies of occurrence.

In addition to the determination of spanwise gust distribution from local pressure distributions, synchronized records from accelerometers located at the center of gravity of the airplane and in the wing were evaluated to obtain the angular acceleration in roll, which is related to the spanwise gust distribution. The results of the evaluation of accelerometer records for 17 flights are shown in table V, which indicates the frequency of occurrence of given values of angular acceleration with the associated values of normal acceleration increment.

Longitudinal gusts.—Rapid airspeed fluctuations have been used to evaluate the magnitude of longitudinal gusts. Figure 20, prepared from an analysis of the XC–35 airplane data, compares the maximum values of the horizontal gust velocities obtained from the rapid airspeed fluctuations with the maximum vertical gust velocities. Each point represents a separate traverse or run. The results of a detailed analysis of airspeed and acceleration records in gusty air from the XBM–1 and Aeronca C–2 airplane investigations are shown in figure 21 and indicate, for both airplanes, the relation of the horizontal gust velocities to the vertical gust velocities for equal frequencies of occurrence.

ACCURACY OF RESULTS

Consideration of instrumental and reading errors in evaluating the data from the several airplanes, together with a knowledge of the problems involved in the reactions of an airplane, indicates that the possible errors in the derived quantities that are of interest are approximately as follows:

Gust velocity based on acceleration, percent	±10
Gust velocity from pressure measurements, feet per second	±4
Gust velocity from airspeed measurements, feet per second	±10
Gust-gradient distance, chords	±1 to ±2
Lateral gust-gradient distance, percent	±20
Spacing, chords	±1½

The accuracy of the gust-velocity measurements, whether true gust velocity or effective gust velocity, from acceleration records depends on the quality of the records obtained, the availability of a gust-tunnel calibration of the airplane, and experience in reading and interpreting the records.

The local gust velocities obtained from wing-pressure measurements were tested for accuracy by comparing the average value of the local gust velocities with the effective gust velocity from acceleration data. The results indicate that the two quantities are equivalent but that the data scatter over a range of about 4 feet per second.

The gradient distances determined from accelerometer records are a function of both the time resolution and the response characteristics of an airplane due to known gusts. Examination of gust-tunnel test results indicates that, under average conditions, the airplane response places two limits on the gust-gradient distance determined from acceleration records. The first limit, for the shorter gradient distances, is specified by the lag in lift. The gradient distances lying above the dash line in figure 4 are not generally recognizable on an accelerometer record. Thus, this limit is from 2 chords to about 4 chords for the average airplane. The second limit, for the longer gradient distances, arises from the fact that, as the airplane penetrates farther and farther into a long gradient gust, the effect of the pitching and vertical motion of the airplane, under the action of the gust, tends to counteract the contribution of lift due to each increment of gust as it is encountered.

The lateral gust-gradient distance is a more questionable quantity than the gust-gradient distance determined from accelerometer records since no single concept as to shape has been obtained. The lack of detailed data and the erratic character of the gust distributions in a spanwise direction (fig. 15) require a great amount of judgment in arriving at any numerical values. Comparison of the actual values of the gust-gradient distance from accelerometer records and the corresponding values of the lateral distance from pressure records indicates that the data are reasonable and in agreement with the actual conditions. From the preceding remarks it is obvious that the error is significant and the value of 20 percent previously mentioned is only a crude estimate.

DISCUSSION

Gust intensity.—Because only a small number of all the acceleration peaks in rough air can be evaluated for true gust velocities, the effective gust velocity has been used as the measure of intensity and frequency of atmospheric gusts. Although the effective gust velocity U_e is a fictitious quantity, it bears a fixed relation to the gust velocity for a given airplane and given conditions of air density, gust shape, and gust size. The effective gust velocity is generally about 50 percent to 70 percent of the gust velocity.

The largest effective gust velocity recorded to date was about 55 feet per second and corresponds to a gust velocity of 100 feet per second for typical conditions. Fortunately, gust velocities this large are not frequently encountered. The distributions of effective gust velocity in figure 8 show that the limiting distributions for a wide range of airplane sizes and weather conditions are reasonably close. Reference 9 concluded, on the basis of these results, that the distribution of gust intensities was essentially independent of airplane size and source of turbulence. Figure 9, in contrast, shows that the XC–35 data for different altitude brackets result in distributions with slopes that vary and, when checked against figure 8, differ from those curves. This discrepancy indicates that the distributions of effective gust velocity may not be independent of the source of turbulence. At this time independency is a reasonable assumption for general use.

Figures 9 and 10 show that, for altitudes above 9,000 feet, the maximum gust intensity in rough air associated with convective clouds is essentially a constant. Below 9,000 feet, the XC–35 data indicate a decrease in intensity due in part, according to reference 10, to the fact that the records were taken in clear air and clouds. Consideration of figure 10 indicates that little difference exists in the expected maximum gust velocities for all altitude ranges.

Gust-gradient distance.—Figure 11 and similar plots for other airplanes show that gust-gradient-distance data are of a random character. Comparisons of such plots indicate that airplane size might be a significant parameter, as in the case of boats where waves of small wave length that are of no concern to a large boat cause the small boat great difficulty. In a similar manner, gusts that cause a rough ride on a small airplane, such as the Aeronca C–2, would be expected to be of such small size as to have little effect on a large airplane, such as the XB–15.

Comparison of figures 12 (a), 12 (b), and 12 (c) indicates that the gradient-distance data show much less scatter on the basis of the mean wing chord than on the basis of span or feet. The scatter of points when the gust-gradient distance is defined in chords is about 1½ to 1 for a given value of U; whereas for the gust-gradient distance plotted in terms of airplane span, the scatter is greater. The data of figure 12(c) show that, when the gust-gradient distance is expressed in feet, the average values of the distance vary from 40 feet to 200 feet for a given gust intensity. Inasmuch as the agreement for the different sets of data is best when the gradient distance is expressed in chords, the gust-gradient distance appears to be roughly independent of the airplane when expressed in wing mean chords.

The adequacy of the average value of the gust-gradient distance for the representation of gradient-distance data deserves some consideration. The relation between the average value and the most probable value shown in figure 13 indicates that the probable gradient distance is about 1 chord to 2 chords less than the average gradient distance.

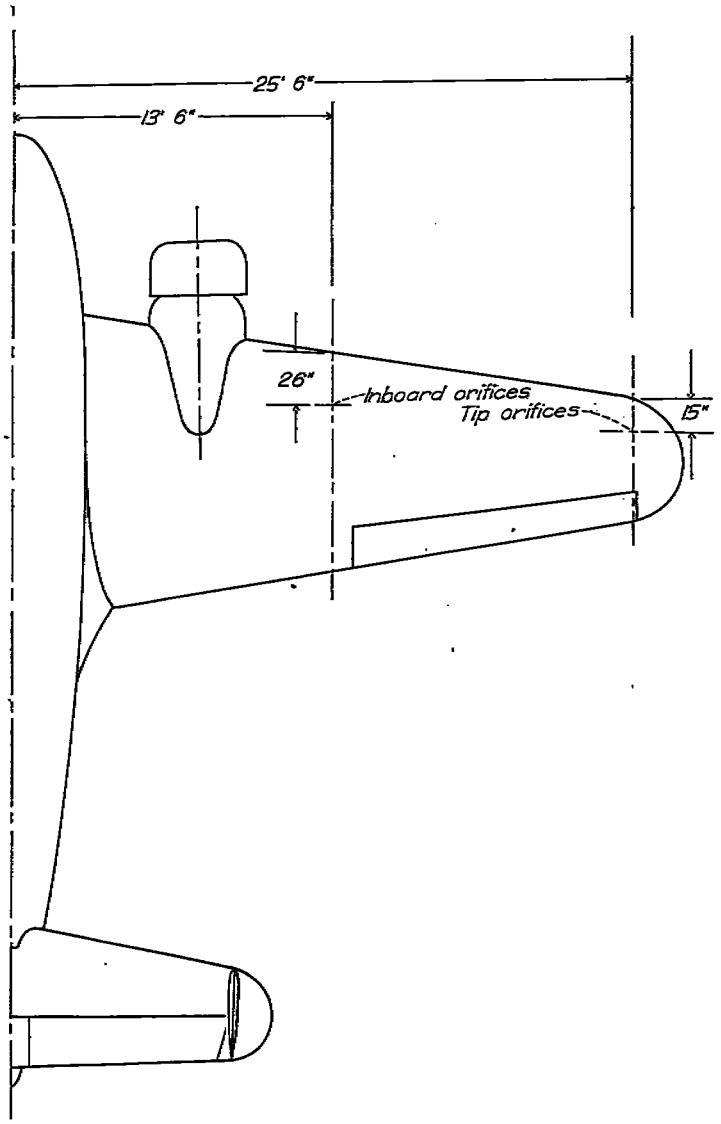

FIGURE 7.—Location of orifices along span of XC-35 airplane.

Since the offset appears to be constant, the use of the average gust-gradient distance, which is generally easier to determine, is believed to be satisfactory for analysis.

As indicated in table II, a variety of weather conditions, from line squalls to gustiness in the ground boundary layer is included in the present data. If the data of figure 12 (a) are assumed to be comparable, regardless of airplane, the type of weather appears to have no effect on the gust-gradient distance.

Figure 14 indicates that the average gust-gradient distance is independent of altitude in convective clouds. The data scatter somewhat but the over-all agreement appears to be good.

General considerations would indicate that the gradient distance might increase with gust velocity. Previous study and figure 12 (a) have indicated such a relation, although the evidence is not conclusive. When the faired curves of figures 12 (a) and 16 are considered, such a variation appears to be a reasonable estimate. The evidence available (fig. 12 (a)) is believed to indicate that for large gusts the average gradient distance is essentially constant but decreases rapidly at the smaller gust velocities.

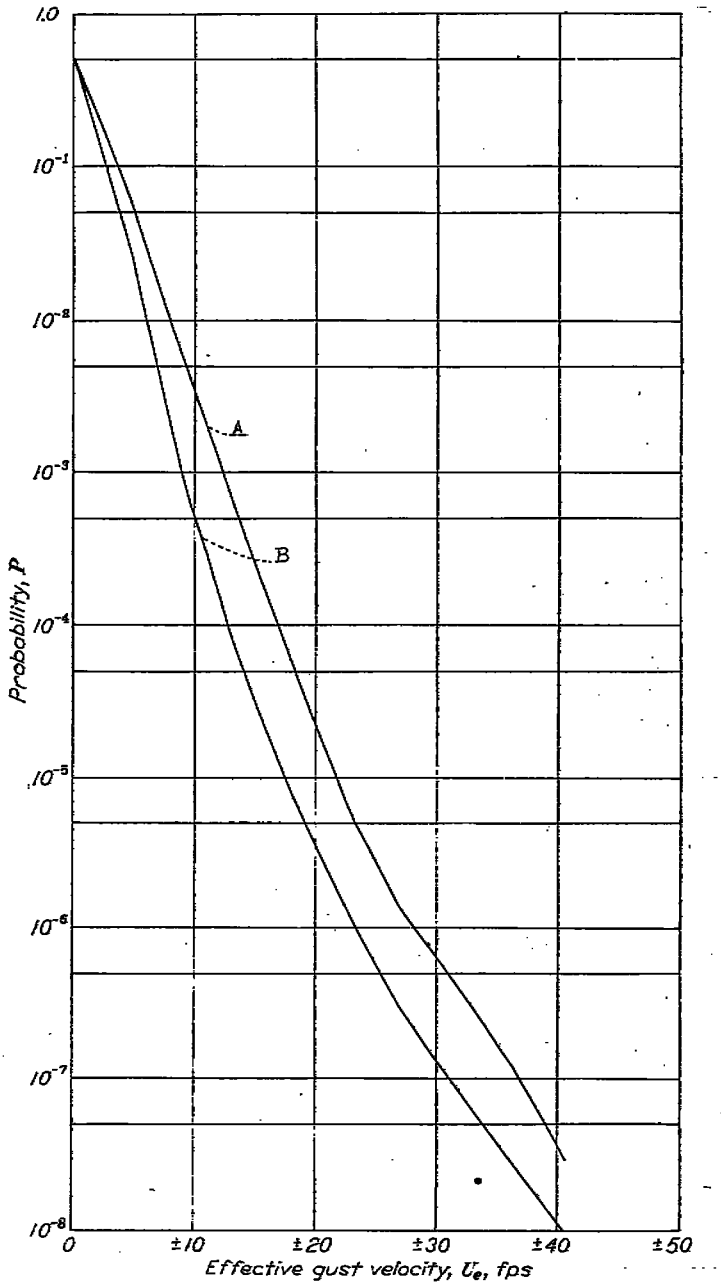

FIGURE 8.—Probability distribution defining limits of gust distributions (from reference 9)

Spanwise gust distribution.—The shapes of the lateral gust distributions, as indicated by figure 15, take many irregular forms. From considerationof the frequency of occurrence, the triangular, double-triangle, and unsymmetrical gust shapes predominate. Inasmuch as the double triangle can lead to wing bending moments along the span equal to those due to a uniform gust distribution, whereas the triangular gust shape would lead to reduced wing bending moments, the selection for design of a uniform gust velocity across the span for the symmetrical load condition is conservative. The relative percentages of the symmetrical (triangle, and so forth) and unsymmetrical gust shapes indicate that the unsymmetrical gust varying uniformly across the span appears quite frequently.

Comparison of the data for the average lateral gust-gradient distance as a function of gust velocity U (fig. 16) with corresponding results for longitudinal gust-gradient

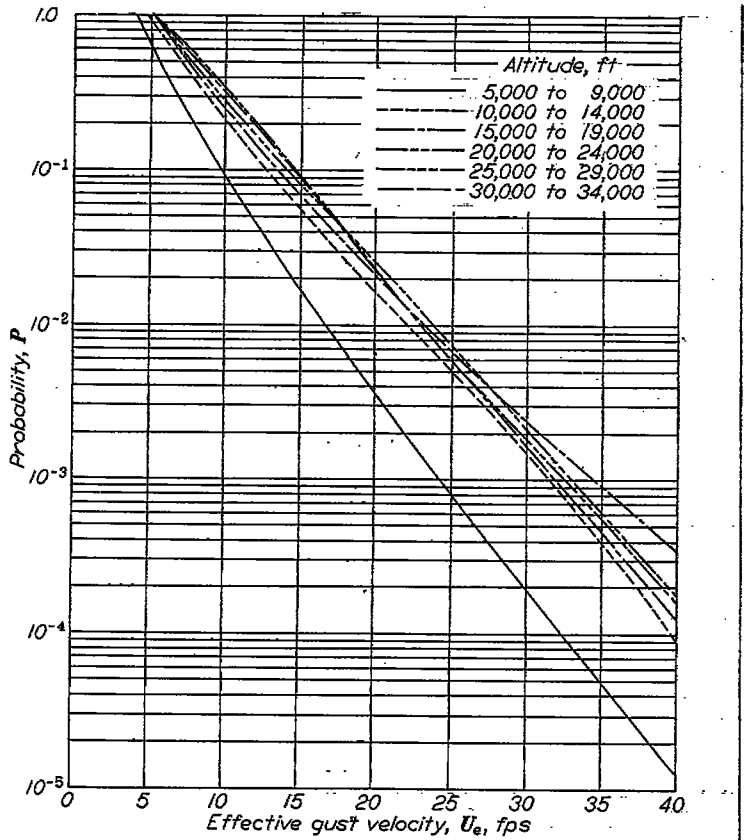

FIGURE 9.—Probability that an effective gust velocity at various altitudes will exceed a given value. Data for XC-35 airplane (from reference 10).

distances (fig. 12 (a)) indicates that the gradient distances are essentially the same in both directions. This agreement is indicated by the fact that the same empirical curve fits both sets of data and the results show the same trend of increasing gust-gradient distance with increasing gust velocity. Because data from only one airplane have been presented and the precision of measurement of lateral values is poor, as previously cited, the excellent agreement between figures 16 and 12 (a) is to some degree fictitious, the degree being unknown. Within the limitations of results the lateral and longitudinal gust dimensions are concluded to be essentially the same.

Inspection of figure 18, relating the unsymmetrical components of the effective gust velocity to the average uniform gust velocity across the span, indicates that no clear relations between the unsymmetrical components and the average gust velocity exists but that two boundaries appear to exist. A fairly definite boundary rising from the lower left-hand corner of the figure and corresponding to equality of the unsymmetrical component of gust velocity and the average gust velocity is indicated. As higher values of the average gust velocity are considered, the results scatter considerably, but an upper boundary is found at from 9 to 10 feet per second. The boundary holds for gust velocities up to 40 to 48 feet per second. On the basis of this upper limit, the unsymmetrical component of gust velocity above 10 feet per

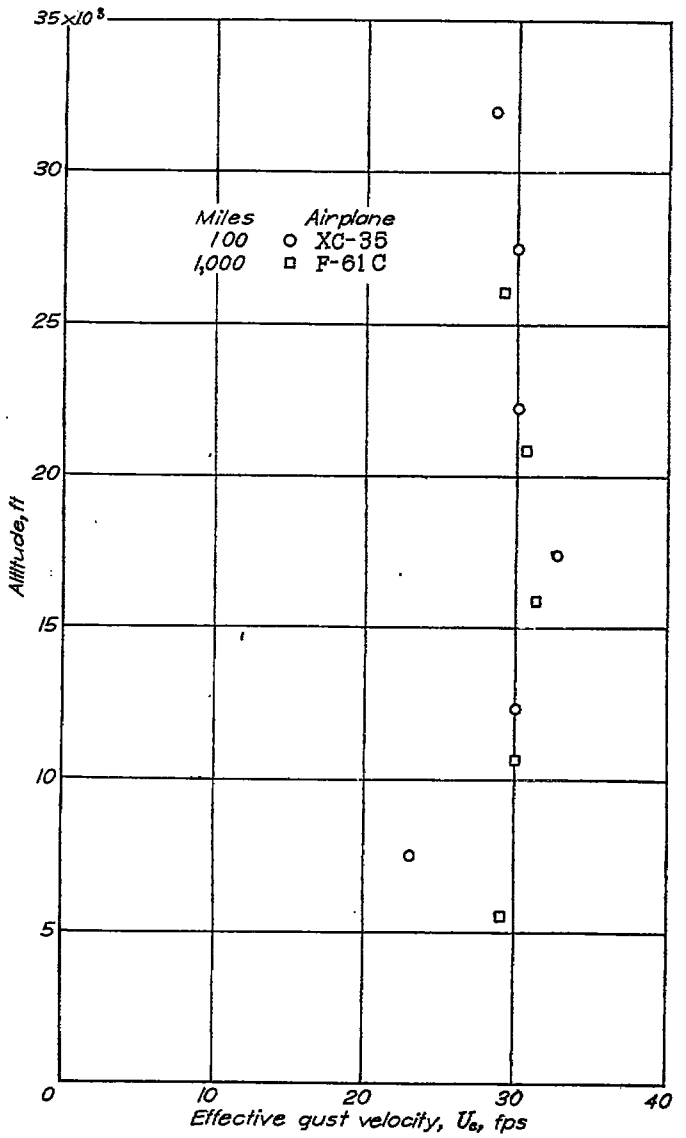

FIGURE 10.—Expected effective gust velocity at various altitudes within convective clouds for 100 and 1,000 miles of flight from data for XC-35 and F-61C airplanes, respectively.

second can be considered rare. Therefore, the unsymmetrical gust can be considered to be composed of two components: an unsymmetrical component amounting to a maximum of about 10 feet per second with opposite signs imposed at each wing tip and a linear gradient across the span, and an average uniform gust velocity of any pertinent value.

A question of some importance is the determination of the magnitude of the unsymmetrical components for other aircraft of entirely different spans. For example, if the span of the airplane were doubled, would the unsymmetrical component amount to twice the value obtained from the data shown herein? In order to obtain information on this question, the maximum value of the unsymmetrical gust components computed in reference 13 from angular-acceleration data was compared with the values obtained herein. It was found that for the XB-15 airplane, which has a span of about

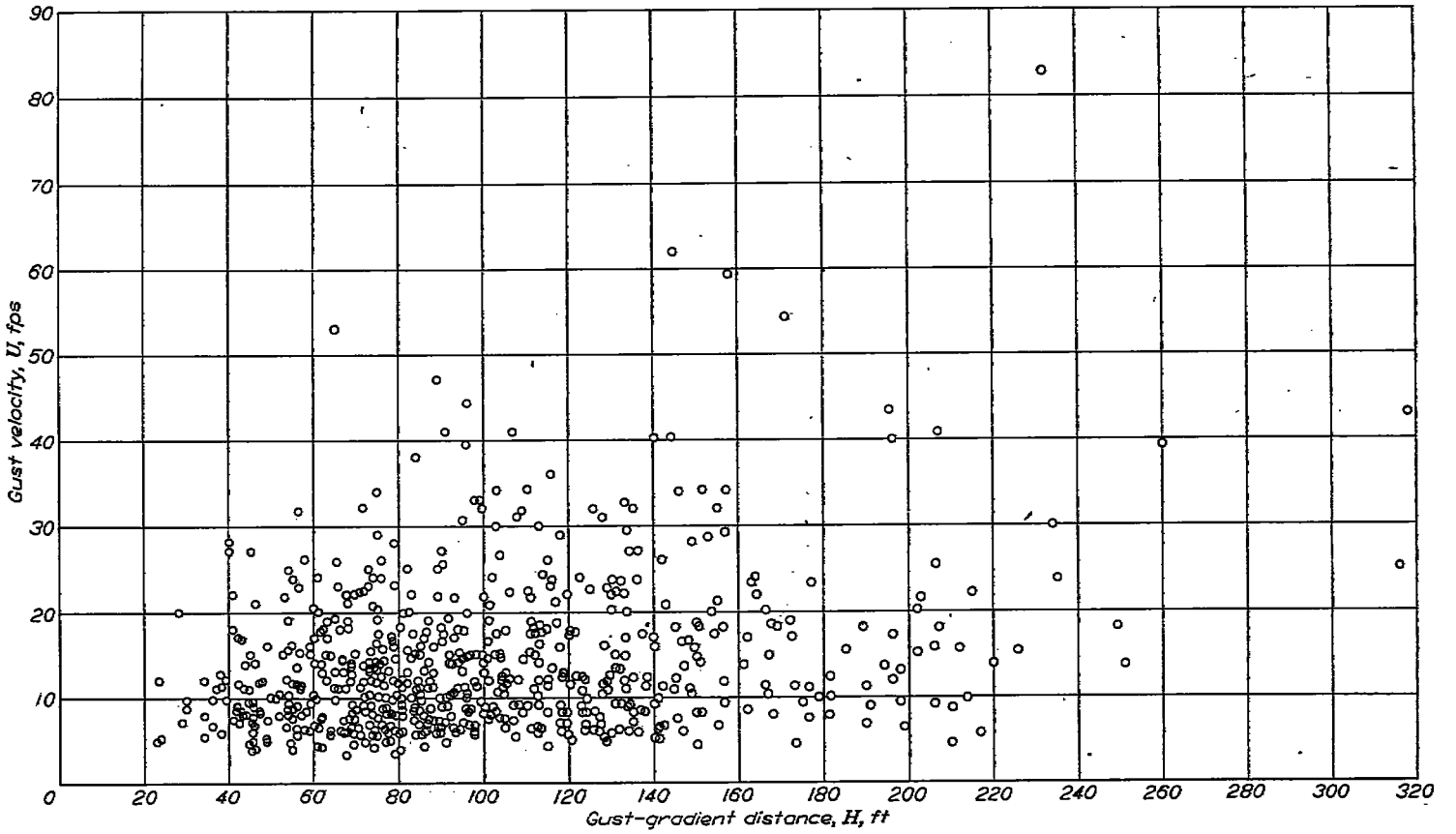

FIGURE 11.—Gust velocity U as a function of gust-gradient distance H.

150 feet, the unsymmetrical components of gust velocity at the wing tip would be about 13.7 feet per second. This value is slightly greater than indicated by figure 18 but is not, by any means, proportional to the span of the airplane. Similar data of a statistical nature obtained for the XC–35 airplane (table V) indicate that the maximum value of the angular acceleration on that airplane varied from about 1.95 to about 2.25 radians per second per second. Computations utilizing the formula given in reference 13 yield a maximum gust-velocity component of about 12½ feet per second. This value is in fair agreement with the one obtained for the XB–15 airplane and indicates that the tip values are independent of span. Since the values based on angular acceleration are somewhat more conservative than those based on wing pressures, more reliance should be placed on these values.

When the information on unsymmetrical gusts is utilized, the average effective gust velocity that should be used in conjunction with the maximum unsymmetrical component of 14 feet per second must be determined. The data of figure 19 indicate that, for an effective gust velocity in the neighborhood of 30 feet per second, the average gust velocity for the unsymmetrical gust would be about 22 feet per second.

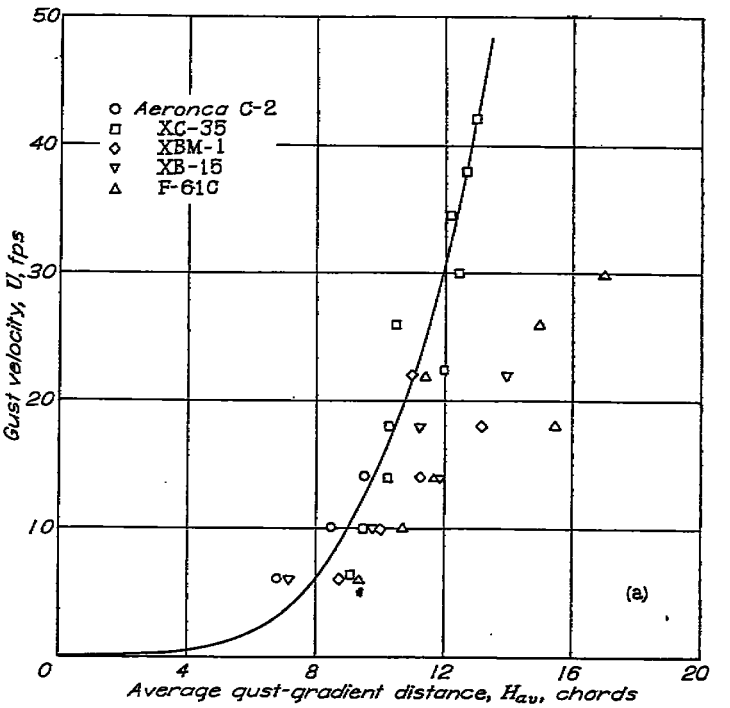

(a) Gust-gradient distance in chords.

FIGURE 12.—Variation of average gust-gradient distance with gust velocity.

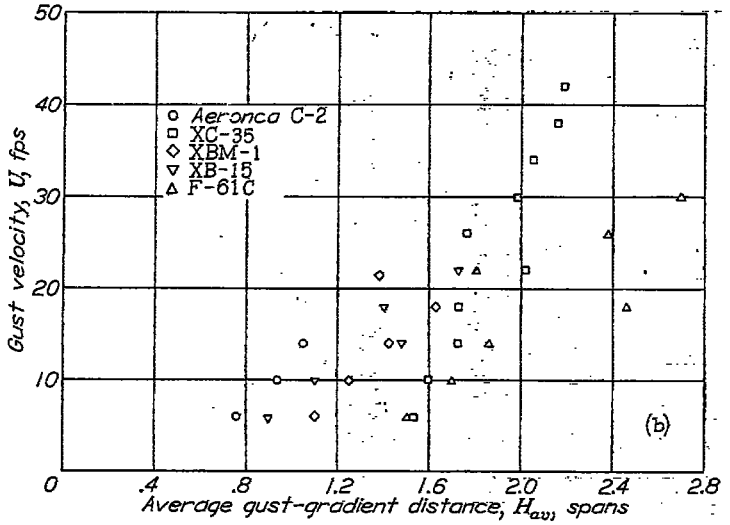

(b) Gust-gradient distance in spans.

FIGURE 12.—Continued.

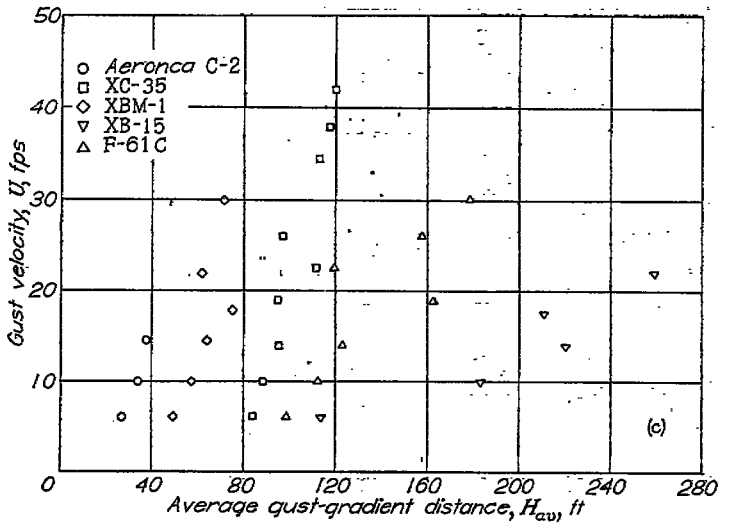

(c) Gust-gradient distance in feet.

FIGURE 12.—Concluded.

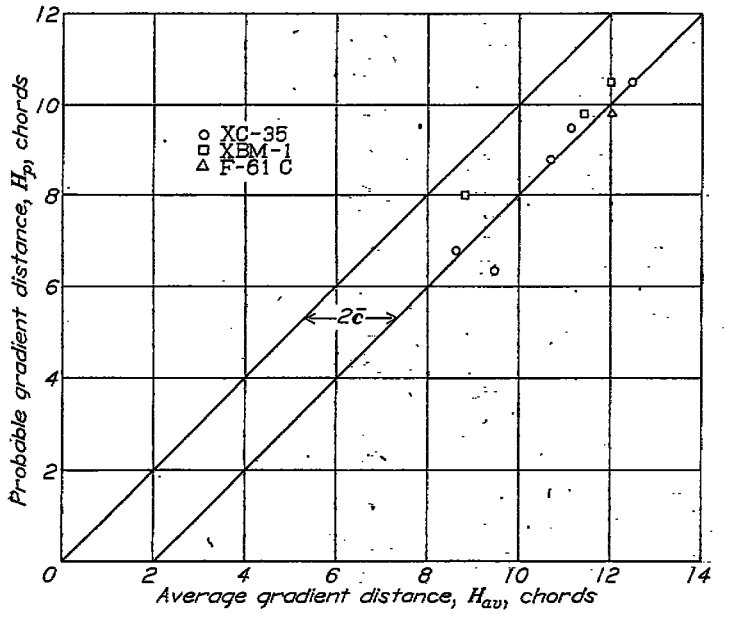

FIGURE 13—Relation between the probable and average gust-gradient distance.

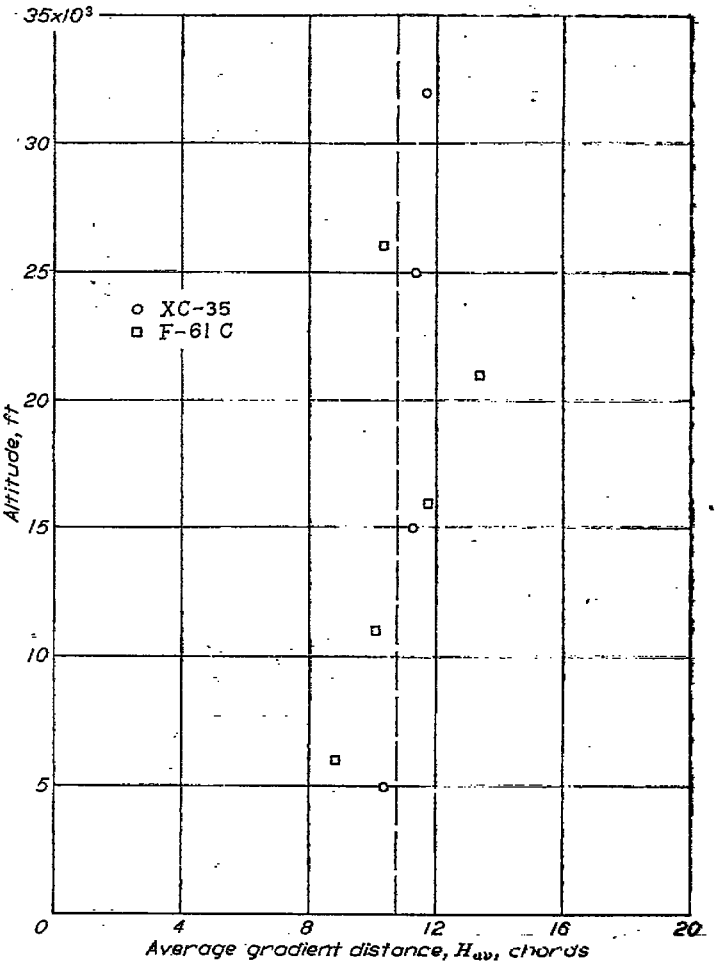

FIGURE 14.—Variation of average gradient distance with altitude.

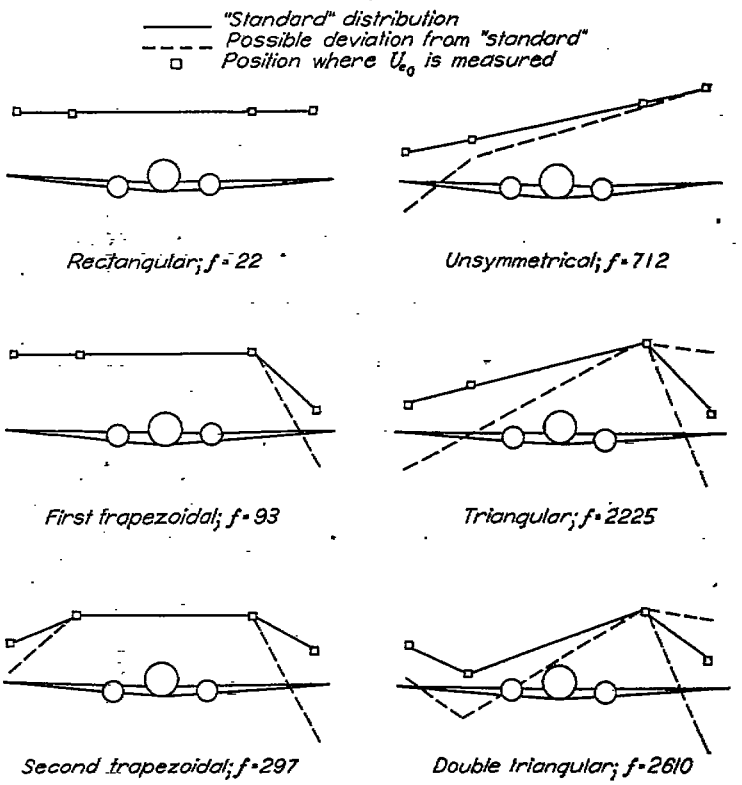

FIGURE 15.—Spanwise gust distributions and frequency of occurrence f for each type.

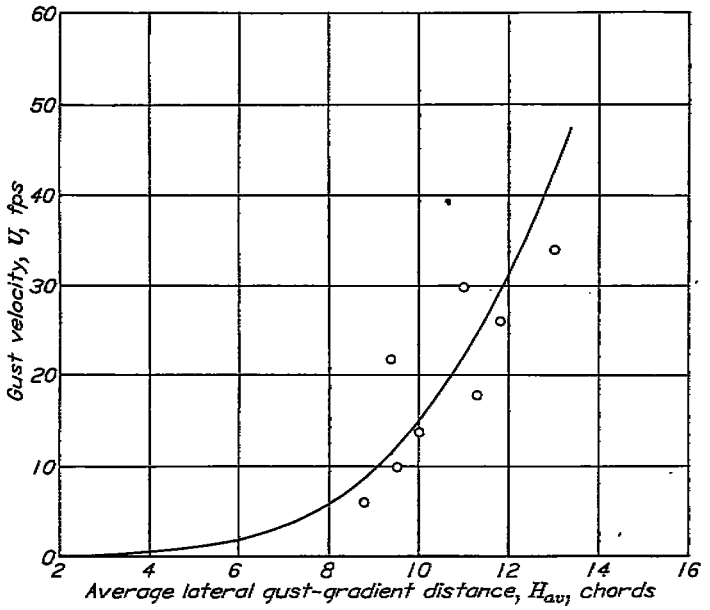

FIGURE 16.—Variation of average lateral gust-gradient distance H_{av} with gust velocity U. Faired curve corresponds to that in figure 12 (a).

Gust spacing.—Inspection of table IV indicates that the spacing of repeated gusts for two or three gusts in sequence is about 22 chords with a spread in actual values of some 20 chords for all sequences. The spacing is approximately twice the average gust-gradient distance of 10 to 14 chords. These data indicate that the gust shape in the direction of flight is either triangular or sinusoidal in character as contrasted to the "flat top" gust assumed in past years.

From time to time, comparisons are made of the gust spacing in reference 11 of 22 chords with the gust spacing that was derived from statistical gust data in reference 9 of 11 chords. The discrepancy between the two figures arises from the fact that the data on gust spacing presented in reference 11 were obtained for the larger gusts and represent data on gust intensities ranging from 5 feet per second up to the maximum value recorded; whereas the gust spacing listed in reference 9 is based on the average spacing of all gusts from a gust velocity of 0.3 foot per second to the maximum value experienced by any of the airplanes considered.

The sequences of gusts found in reference 11 were such that in about two-thirds of the cases of sets of two the gusts

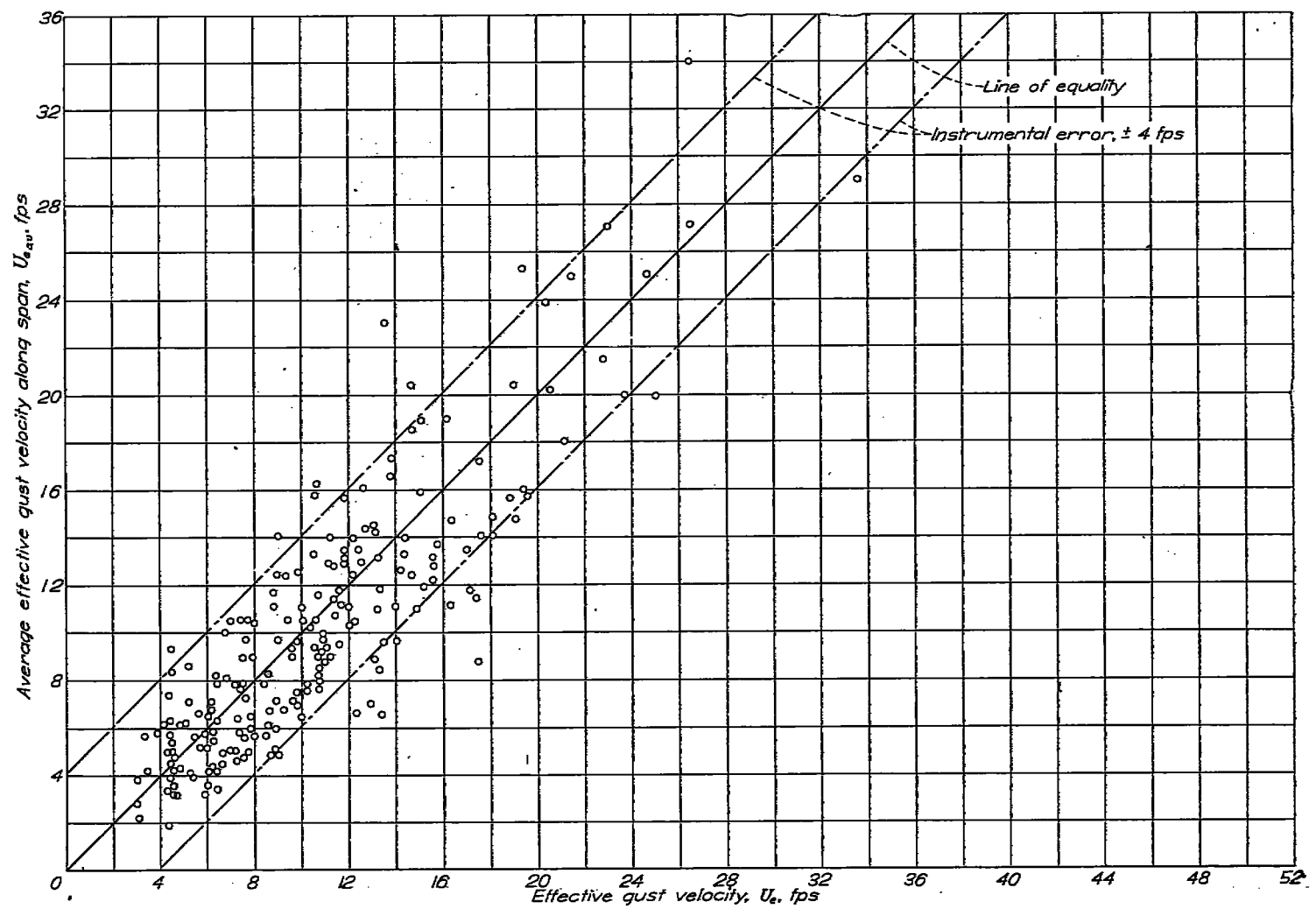

FIGURE 17.—Comparison of the effective gust velocity obtained from acceleration records with the average effective gust velocity along the span of the XC-35 airplane. (Data chosen at random from 25 percent of the total number of flights given in reference 12.)

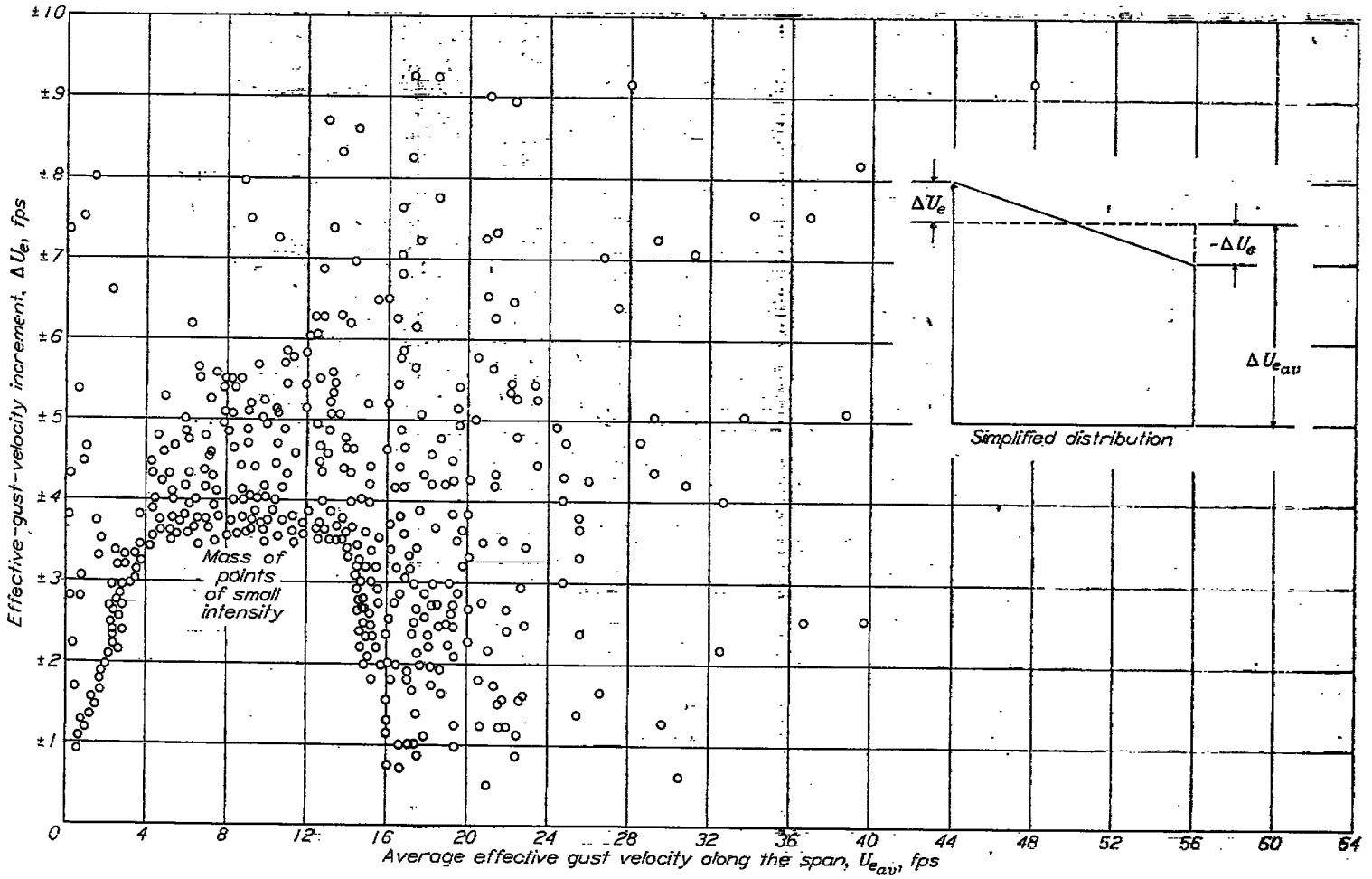

FIGURE 18.—Effective-gust-velocity increment $\pm\Delta U_e$ as a function of the average effective gust velocity $U_{e_{av}}$.

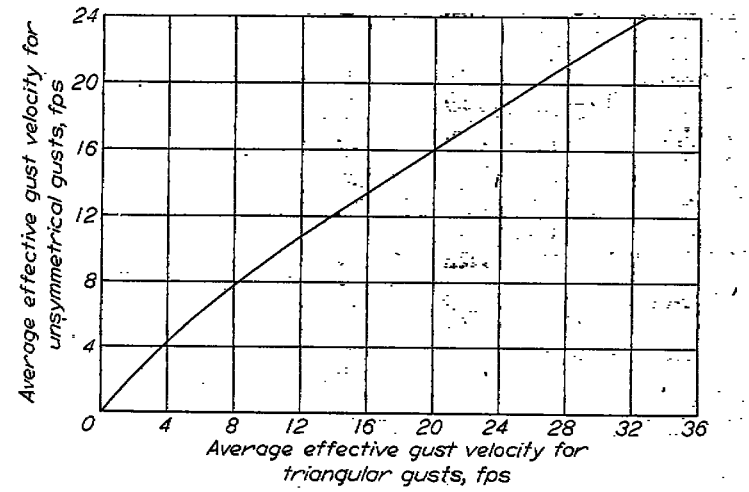

FIGURE 19.—Comparison of the gust intensity at equal frequencies of occurrence for the two predominating gust shapes.

were of opposite sign, whereas the remaining sets of two were composed of gusts of like sign. The larger gust intensity could be found at any point in the sequence under consideration.

Longitudinal gusts.—Inspection of the data for the maximum values of the horizontal and vertical gust velocities in the same traverse (fig. 20) indicates equality of the gust intensities in the two directions. Figure 21 for the XBM–1 and Aeronca C–2 airplanes gives essentially the same indication, but the agreement is not exact and the discrepancy between the values of the gust velocities is an offset of roughly 1 foot per second. The data obtained from the Aeronca C–2 airplane show the larger discrepancy. Some of this discrepancy may be due to the fact that the amount of horizontal-gust data was larger than the amount of vertical-gust data for the Aeronca C–2 airplane and smaller than the amount for the XBM–1 airplane.

Since the maximum gust intensity in the horizontal direction is equal to the vertical gust intensity for the same region of turbulence and since a preliminary investigation of frequency distributions indicates that the frequency distributions are essentially the same, the atmospheric turbulence seems to be isotropic. Previous indications as to structure of vertical gusts—that is, gust spacing, gust-gradient distance, and lateral distributions of gust velocity—would be assumed to apply to horizontal gusts.

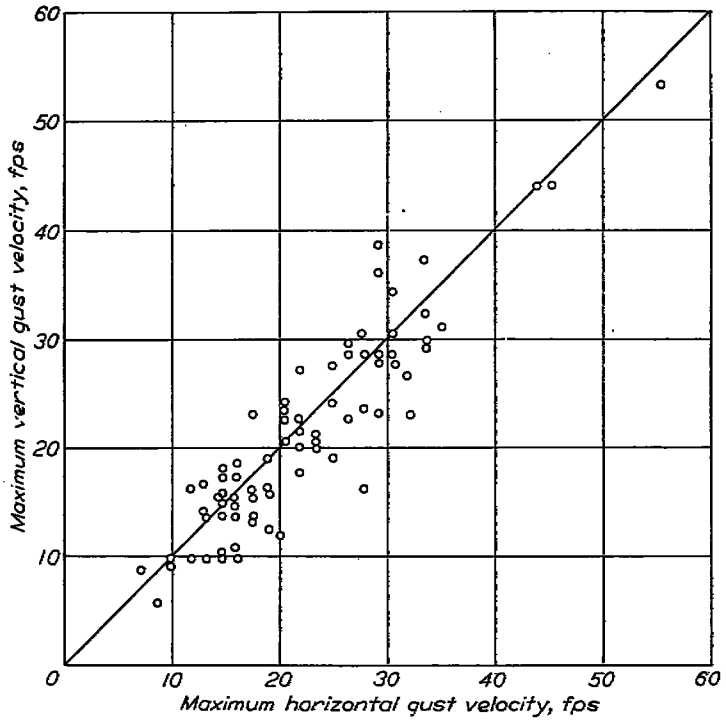

FIGURE 20.—Comparison of the maximum vertical gust velocity with the maximum horizontal gust velocity for separate traverses in rough air. Data for XC-35 airplane.

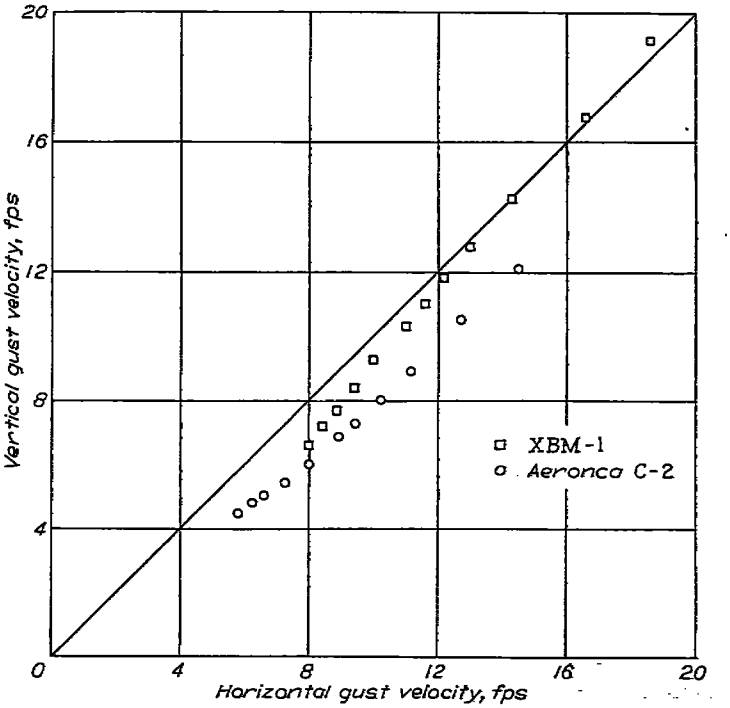

FIGURE 21.—Variation of vertical gust velocity with horizontal gust velocity for equal frequencies of occurrence.

The preceding results indicate equal gradient distances for the longitudinal and lateral faces of the gust velocity distribution, and this equality suggests that the gust is symmetrical about a vertical axis. In keeping with this concept, the findings suggest that the distribution might be visualized as a four-sided pyramid with a base length of 20 to 28 chords. While such a velocity distribution may represent the average gust, because of the wide variations in shape, a wedge-shaped velocity distribution such that the velocity distribution along the span is uniform and the longitudinal shape is either triangular or sinusoidal is recommended for load calculations.

CONCLUDING REMARKS

Although much of the information on gust structure can be rationalized to obtain a "standard" gust, this material should be used with caution for unconventional types of aircraft. The gust structure of interest is, of course, dependent to some degree on the airplane characteristics. Many other sizes of gusts exist and those that affect the airplane may be only a small part of the random variations that exist in the atmosphere.

Available information on the structure of atmospheric gusts has shown that, when the gust size and the gust-gradient distance are expressed in mean wing chords, the gust size is independent of airplane, weather, topography, and altitude. The probable size of the gust is 20 chords, and the probable gust-gradient distance for the standard gust is about 10 chords. A wedge-shaped gust with the gust velocity uniform across the span and either triangular or sinusoidal in shape with a base of 20 chords is believed to be the proper type for most load calculations.

For a sequence of gusts, the gusts may be of either like or unlike sign and will be continuous with the gust peaks spaced 20 chords apart.

Since the maximum horizontal and vertical gust intensities and frequency distributions are essentially the same within any region of rough air, the gust structure obtained for vertical gusts should apply equally well for horizontal gusts. Such information is pertinent where gust loads are under consideration for diving airplanes or missiles.

Since the data are influenced by the reactions of the airplane, the application to unconventional configurations should be investigated by a detailed analysis of several possible combinations of gust shape and size.

AIRPLANE REACTIONS

The second phase of the gust-load problem is that of determining the reaction or forces imposed on an airplane due to a known gust. The factors considered are the aerodynamic coefficients and the possible effects of stability and elasticity. The purpose of this section is to indicate what is known about these factors by coordinating the available information. In most cases, specific procedures or numbers to be used in load calculations are not obtained. In regard to some factors, the state of available information is unsatisfactory, but the factor is considered and its status is indicated.

956646—51——53

METHODS

The three methods utilized in the study of airplane reactions were an analysis and two experimental methods. The experimental methods consist of tests of models in the Langley gust tunnel and flight tests with full-scale airplanes.

ANALYSIS

Inspection of the equations given in references 14 and 15 indicates that the inclusion of unsteady lift leads to variable coefficients, which result in integral equations when the unknown appears under the integral sign. In all cases the integrals that appear are of the same form and represent the application of the principle of superposition to unit-jump solutions to obtain the response to arbitrary or known disturbances.

The principle cited is illustrated in figure 22 for a linear variation in angle of attack for which the lift on an airfoil after s_1 chords of penetration is desired. In figure 22 (a) the angle of attack is assumed to vary directly with s and the development of lift per unit change in angle of attack is assumed similar to that shown in figure 3. The angle-of-attack variation is assumed to be approximated by a series of unit changes in angle of attack superimposed in the s direction. For steady lift, the corresponding variations of lift with s are indicated by the straight line and steps in figure 22 (b). The unsteady lift develops for each step in angle of attack according to the dash curves and the approximate lift at s_1 is the sum of the contributions of each step at s_1. The result at s_1 can be written as

$$\Delta C_{L_1}=\frac{dC_L}{d\alpha}\sum_0^{s_1} C_{L_\alpha}(s_1-s)\Delta\alpha=\frac{dC_L}{d\alpha}\sum_0^{s_1} C_{L_\alpha}(s_1-s)\frac{\Delta\alpha}{\Delta s}\Delta s$$

or for an analytic expression of differential increments

$$\Delta C_{L_1}=\frac{dC_L}{d\alpha}\int_0^{s_1} C_{L_\alpha}(s_1-s)\frac{d\alpha}{ds}\,ds$$

This expression is commonly known as Duhamel's integral and is illustrated by Berg in reference 16. The integral can be evaluated analytically step by step as indicated in figure 22 or graphically by Carson's theorem (reference 17).

As previously mentioned, the type of equation obtained is of the form

$$C_{L_{w_1}}=A\int_0^{s_1} C_{L_\alpha}(s_1-s)\frac{d\alpha}{ds}\,ds-B\int_0^{s_1} C_{L_\alpha}(s_1-s)\frac{dC_{L_w}}{ds}\,ds$$

where $C_{L_{w_1}}$ is the local value of C_{L_w} at s_1. The difficulty in solving the equation arises from the fact that the relation between C_{L_w} and s must be known before the second integral on the right side can be evaluated. The equation shown is a simple case and the more complete equations of motion consist of additional integrals and, in some cases, derivatives of integrals.

Solutions of equations of the type shown have been obtained by methods of successive approximation, Fredholm's solution (reference 6), Laplace transforms (reference 14), or by assuming, as in reference 18, that the function is known. The need for solutions for arbitrary disturbances and the complicated nature of solutions generally lead to graphical or approximate methods in all but a few cases.

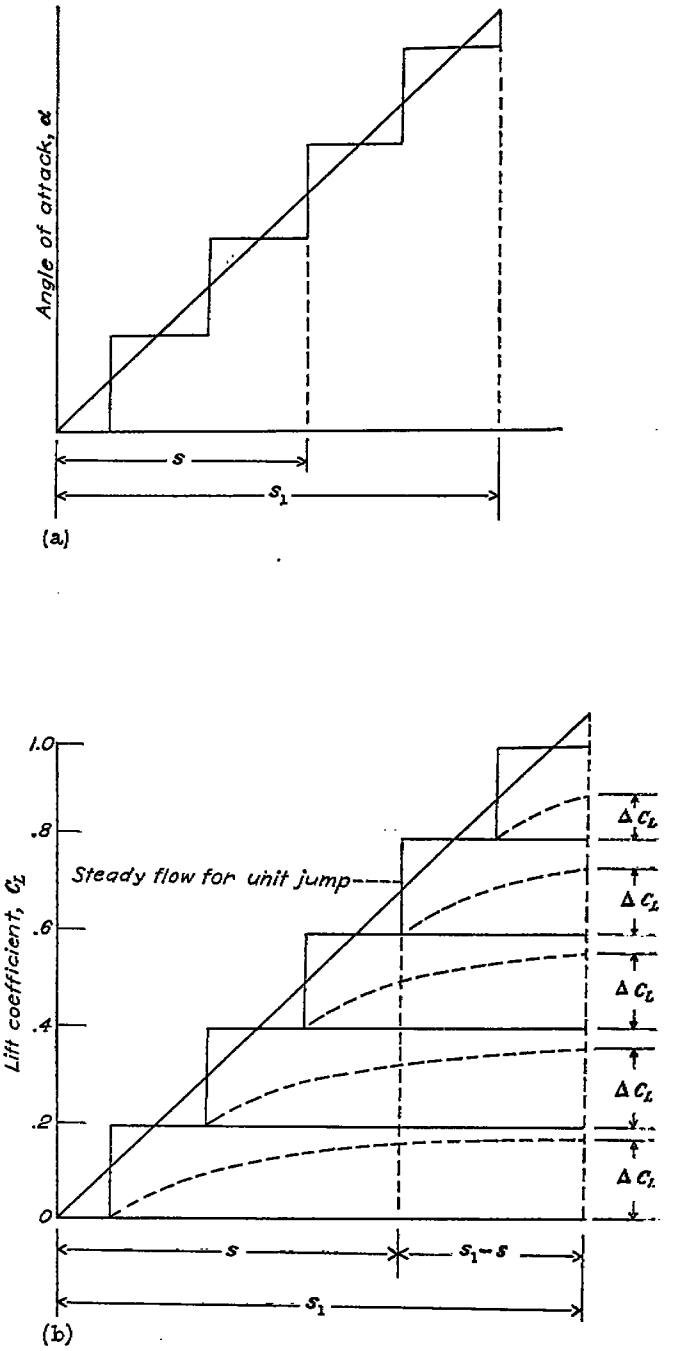

(a) Angle-of-attack change.
(b) Lift-coefficient change.

FIGURE 22.—Diagrammatic illustration of the superposition (Duhamel) integral for evaluation of lift following arbitrary variation in angle of attack.

GUST-TUNNEL TESTING

The Langley gust tunnel (fig. 23) was built to permit the determination of airplane reactions and other pertinent quantities under controlled and known conditions. It consists of a catapult to launch a dynamically scaled airplane model into steady level flight through a vertical jet of air having characteristics that are under control, a means of catching the model, and, finally, suitable equipment to record the required information. The old NACA gust tunnel described in reference 19 was capable of handling 3-foot-span models of airplanes at speeds up to about 50 miles per hour but in 1945 was replaced by a tunnel that is able to handle 6-foot-span models at speeds up to 100 miles per hour.

The accuracy of measurement at present is about $0.05g$ for acceleration, 0.3 foot per second for speed, and 0.01 inch for deflection of the wing or flap. Angular motions are determined within 0.1° of pitch-angle increment and about 0.2° for the position of any flap. All measurements except that of speed are incremental values from steady conditions and, as such, depend upon the steadiness of flight prior to entry into the gust. At peak acceleration for sharp-edge gusts the acceleration increment is considered accurate to within $0.1g$ and the pitch-angle increment, to about 0.1°, but the accuracy is questionable for the longest gust-gradient distance of about 16 chords.

In fundamental studies such as the determination of unsteady-lift functions, the solution obtained from gust-tunnel tests is an indirect one since the acceleration increment due to a gust is dependent on the difference between two terms. Thus, it is not possible to determine whether the correct values of the unsteady-lift functions are used, but only whether the use of unsteady-lift functions for a given shape is adequate. If sufficient data are collected utilizing different models of many sizes and shapes in different gusts, the various unsteady-lift functions can be evaluated to a limited degree.

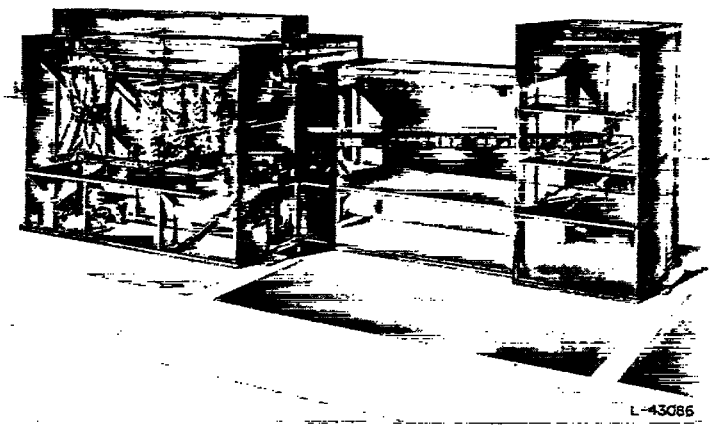

FIGURE 23.—Schematic sketch of Langley gust tunnel.

FLIGHT INVESTIGATIONS

Two approaches have been utilized for flight investigations of airplane reactions: one consisting simply of detailed analysis of flight records to obtain the relations desired—for example, between the pitch of an airplane and the acceleration imposed on the airplane—and the other consisting of flying an airplane in rough air to obtain statistical data for different conditions and then statistically comparing the reactions of the airplane. The first approach was used in a rather crude manner in reference 3, in which a determination was made of the effect of airplane wing loading and speed on the gust load factor. The statistical approach may permit checks to be made of both theoretical and gust-tunnel results, but the procedures and techniques have not been developed to the point where precise results can be obtained.

TRANSIENT AERODYNAMICS

The material presented in this section covers the development of the lift force and downwash but does not cover the variation in moment coefficient. The development of lift following a sudden change in angle of attack is assumed to be independent of the slope of the lift curve and can be treated as a separate subject. The neglect of possible variations in moment coefficient appears justified at this time on the basis that theory indicates that the zero-lift moment coefficient is unaffected.

UNSTEADY-LIFT FUNCTIONS

In the present report, the variation of lift coefficient for a unit change in angle of attack has been referred to as C_{L_α} or as the Wagner function, and the corresponding variation in lift coefficient following a change in angle of attack due to penetrating a unit gust has been called C_{L_g} or the Küssner function. The Küssner function is related to the Wagner function in that it has been derived from it by considering the airfoil penetrating a gust to be replaced by a deforming airfoil where the deformations correspond to the chordwise angle-of-attack distribution due to gust penetration. Unless otherwise stated, the lift at any time after the start of the angle-of-attack change is expressed as a fraction of the final lift coefficient.

Infinite aspect ratio.—Both the Wagner function and the Küssner function for unsteady lift have been derived a number of times. The former was originally given by Wagner in reference 20 and has been checked experimentally by Walker in reference 21 by measuring the circulation about a wing following a sudden change in forward speed. Figure 24 summarizes the computed and observed circulations obtained by Walker. Although the amount of direct experimental verification is limited, several analytical studies agree and indicate that the Wagner function should be close to correct.

The Küssner function has also been computed a number of times and different results have been obtained. Figure 25, which is based on data taken from references 2, 5, and 22 to

25, presents the results of six separate computations of the lift ratio C_{L_g} as a function of the distance penetrated into a sharp-edge gust and shows considerable scatter. The derivation given by Küssner in reference 5 is probably the best. No direct experimental verification of this factor is available, but Küssner has made several attempts at verification by dropping airfoils equipped with end plates through the boundary of a wind-tunnel jet. The tests made by Küssner have been described in reference 5 and the comparisons of the computed and experimental flight-path curvatures indicate good agreement, at least for penetrations up to 3 to 4 chords.

The values of C_{L_α} and C_{L_g} for the infinite-aspect-ratio wing are presented in figure 26. If the pitching motion of the airplane is not considered, the exact shapes of the unsteady-lift functions are unimportant and the discrepancies noted in figure 25 do not appear to be significant.

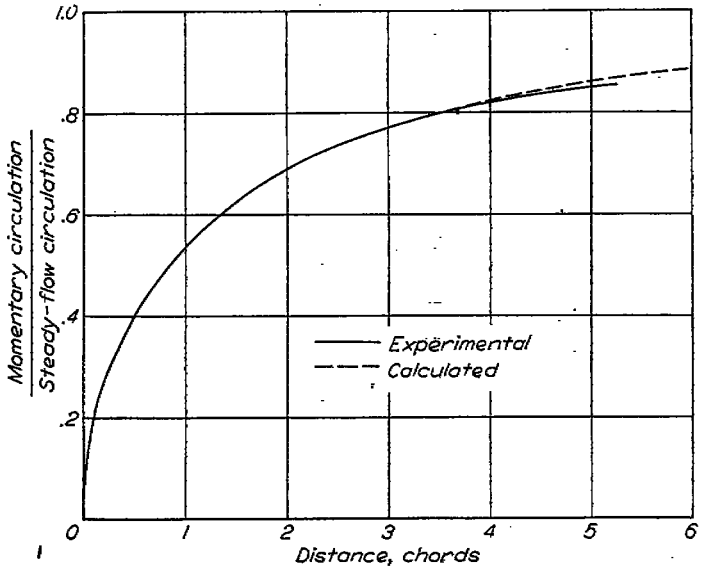

FIGURE 24.—Comparison of calculated and experimental circulation following abrupt increase in speed (from reference 21).

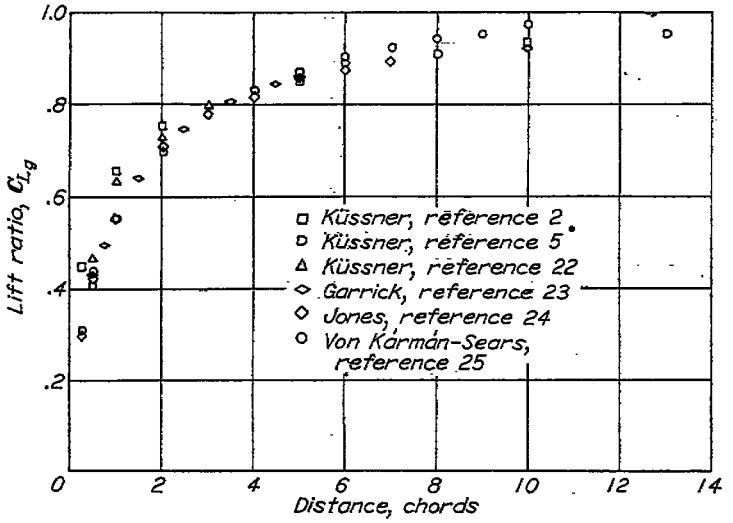

FIGURE 25.—Unsteady-lift function for an airfoil traversing a sharp gust.

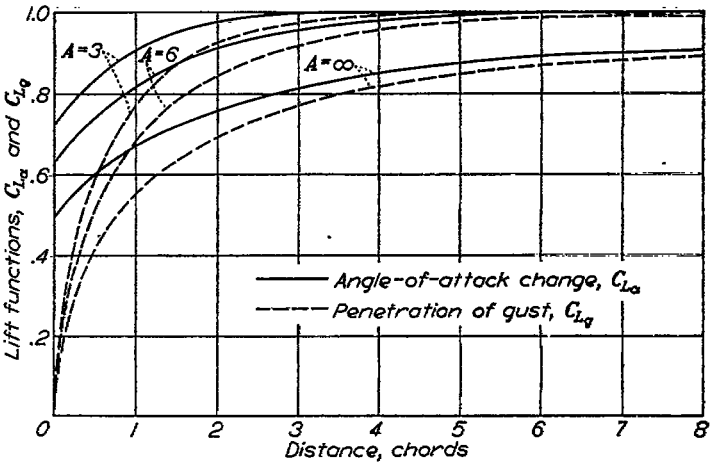

FIGURE 26.—Unsteady-lift functions C_{L_α} and C_{L_g} for aspect ratios 3, 6, and ∞.

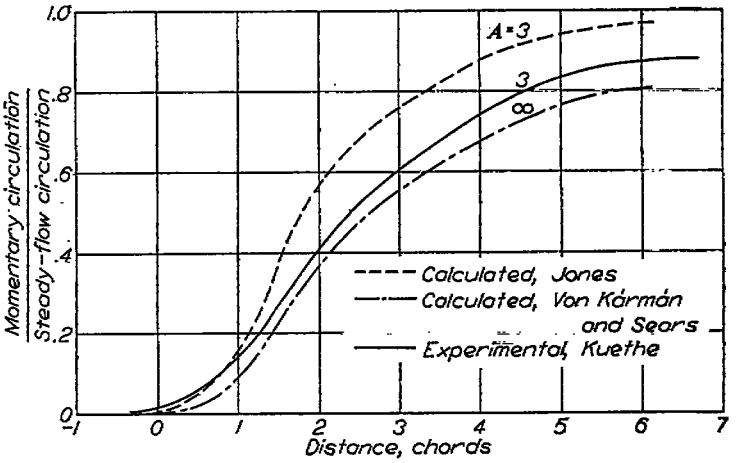

FIGURE 27.—Comparison of calculated and experimental circulations for aspect ratios 3 and ∞.

Finite aspect ratio.—The effect of finite aspect ratio on the unsteady-lift functions has been investigated by Jones in reference 14 and these results are shown in figure 26. This figure indicates that, as the aspect ratio decreases, the lift develops more rapidly, particularly at the start, until for the limiting case of zero aspect ratio the variation in lift might be expected to correspond to that for steady flow conditions. The estimation of the unsteady-lift functions for lower aspect ratios than those shown in figure 26 has been made by extrapolating the data by assuming that at zero aspect ratio, the unsteady-lift function disappears. Unpublished tests made with a flying wing having an aspect ratio of about 1.27 showed that this method led to reasonable values. The calculated value of the acceleration ratio was 0.92 as compared with an average experimental value of 0.93. These results indicate, therefore, that for flying wings finite theory applies. Other results, shown in figure 27 and given by Kuethe in reference 17 and by Sears and Kuethe in reference 26, indicate that the unsteady lift developed on a low-aspect-ratio wing subjected to a gust more closely approximates the unsteady-lift function for the two-dimensional case than that for aspect ratio 3.

An indirect verification of unsteady-lift functions has been obtained by comparing the calculated and actual response of airplane models to a sharp gust. The curves in figure 28 show the calculated acceleration ratio $\Delta n/\Delta n_s$ as a function of the mass parameter μ_g. The calculation for aspect ratio 6 is based on the unsteady-lift function given in figure 26 and that for infinite aspect ratio is based on the unsteady-lift functions given by Rhode in reference 4. The test points shown in figure 28 represent experimental values of the acceleration ratio determined from tests in both the old and the new gust tunnels. The results are for all types of airplanes from tailless high-speed configurations with wings swept back 35° to transports. As can be seen from figure 28, the experimental data scatter about the curve based on the unsteady-lift functions for aspect ratio ∞ and below the curve for aspect ratio 6. The results indicate that, for airplanes that include a fuselage, the use of the unsteady functions for infinite aspect ratio has given adequate and in most cases more accurate predictions of the acceleration ratio than the computations based on the finite-aspect-ratio theory of Jones.

The discrepancy between experiment and theory was considered as to the effect of interference on the experimental results. If the fuselage is considered as an elongated wing having a chord three times that of the wing, then at peak acceleration in a sharp gust the wing has traveled about 4 chords while the fuselage has traveled 1. On this basis, the lift on the fuselage might be considered zero or at most about half of its steady-flow value. If this hypothesis is compared with the material given in reference 19 (some of the values were in error and have been recomputed), the results shown in table VI are obtained. The results in table VI indicate that, although Jones' unsteady functions are much too high on the basis of gross area and the functions from reference 4 are somewhat high, the use of a net wing area plus one-half the fuselage intercept brings all calculations into closer agreement. In fact, for the infinite-aspect-ratio functions, the discrepancies are less than the precision of the data. If the net wing area is assumed, then both

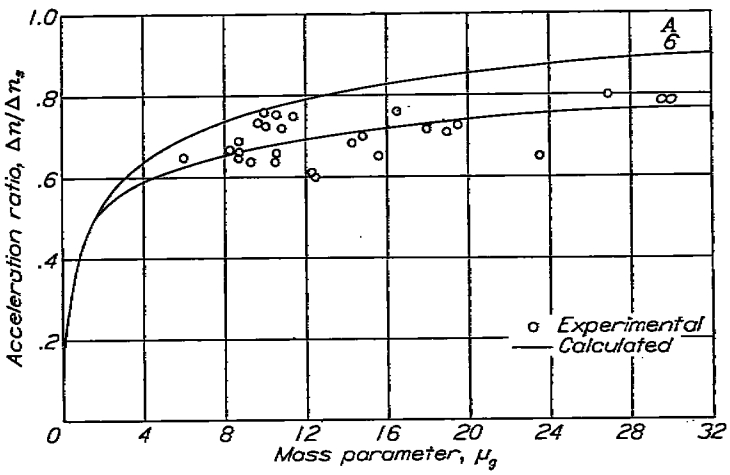

FIGURE 28.—Comparison of calculated and experimental acceleration ratios for a sharp-edge gust. Pitch assumed zero.

finite- and infinite-aspect-ratio functions differ from experiment by about the same amount, the results based on reference 14 being high and those based on reference 4 being low. Similar corrections may apply to Kuethe's results (fig. 27). Although the evidence indicates that the unsteady-lift functions for infinite aspect ratio should be used for conventional airplanes in conjunction with the net wing area plus half the fuselage intercept, the use of net area is recommended and is discussed subsequently.

Unpublished tests of a skeleton airplane equipped with a wing swept back 45° showed that the installation of the fuselage had no appreciable effect on the maximum acceleration increment. In this particular case, however, the length of the wing from the leading edge of the root section to the trailing edge of the tip section was almost equal to the length of the fuselage. Since one effect of sweep would be to modify the rate of development of lift on the wing, the difference between the lift developed on the wing and that on the fuselage for a given gust penetration may have been too small to be noted during the test. Although the evidence is still scant and conflicting in some respects, the use of net wing area appears to be better than the use of gross wing area for the sharp-edge gust except when the side projections of the wing and the fuselage are about the same length.

The determination of the proper wing area for the gradient gust is complicated by the introduction of the pitching motion of the airplane, and comparisons must be made between the detailed calculations and experiment. In the investigations that have been made (reference 15), the results have indicated that the use of the net wing area yields the best over-all agreement between calculations and experiment for gradient distances between 0 and 16 chords.

The use of tapered and swept wings for modern aircraft leads to problems in the computation of the gust load factor. Relatively little information is available on either problem, but the data of reference 19 indicated that moderate amounts of taper (up to 2:1) have little or no effect and can be neglected at least until experimental evidence of a more accurate nature is available. Large values of taper (for example, of about 3:1) and large sweep angles (30° to 40°) lead to concern as to the adequacy of the unsteady-lift functions, particularly the Küssner function C_{L_g}. The concern arises from the fact that for wings of high taper, the root section with the larger chord will have a rate of development of lift for a given distance penetrated into a gust considerably less than that of the narrower tip chord. In the case of sweep, the root of a sweptback wing penetrates the gust first and the lift may develop an appreciable value before the tip sections ever enter the gust.

With regard to the effect of wing taper on the unsteady-lift function, no theoretical developments are available to permit accurate computation, and calculations have been made by utilizing strip theory to develop the unsteady-lift functions for the finite wing from the two-dimensional functions of Küssner and Wagner. Experimental data available

to check the effect of taper on the unsteady-lift functions are indirect and are the result of tests of two specific airplanes. In both cases, calculations based on the results presented in reference 4 were in agreement with the experimental data for the sharp-edge gust in which pitch can be neglected. In the case of the large flying boat with 3½:1 taper ratio, the discrepancy amounted to about 2 percent. The maximum discrepancy was well within the experimental error. On the basis of these limited results, the effect of taper, at least up to 3½:1, appears to be negligible insofar as the calculation of total loads is concerned.

No theoretical studies are available for the sweptback wing, but recent test results for a straight and a 45° sweptback wing are available. Tests were made on a straight wing with a 2:1 taper and on the equivalent of the straight wing where each half-wing was rotated about the midchord point at the root so that the span changed with the angle of sweep. The sweep was such that the midchord line was at an angle of 45° to its original position. Flights were made through a sharp-edge gust, and an average time history of acceleration increments as a fraction of the maximum value is shown in figure 29. For comparison with the experimental results, two curves are shown: one based on the theory presented in reference 4 which disregards the effect of sweep on the unsteady-lift functions, and the other represents the calculated time history of acceleration based on the assumption that strip theory could be applied to derive the Küssner function for the swept wing.

Figure 29 shows that strip theory is in good agreement with experiment throughout the entire history, but the neglect of the effect of sweep on the lag in lift is in error at the start of the motion although good agreement is obtained for distances greater than 4 chords. Both calculations should yield essentially the same values for the larger distances since the conditions tend to approach the steady state. The discrepancy between experiment and strip theory appears to be due in part to positive pitch of the model during the traverse of the gust. Therefore, the effect of sweep on the unsteady-lift functions cannot be neglected if the shape of the curve is considered important.

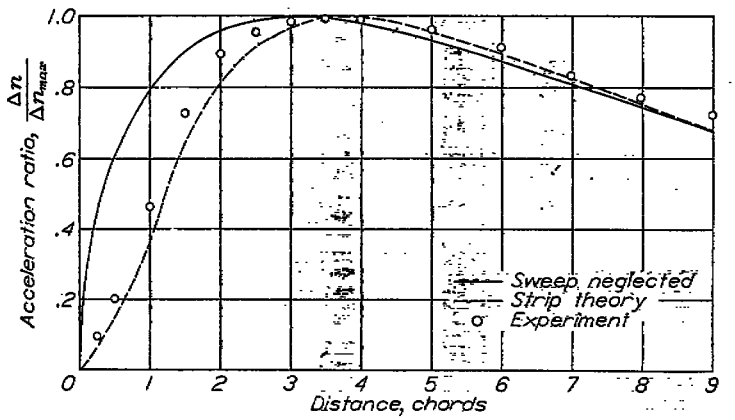

FIGURE 29.—History of acceleration for an airplane with a 45° sweptback wing in a sharp-edge gust.

The unsteady-lift theory as developed by Wagner, Jones, and others has been evolved for monoplanes only but the unsteady-lift functions for biplanes may be needed in connection with gust-load calculations. No theory is available on this problem, but consideration of the vortex sheets associated with the biplane indicates that, for the first few chords after a sudden change in angle of attack, the tip vortices of the wings are short and have a negligible effect on the mutually induced angle of attack of one wing upon the other. Since the equivalent monoplane theory assumes completely developed vortex systems with the shed vortex at infinity, it might be expected that for a biplane in a sharp gust the two wings would act independently, and, therefore, the unsteady-lift functions and other associated aerodynamic parameters for the biplane should be based on the characteristics for each individual wing. Figure 30, which has been reproduced from reference 8, shows the results of tests of a biplane. The results in the figure are the accelerations obtained as a result of experiment in the Langley gust tunnel, the curve predicted by assuming that the two wings act independently, and the curve predicted by assuming that the equivalent-monoplane theory holds. Infinite-aspect-ratio unsteady-lift functions were used. For the shorter gust-gradient distances where the tip vortices might be expected to have little effect, theory and experiment are in excellent agreement if the two wings are assumed to act independently. The computed curve for acceleration increment, based on reference 4, is considerably below the experimental data; thus the tip vortices have little effect, at least up to 8 or 10 wing chords. As the gradient distance is increased to 20 chords, the experimental data fall below both calculated curves because of the pitching action of the airplane.

The effect of compressibility on the unsteady-lift functions is of interest because it may change the shape of the curves, but little or no information on this problem is available. Jones has indicated that for subsonic speeds the effect of compressibility would be to reduce the aspect ratio of the

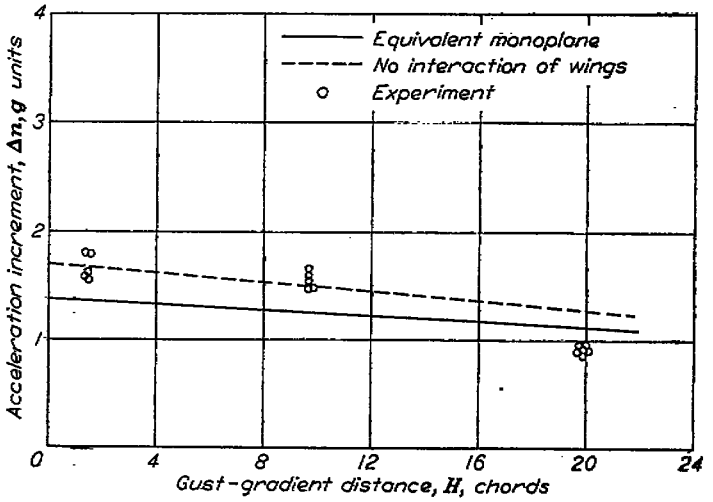

FIGURE 30.—Variation of acceleration with gust-gradient distance for a biplane (from reference 8).

wing according to the relation $\sqrt{1-M^2}$. The E correction of reference 27 is changed at the same time to correspond. For the transonic range where mixed flows occur the variation in the unsteady-lift functions is unknown. At supersonic speeds the effect of unsteady lift would be expected to disappear since the effect requires the transmission of pressures forward. It would be expected that the unsteady-lift functions would change only slightly up to high subsonic speeds and that at supersonic speeds the functions would disappear.

SLOPE OF LIFT CURVE

Investigations to determine the proper slope of the lift curve to be used in gust-load calculations have been made mainly in the Langly gust tunnel. The information available for presentation is indirect and in many instances inconclusive because of interrelations of many factors. The factors involved in the computation of the proper slope of the lift curve include the determination of the airfoil section characteristics, aspect-ratio corrections, interference effects, the effects of configuration with reference to sweep and multiplanes and the effects of compressibility and power.

Section characteristics.—As indicated by the results presented in figure 28, the conventional estimates of the lift-curve slope together with the unsteady-lift functions for infinite aspect ratio gave the best results in predicting the acceleration increment due to a sharp-edge gust for ordinary airfoils. The use of the laminar-flow section introduced airfoils having higher slopes of the lift curve. The increase was of concern since it amounted to an increase of 10 percent in the load-factor increment. Brief consideration indicated that the slope of the lift curve depends on the steady-flow relation between the boundary-layer thickness and angle of attack. It was believed that under unsteady flow conditions the relation for steady flow would not apply and, therefore, the boundary layer would not have time to adjust itself during a sudden change in angle of attack. Since no experimental or theoretical information was available in connection with the probable slope of the lift curve, experimental evidence was needed.

For this purpose a skeleton model with a laminar-flow wing was tested in the Langley gust tunnel. The characteristics of the test model are given in table VII and figure 31. For the first tests the wing had a smooth surface. For the second tests, carborundum grains were glued over the leading edge of the wing back to 7.8 percent of the chord on both the upper and lower surfaces. The slopes of the lift curve for the smooth and rough wings have been included in table VII and are based on experimental data presented in reference 28 corrected to finite aspect ratio according to reference 27. In addition to the lift-curve slopes obtained from low-turbulence wind-tunnel tests, the theoretical lift-curve slope, based on the theory presented in reference 29, is also included in the table.

The average values of the acceleration increments for the smooth and rough wings and the probable errors are given

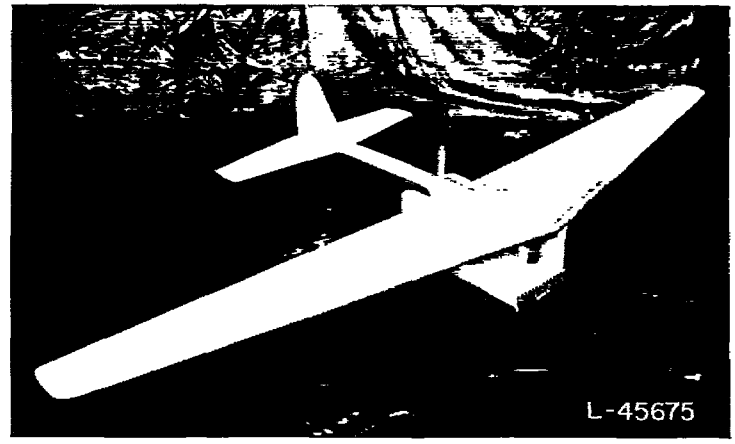

FIGURE 31.—Test model.

in table VIII. The acceleration increments computed on the basis of the characteristics in table VII have also been included. Table VIII shows that the maximum acceleration increments for the two test conditions are essentially the same. Comparison of the $0.02g$ experimental difference with the calculated difference of $0.26g$ shows that roughening an airfoil to produce a turbulent boundary layer has no effect on the slope of the lift curve that is applicable in the unsteady flow conditions of a sharp-edge gust. If these results are extended by the assumption that the flow conditions for a conventional airfoil in the steady state are simulated by those for the roughened low-drag wing, airfoil section characteristics are concluded to have no significant effect on the acceleration increment obtained in unsteady flow conditions of a sharp-edge gust.

Since the most probable gust is one with a gradient distance of 10 chords, the averages of the maximum acceleration increments for the two test conditions were calculated for gusts with gradient distance up to 12 chords by applying the principle of superposition to the test results for the sharp-edge gust. The results of these calculations showed only 2½-percent difference between the average values. On the basis of this simple analysis, airfoil section characteristics have no significant effect on the acceleration increments for gusts with gradient distances from 0 to 12 chords. From the present data, however, it is not possible to specify the gradient distance at which the difference would become noticeable as the result of attaining quasi-steady conditions.

For the laminar-flow type of airfoil, tests in low-turbulence wind tunnels together with the aspect-ratio corrections of reference 27 should yield an adequate prediction of the acceleration increment due to a sharp-edge gust. The use of the corrections and the determination of section characteristics for an arbitrary airfoil are, however, still open to question since tests in low-turbulence tunnels on the arbitrary airfoil sections tend to show low slopes of the lift curve. In view of the many interrelated factors, some of which are discussed in subsequent paragraphs, it appears that the selection of an arbitrary section lift-curve slope of about 6 pre radian will be adequate for gust-load calculations.

Aspect-ratio corrections.—As previously noted, the data in figure 28 were obtained for conventional airplanes, but the data in table VIII apply to a skeleton airplane with little or no fuselage. The combined effects of fuselage interference, aspect-ratio corrections, unsteady-lift functions, and section characteristics are all involved and at the present time cannot be entirely segregated. For the time being, simple aspect-ratio correction factors appear to be adequate. The factor $\frac{6A}{A+2}$ has been used with satisfactory results in connection with gust-load studies.

Swept wings.—Table IX (from reference 30) shows the results of gust-tunnel tests on a wing swept back 45°. The tests were made in a sharp-edge gust and the acceleration increments for a gradient distance of 9 chords were obtained by superposition. All results are corrected to zero pitch of the model. Calculated values are also included. One set of values is based on the results of wind-tunnel tests of the airplane model, tail off, and the other set differs from the first in that the slope of the lift curve for the swept wing was taken as that for the straight wing multiplied by the cosine of the sweep angle. In both calculations, the unsteady-lift function for the wing C_{L_g} was obtained by means of strip theory.

Inspection of the results given in table IX shows that the use of the cosine law for predicting the slope of the lift curve for the swept wing gives excellent results, the differences between experiment and calculation being within the experimental error. The use of lift-curve slopes from steady-flow tests to calculate the acceleration increments for the swept wing yields values some 20 percent below experimental results. Similar tests on a 45° sweptforward wing verify this result.

The low value of acceleration increments calculated from the results of wind-tunnel tests has been of concern. At present, no definite evidence is available to explain this discrepancy, but it is believed that the difference can be ascribed to the behavior of the boundary layer in the unsteady flow condition that exists during traverse of a gust. The discrepancy emphasizes the importance in the prediction of gust load factors of using the proper lift-curve slope. On the basis of limited data better results seem to be obtained if the cosine law of variation is used rather than wind-tunnel results.

The results obtained to date apply to a definite method of sweeping the wing (rotating the wing panel) to obtain the equivalent straight wing. Other systems lead to other combinations of aspect ratio and sweep and may yield different results. In such calculations, the same procedure as that described in the present report should be utilized.

Scale effects.—Tests in the old and new gust tunnels of models of the Boeing B–247 airplane (table X) were made to obtain a measure of any scale effects. A 3-foot-span model was tested in the old gust tunnel as a reference for design requirements. When the new gust tunnel was built, this model and one dynamically similar but twice as large were tested. The results of all three tests are shown in figure 32 as a plot of the acceleration ratio as a function of gradient distance in chords.

Inspection of figure 32 shows excellent agreement between the results for the two models; this fact indicates that for the conditions tested no scale effect was present. The largest discrepancy is for a sharp-edge gust and is no greater than differences in results for tests of the same model in two tunnels. Some of the discrepancy may be due to the fact that the gust shape was the same in absolute dimension but differed slightly on the basis of chords of the two models.

Effect of power.—When the slipstream covers the entire span of the airplane, the steady-flow slope of the lift curve has been shown to increase about 100 percent for the slipstream corresponding to the climb condition. Since the working velocity has been increased by the introduction of power, a real increase in the lift-curve slope has probably been obtained. Under these circumstances, the angle-of-attack change due to the gust would be utilized in connection with the increased slope of the lift curve. In actual practice, the suggestion that the power-on slope of the lift curve should be used where the slipstream covers most of the airplane span is not as serious as it appears at first sight. The highest lift-curve slope is obtained at relatively low forward speed, a condition at which the load factor due to the gust is small. For conventional airplanes, the power-off lift-curve slope appears correct.

Multiplanes.—For steady flow conditions the biplane is usually represented by an equivalent monoplane. This assumption no longer applies for the transient lift conditions that exist in a gust. The question of the proper slope of the lift curve to use for the transient conditions is in part answered by the results presented in figure 30. On the basis of the agreement shown in figure 30, the wings should be considered as acting independently and the slope of the wing lift curve as being computed on the basis of the average geometric aspect ratio of the two wings.

Compressibility.—The effect of compressibility on the slope of the lift curve under unsteady flow conditions is a subject of much interest and one for which no experimental evidence is available. It is thought that the lift-curve slope should follow the Glauert factor in the subsonic range, but in

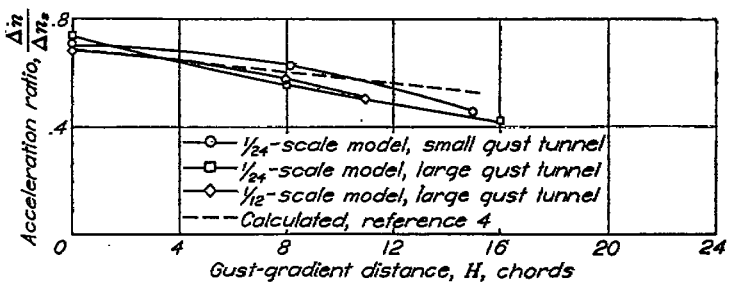

FIGURE 32.—Experimental acceleration ratio for Boeing B-247 airplane as a function of gust-gradient distance.

the region near the critical Mach number and through the transonic region the mixed flows combined with transient conditions might delay or cancel the effect of compressibility on the lift-curve slope. For the time being the usual compressibility factors could be applied up to the critical Mach number and above that, the results of wind-tunnel tests should be utilized.

DOWNWASH

Figure 33 (fig. 9 of reference 31) shows the change in vertical velocity at the tail following a sudden increase in wing circulation for several values of the distance from the trailing edge of the wing to the leading edge of the tail. The change in vertical velocity is plotted as a function of the distance of the tail surface from the vortex shed by the wing.

Figure 33 indicates that the tail surface first encounters a gradual increase in upwash until the leading edge crosses the center of the shed vortex when, following a violent change in direction, the downwash approaches its steady-state value. The curves for different tail lengths indicate quite clearly that the effect of increasing the tail length is to increase the time delay of the velocity change in proportion to the tail length. The violence of the direction change as the tail penetrates the vortex depends on the vertical location of the tail relative to the vortex and until more accurate predictions can be made of the location of the vortex, such changes might be disregarded. Figure 33 indicates that the assumption proposed in references 31 and 32 of a space lag between the change in lift on the wing and the change in angle of attack at the tail is reasonable and should be taken into account in any detailed calculations.

The indications to date are that the results obtained by utilizing a space lag of downwash have been in fair agreement with experiment, but the corresponding calculations neglecting the space lag of downwash have not been made to determine the seriousness of the error of neglecting this quantity.

MAXIMUM LIFT COEFFICIENT

Reference 19 shows that, for an airplane model traversing a sharp-edge gust at its steady-flow maximum lift coefficient, the maximum lift coefficient during the action of the gust was not limited to the steady-flow value. Farren in reference 33 made tests of two-dimensional airfoils at constant angular velocities through maximum lift and return. Angle-of-attack variations range as high as 12½° per chord of travel, and the results indicated that the maximum lift coefficient could range from 30 to 50 percent above the steady-flow value.

No concise estimates of maximum lift coefficient during sudden changes in angle of attack can be made, but the sketchy information that is available indicates that a conservative estimate for incompressible-flow conditions is an increase of about 25 percent over the steady-flow value. In the transonic region, the effects of compressibility may limit the maximum lift coefficient, and in this range the investigations made in the various wind tunnels would be pertinent.

RIGID-BODY REACTIONS

The available data on gust structure and aerodynamics have been analyzed and the next problem is the determination of the behavior of the airplane as a whole since the motions of the airplane have an important bearing on gust-load calculation. The significant parameters of airplane behavior as determined from analytical and experimental investigations are subsequently summarized and possible simplifications are investigated.

ANALYTICAL AND EXPERIMENTAL STUDIES

The material presented is the result of analytical and experimental study of arbitrary and special configurations. The analytical studies have been of a general nature and about two-thirds of the experimental studies can be so classed. The rest of the experimental research has been done in connection with specific problems or airplane designs. The scope and results of the analytical studies are presented first, followed by the experimental studies. In addition to the behavior of and the loads on airplanes caused by vertical gusts uniform across the span, limited research and studies on unsymmetrical and lateral gusts are described and reported in appropriate sections.

Analytical studies.—The analytical studies of the loads on and behavior of an airplane traversing a gust have been performed for a uniform upward-acting vertical gust. Current theory indicates that the incremental loadings for a downward-acting gust are equal in magnitude but opposite in sign. Further assumptions are that:

(1) The airplane maintains a constant forward speed during the traverse of the gust

(2) The airplane is in equilibrium prior to entry into the gust

(3) The aerodynamic center of an aerodynamic surface is at the quarter-chord point

(4) The moment coefficient at zero lift is a constant for transient conditions and has the same value as for steady flow conditions

(5) The control surfaces of the airplane are locked.

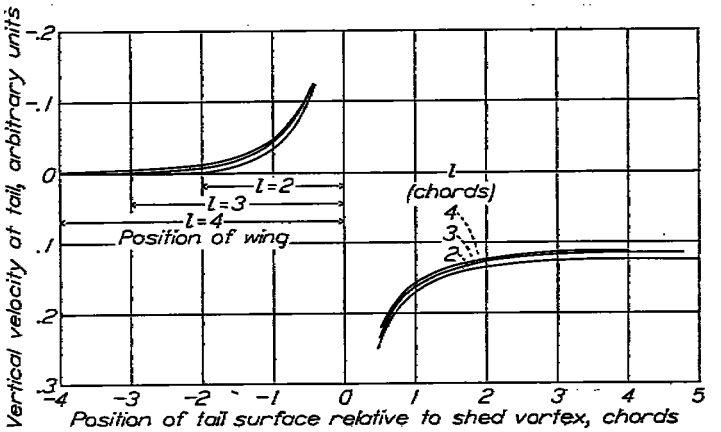

FIGURE 33.—Effect of tail length on the vertical velocity at the tail surface following a sudden increase in wing circulation. Figure 9 of reference 31

Extended analyses in which the airplane is considered free to pitch as well as to rise under the action of a gust have been made by the NACA for conventional, canard, and tailless airplanes. In the case of the conventional airplane, the analysis was rather wide in scope; whereas for the other two types of aircraft, the analyses were limited to specific cases. The procedure used was an iteration process.

The calculations were aimed at covering all configurations and values of stability which would be reasonable for conventional airplanes and such values of the mass parameter and moment of inertia which would fall within the capacity of the gust tunnel. The pertinent airplane characteristics assumed in the analysis are given in table XI for all the combinations considered. As can be seen from the table, the static margins range from 0.009 to −0.503 and the mass parameter ranges from 10.25 to 30.75. The calculations were made for three gust-gradient distances—0, 8, and 16 chords. The flight conditions assumed were a gust velocity of 6 feet per second and a forward speed of about 40 miles per hour. The calculations were not made for all combinations of variables noted in table XI, but some intermediate values were interpolated.

The results of the calculations are shown in tables XII (a), XII (b), and XII (c) as the acceleration increments at maximum acceleration for the airplane with the center of gravity at 15, 25, and 35 percent of the mean aerodynamic chord, respectively. Each table shows the results for the three gust-gradient distances and for various combinations of tail area and tail length. The incremental values of acceleration which are contributed by each motion or source are tabulated and then totaled to obtain the wing acceleration, the acceleration increment resulting from the lift on the tail, and finally the total acceleration increment impressed on the airplane.

In addition to the results of the analysis being presented in tabular form, figures 34 and 35 indicate the effect of pitch on the total wing load. In figure 34, the ratio of the total wing load increment, including the effect of pitch, divided by the total wing load increment, assuming the pitch equal to zero, is shown. A value of 1 indicates that the effect of pitch was negligible, and values greater than 1 indicate that the effect of pitch increased the total wing load. The results are shown as a function of the static margin for three gust-gradient distances. The individual curves shown in the figure represent given configurations but different center-of-gravity positions. Figure 35 is a similar plot of data from tables XII (a), XII (b), and XII (c) of the total acceleration increment as a function of the static margin for comparison with the experimental data from the gust tunnel.

Figure 36 shows the wing lift increment resulting from pitch of the airplane in terms of the total wing lift as a function of mass parameter. The three solid curves represent the three center-of-gravity positions. The curves represent the "average" airplane with medium tail length and medium tail area traversing a flat-top gust with a gradient distance of 8 chords. The dash lines included in the figure represent the pitch-increment ratio $\frac{\Delta\theta}{U/V}$. This ratio has been used to correct for pitching effects on the basis that the change in acceleration due to pitch is proportional to the ratio of the pitch increment to the gust angle. The distance between the dash and solid lines is a measure of the error of this assumption.

The data in tables XII (a), XII (b), and XII (c) were also utilized to obtain the total tail load increment divided by the tail load if the downwash, the vertical motion, and the pitch are assumed to be zero. The results are shown in figure 37 as a function of the static margin $dC'_{m_{cg}}/dC_L$ for the

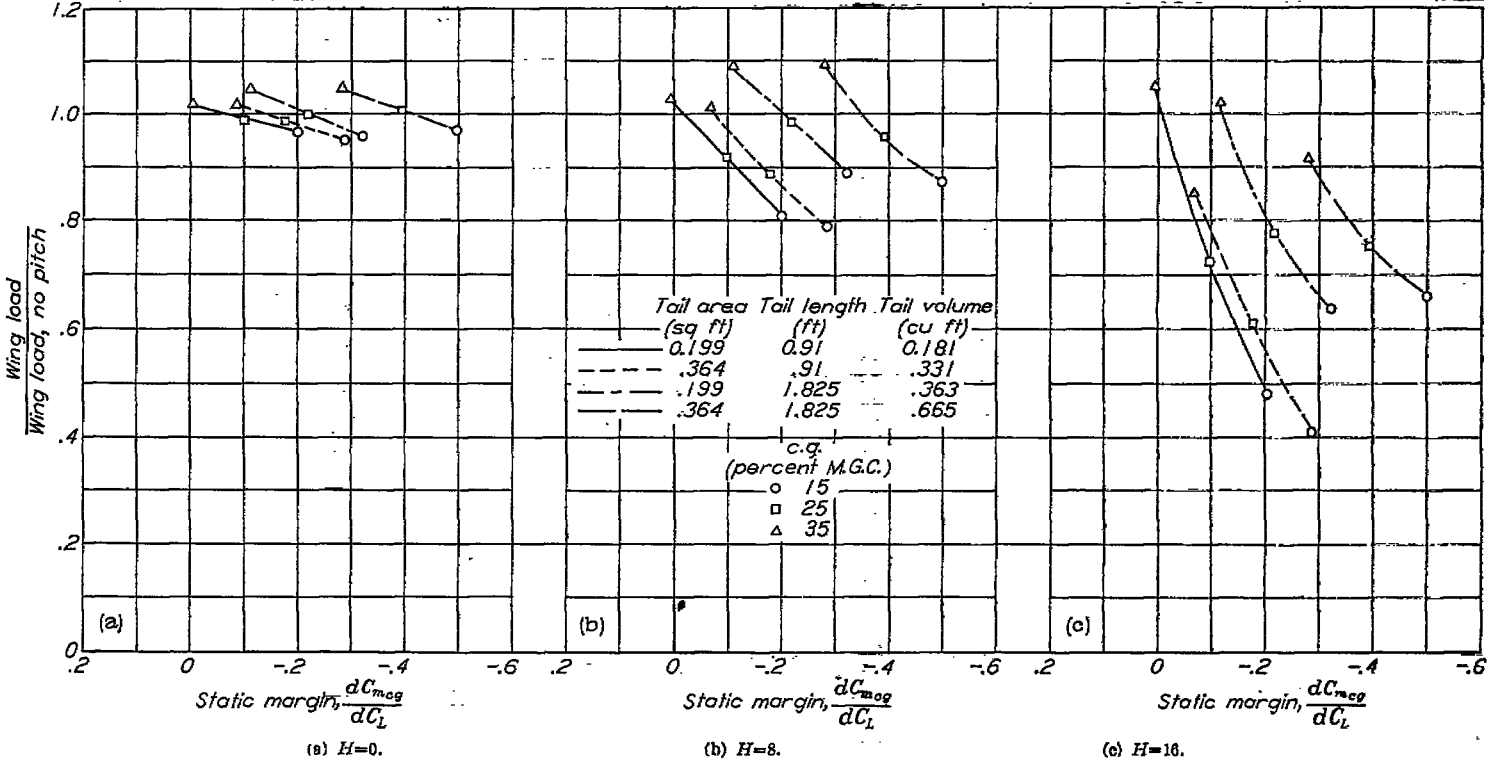

(a) H=0. (b) H=8. (c) H=16.

FIGURE 34.—The ratio of total wing load to the wing load with no pitch as a function of static margin for a conventional airplane.

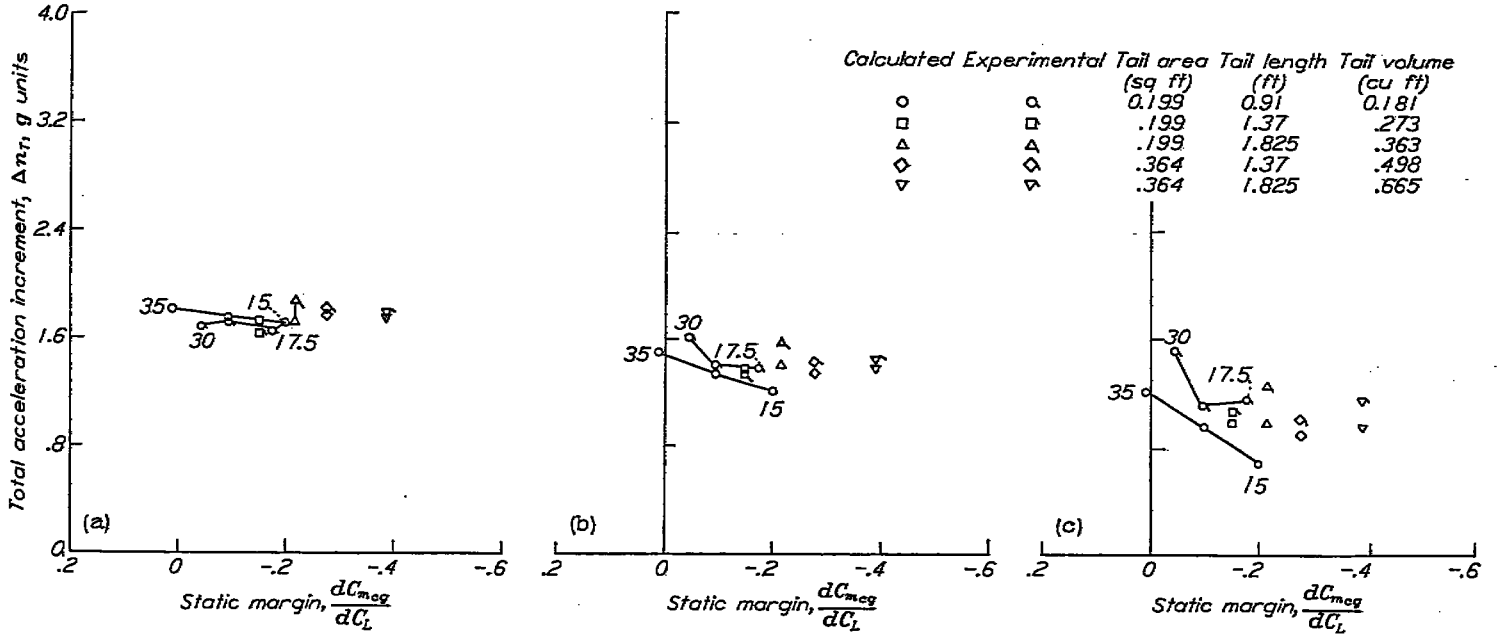

(a) H=0. (b) H=8. (c) H=16.

FIGURE 35.—Comparison of calculated and experimental acceleration increments for conventional airplane. All points except where noted have center of gravity at 25 percent mean geometric chord.

three gust-gradient distances. The total tail load shown is that at the time of maximum total airplane load. The lines connecting the points represent the same configuration and the movement along the line to the right indicates increasing static stability.

Detailed calculations have also been made for a flying wing with about 25° of sweepback and for a canard airplane. The characteristics of the airplanes are shown in table XI. The calculations for the flying wing were made for two center-of-gravity positions and for three gradient distances — 0, 8, and 17.5 chords. Table XIII shows the results of the calculations and includes the contributions from the different sources for the two center-of-gravity positions. The total wing load increments are shown for each center-of-gravity position. Calculations were made by using finite-aspect-ratio unsteady-lift functions on the basis that no fuselage was present. The total acceleration increment has been plotted in figure 38(a) for each center-of-gravity position. The canard airplane had the same general characteristics as the conventional Boeing B–247 transport airplane. The calculations for the canard airplane for net wing area and for the two unsteady-lift functions have been obtained from reference 15 and are presented in table XIV. The calculated total acceleration increments for the canard are shown in figure 38(b) as a function of gradient distance.

Figure 39 indicates the effect on the calculated loads of substituting the wing loading for the mass parameter. This figure is a plot of the acceleration based on wing loading divided by that based on the mass parameter as a function of wing loading. The calculations were made for three classes of airplanes—transports, personal airplanes, and flying boats. The results are shown as a function of the wing loading. Points lying above the line indicate overestimation of the acceleration increment, and points below the line represent underestimation of the acceleration increment.

As mentioned in the section about gust structure, the suggestion was made of either a triangular or sinusoidal gust

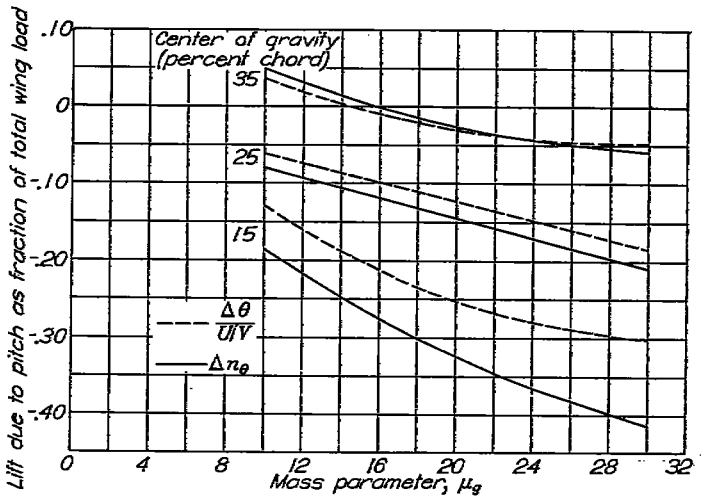

FIGURE 36.—Variation of relative lift due to pitch with mass parameter for a gust-gradient distance of 8 chords.

shape in the direction of flight. As a check on the interchangeability of the two gust shapes, figure 40 shows the ratio of the acceleration due to a sinusoidal gust to that for a triangular gust as a function of the mass parameter when the unsteady-lift functions for infinite aspect ratio and aspect ratio 6 are used. The calculations were performed by a step-by-step procedure that took into account the possible lack of coincidence in the gust peaks. Other calculations indicated that, for gusts with a distance of 10 chords, the maximum lag in the acceleration peak would be about 2 chords when the wing had an infinite mass parameter.

Experimental studies.—Most of the experimental data available are from general tests in the Langley gust tunnel with upward-acting gusts perpendicular to the flight path. Most of the research can be classed as general and includes the material presented in reference 19. The results of tests of specific models that are applicable to general studies are included.

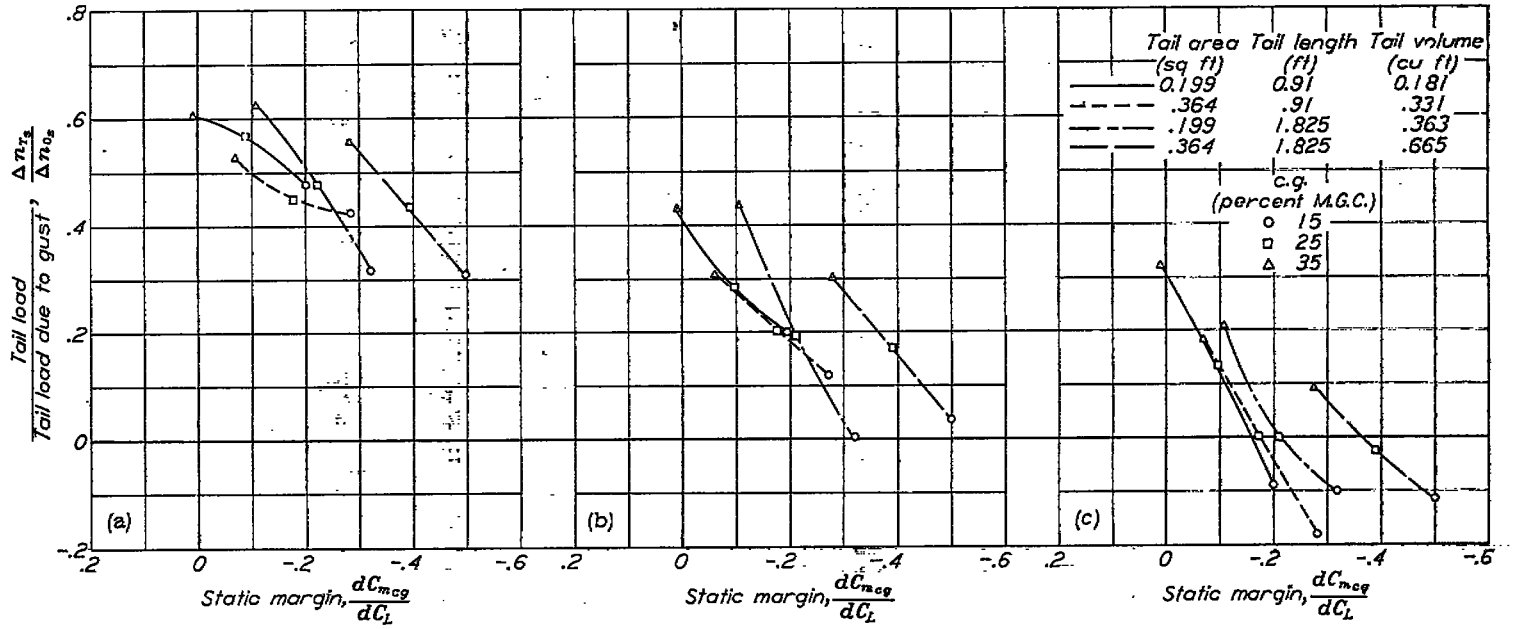

(a) H=0. (b) H=8. (c) H=16.

FIGURE 37.—Tail load increment as a fraction of tail load due to gust only for a conventional airplane.

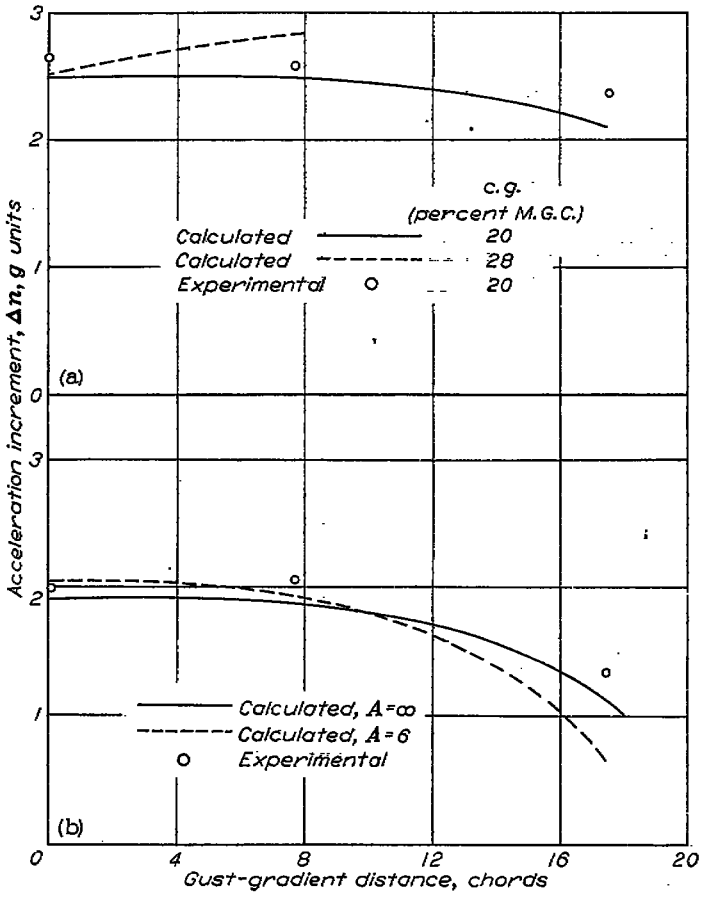

(a) Tailless airplane.
(b) Canard airplane.

FIGURE 38.—Comparison of calculated and experimental acceleration increments for unconventional airplanes.

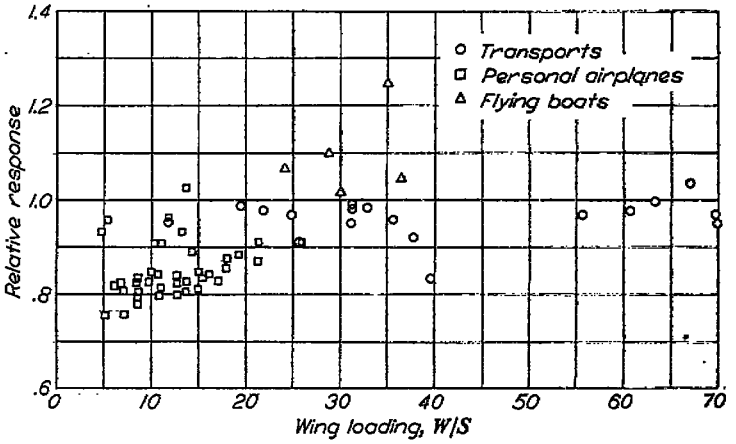

FIGURE 39.—Relative response of representative airplanes as a function of wing loading. (Acceleration based on W/S divided by acceleration based on mass parameter.)

A general study was made of the effect of the stability of airplanes on the gust load factor; the stability characteristics were varied over a wide range within which conventional airplanes would be expected to fall. The tests were performed on an arbitrary "stability" airplane model for correlation with the extended analysis previously described. The characteristics of this model are given in table XI and the total acceleration increments obtained from the tests are shown in figure 35. The tests were made for three gust-gradient distances and with the center-of-gravity positions at 17.5, 25, and 30 percent of the mean geometric chord. The combinations of tail area and tail length used on the test model are listed in figure 35.

The unconventional airplane models listed in table XI include a flying wing and a canard airplane. Tests of the

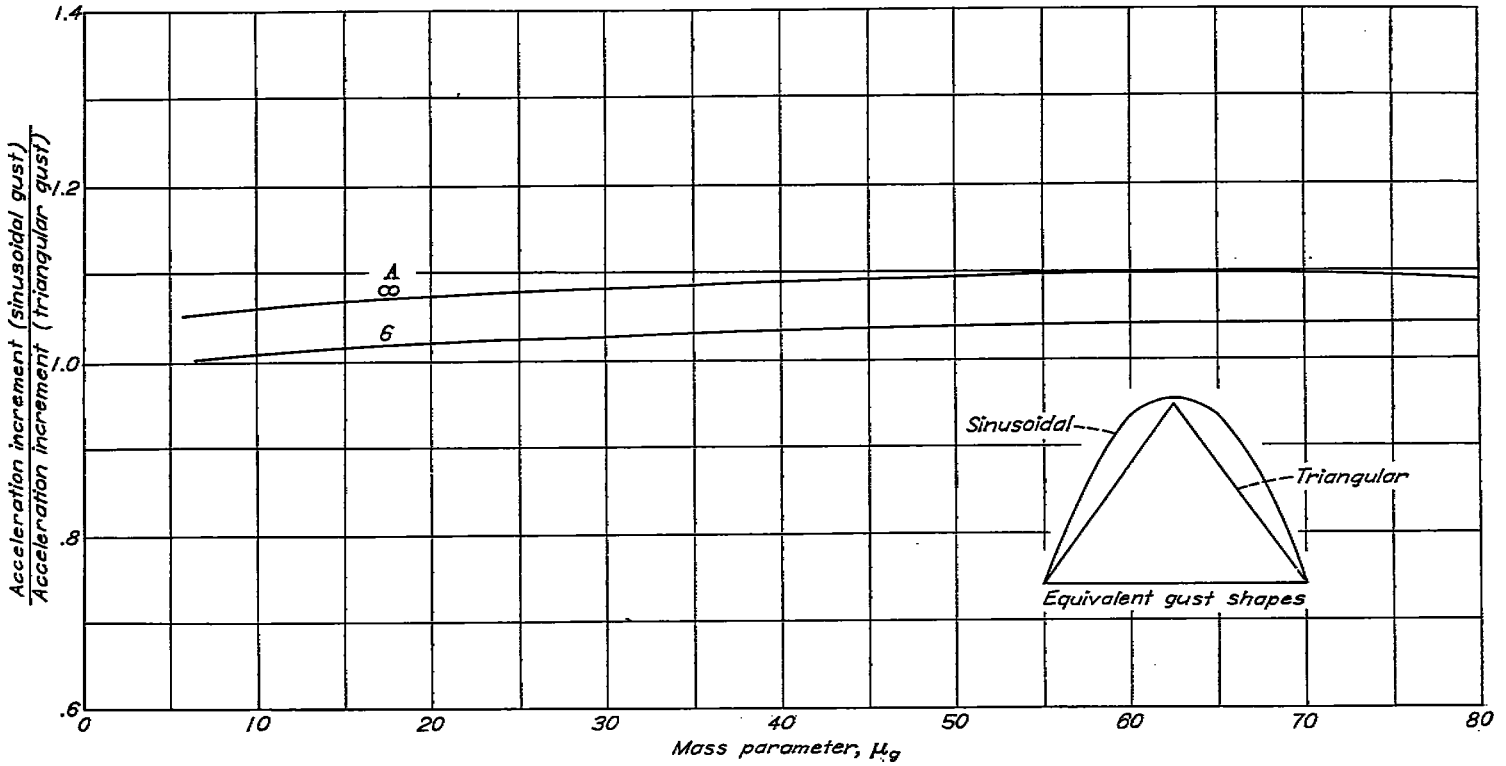

FIGURE 40.—Relative response of an airplane encountering sinusoidal and triangular gusts as a function of mass parameter.

flying wing were made with the center of gravity at 20 percent of the mean geometric chord. The acceleration increment, forward speed, gust velocity, and pitch of the model were measured during each test flight. The tests consisted of a series of five or more flights of the airplane at a forward speed of 40 miles per hour through vertical gusts with gradient distances of 0, 8, and 16 chords. The test results have been included in table XIII and are shown in figure 38 (a). The test conditions for the canard airplane have previously been reported in reference 15. The pertinent characteristics of the model have been included in table XI and the results of the experiments are given in table XIV and in figure 38 (b).

A few flight tests have been made to obtain data on the behavior of an airplane subjected to unsymmetrical gusts and on the gust loads on the vertical and horizontal tail surfaces. The results for the unsymmetrical gusts have been discussed previously in the section entitled "The Structure of Atmospheric Gusts" and indicate reasonable agreement between calculation and experiment. The results of investigations of gust tail loads on the 0–2H and XB–15 airplanes are given in table XV as ratios of the effective gust velocity on a tail surface to that determined for the wing. The XB–15 airplane is shown in figure 6 and described in the section on gust structure and the general characteristics of the 0–2H airplane can be found in reference 34. Because of the use of improved instruments, the results from work with the XB–15 airplane are considered better than those obtained on the 0–2H airplane.

DISCUSSION

Wing area.—The results presented in figures 35 and 38(b) show good agreement between experiment and the detailed calculation based on net wing area. If gross area were used, the calculated values would be higher than the experimental values for a sharp gust. For a gradient gust the reverse would be true since the amount of alleviation due to pitch would be increased. A similar result applies to the canard airplane of figure 38(b) as indicated by table II of reference 15, which shows a decrease in acceleration of 30 percent for a gradient distance of 16 chords ($A=\infty$).

Mass parameter.—Analytical studies that are based on extensive equations indicate that the mass parameter is the significant variable in that it affects the amount of alleviation due to vertical motion. The mass-parameter term has a negligible effect for a sharp-edge gust but is important for long gradient distances. This result is due to the fact that for a sharp gust the airplane does not acquire much vertical velocity, but in a long gust the vertical velocity approaches the gust velocity.

In addition to its effect on the vertical motion of the airplane, an increase in the mass parameter for a given airplane, by increasing the gross weight, unexpectedly increases the alleviation of the total wing load due to pitch. (See fig. 36.) As the mass parameter increases, the resistance of the airplane to rotation would be expected to increase and therefore the amount of pitch and the alleviation due to the pitching motion would be decreased. The result just noted

arises from the fact that the pitching moments on the airplane arise not only from the action of the gust but also from the vertical motion of the airplane. By reducing the vertical motion of the airplane, the adverse pitching moment is decreased, and thus the favorable effect predominates and provides more alleviation.

In some cases, such as in computing the factor K, wing loading instead of mass parameter has been taken as the significant variable. Such a substitution presumes a fixed relation between wing loading and mass parameter. Figure 39 indicates that this substitution may result in either underestimation or overestimation of imposed acceleration increments. The answer in any case depends on the relation between wing loading and mass parameter. Figure 39 shows that the substitution of wing loading appears satisfactory for transports but results in too-low acceleration increments for personal airplanes and too-high values for flying boats.

Phase lag.—The data from the general analysis were utilized to obtain the lag in chords of the acceleration peak behind the flat-top-gust peak. Figure 41 shows that the lag is primarily a function of the gradient distance for a given mass parameter although some variations due to the tail area and tail length are noted. No effect due to a variation in the center-of-gravity position from 15 to 35 percent of the chord is noted. The results indicate that, for a mass parameter of approximately 10, the lag in the gust peak could be as much as 2 chords for an 8- to 10-chord gust. Computations indicate that this lag increases to 3 chords for a gradient distance of 8 chords when the mass parameter is about 30.

In the calculations for the triangular and sinusoidal gusts, the lag of the acceleration peak behind the gust peak for infinite mass parameter, the most adverse case, does not exceed 2 chords. The effect of the phase lag of the acceleration behind the gust can probably be neglected since, for many calculations of acceleration increments and load factors, a change of 1 chord in 8 has a negligible effect on the acceleration ratio.

Static margin.—Figure 34 indicates that the total wing load on a conventional airplane decreases with increasing stability and increasing gradient distance because of the resulting increase in pitch. The figure also shows that the method of obtaining a given static margin is more important than the actual value of the static margin. The results for tailless airplanes are discussed in the following section.

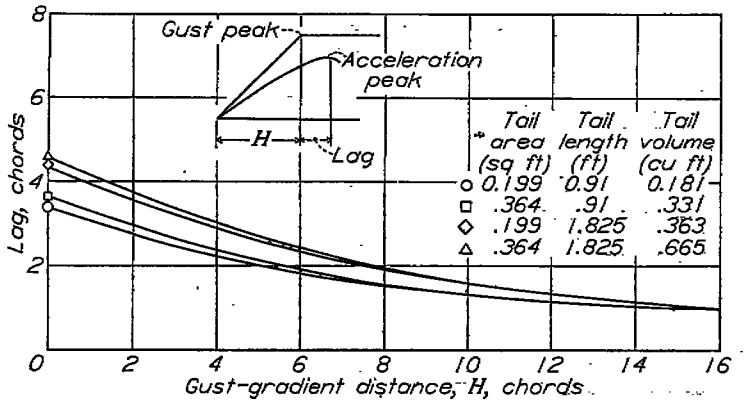

FIGURE 41.—Lag of acceleration peak as function of gust-gradient distance for a flat-top gust. Center of gravity, 15 to 35 percent mean geometric chord.

Although no data are available for canard airplanes, a comparison of figures 38(b) and 32 (both airplanes have the same static margin) show a marked effect on the acceleration increment due to the radical change in configuration. From the results obtained, it is concluded that the effect of airplane pitch on the wing load cannot be specified by static margin alone.

Center-of-gravity position.—Inspection of figure 34 indicates that, for a given configuration, the alleviation due to pitch varies almost directly with the center-of-gravity position. The rate of change of pitch effect with center-of-gravity position is roughly independent of the configuration for the conditions analyzed and depends mainly on the gust-gradient distance. For a gust with a gradient distance of 8 chords, figure 34 indicates that a 1-percent change in center-of-gravity position gives a 1-percent change in load factor. The change in load is doubled for the gust with a gradient distance of 16 chords and about halved for a sharp-edge gust.

The results shown in figure 34, which are for a single value of the mass parameter, and those presented in figure 36 indicate that the effect of pitch on the gust load factor will increase as the mass parameter is increased. Figure 36 shows that for a mass parameter of 10 a 1-percent change in center-of-gravity position represents about a 1-percent change in load factor; whereas tripling the mass parameter to a value of about 30 increases the rate of change in the total wing-load increment 2 percent for each 1-percent shift in center-of-gravity position.

The tailless airplane for which calculations were made had a mass parameter of about 26, and a 1½-percent increase in load for a 1-percent rearward movement of the center of gravity for 8 chords was indicated (fig. 38 (a)), which is in fair agreement with the curves shown in figure 34 for the conventional airplane. Although the analysis is crude, the results indicate that, for both the conventional and tailless airplanes, the effect of the center-of-gravity position is about the same. Consideration of figure 34 indicates that, although the center of gravity is significant in determining the changes in load on the airplane, the center-of-gravity position is not significant in setting the absolute level of the total load for any particular airplane.

Tail volume.—The two middle lines of figure 34 for approximately equal tail volume indicate that this quantity by itself is not of prime importance. Inspection of the results for a gradient distance of 8 chords shows that for equal tail volumes but different tail lengths a variation of 10 percent in the effect of pitch on the applied wing load increment can be obtained for a given static margin. For similar conditions and a gust with a gradient distance of 16 chords, the change in load increment is about 20 percent. A change in tail volume obtained by increasing the tail length and reducing the tail area results in higher loads on the airplane.

The results shown in figure 34 for the same static margin indicate that the change in tail area does not yield significant variations in load; whereas the change in tail length results in a significant modification of the amount of wing load imposed on the airplane. The data thus indicate that, for the maximum alleviation of load by means of pitch of the airplane, a short tail length and large tail area appear to be most beneficial, although the combination will probably lead to an uncomfortable ride due to the violent pitching motion of the airplane. The use of a small area with a short tail length will yield results not too different, although the reduction of damping in pitch may emphasize the pitching oscillation to the detriment of passenger comfort and control of the airplane in continuous rough air.

On the basis of these analytical results, it is concluded that the tail volume is a secondary factor in establishing the level of wing load. The results indicate that the larger the tail length for a given static margin the greater the load imposed on the wing. For a gradient distance of 8 chords the effect on the total wing load due to the various elements of configuration can vary from 10 to —20 percent.

Piloting and continuous rough air.—Previous analytical and experimental studies were made for a single gust isolated in space and with elevator fixed; whereas airplane flights are in continuous rough air with a pilot modifying the reactions of the airplane. Although there are few available data covering this condition, on the basis of statistical analysis, significant differences have been found to exist between pilots and between airplanes of the same type. The effect of different pilots was as much as 20 percent and differences between airplanes were 5 to 10 percent. It appears from these results that the pilot is more important than the variation between airplanes of the same type in determining the loads applied to the airplane. The variation due to both factors is estimated to average 15 percent.

Little or no correlation between the maximum angular motions of an airplane and the maximum loads in the same traverse has been found. It was found in another flight test that one pilot moved the controls five times as often as another pilot and no significant difference in the loads imposed was found. These results led to the conclusion that the effect of the pilot on the imposed load is due to his past actions and is not directly related to the effect of any single gust.

At the present time the question of the effect of piloting and airplane motion in continuous rough air on the prediction of gust load factors is only being approached. The redeeming feature at present is the fact that the evaluation of flight load experience under actual operating conditions will include piloting effects for the airplanes tested. The question still to be answered is whether data on piloting effects taken in the past on older types of airplanes are valid for modern high-speed airplanes flown by pilots with different training and with airplanes designed for different requirements of flying qualities and stability.

Unsymmetrical gusts and airplane response.—Little is known concerning the response of airplanes under the action of a gust which strikes only one wing. The only material available is empirical in character and has been previously presented in this report in connection with the studies of gust structure. In that material it was indicated that calculation by a simplified method, neglecting the alleviation effects of motion, would have to be adequate until more information concerning the significant parameters and the motions of the airplane is obtained.

Horizontal tail loads.—The results given in figure 37 indicate that the static margin and the tail volume are not of primary importance in the determination of tail load. The data indicate a reasonably ordered variation of tail load with center-of-gravity position. The magnitude of the tail load varies rapidly with gradient distance, the variation ranging from about 50 percent for a gradient distance of 0 chords to 0 percent for a gradient distance of 16 chords. Inspection of tables XII (a), XII (b), and XII (c) indicates that the decrease is due mainly to the increasing importance of the effect of pitch-angle increment as the gradient distance is increased and due to the fact that the total tail load is composed of one large term due to the gust, to which is added many small contributions from various sources which may be of either sign. The net result is that the tail load is, in many cases, small and equal to some of the small components. The calculation of the tail load thus requires an extremely high degree of accuracy in order to obtain an accurate answer.

As previously noted, the material presented in figure 37 and table XII shows the tail load at the time of maximum airplane acceleration. It is thought that the maximum tail load may result from a different sized gust than that which is critical for the wing or it may occur at a different time than at maximum acceleration. In view of the many uncertainties in the calculation of tail loads due to gusts, it has been suggested from time to time that the tail load be calculated as the increase in lift due to the gust alone multiplied by the factor $1-\frac{d\epsilon}{d\alpha}$. A slightly different concept would be to assume the gust velocity equal to about half that on the wing.

The few experimental data that are available from flight tests appear to be in essential agreement with the preceding suggestion. Table XV indicates that the ratio of the effective gust velocity on the tail as determined from tail-load measurements to the effective gust velocity for the wing is equal to 0.53 and 0.64 for the XB–15 and 0–2H airplanes, respectively. The results compare favorably with an estimated value for $1-\frac{d\epsilon}{d\alpha}$ of 0.5.

In the case of the canard airplane, inspection of the data in table XIV indicates that for a gust with a gradient distance of 8 chords the effects of pitch and vertical motion cancel so that the total stabilizer load is approximately equal to the load that would be imposed on the tail surface due to the gust

alone. For the longer gradient distance of 17.5 chords, the cancellation is not complete, and the total tail load amounts to about two-thirds of the tail load resulting from the action of the gust. For the practical case, calculations of the horizontal tail load for canard airplanes might be based on the lift due to the change in angle of attack resulting from the gust if both the vertical motion and pitching motion of the airplane are neglected.

In summary, the available results indicates that it is not possible by means of detailed calculations to obtain an accurate estimate of the horizontal tail load due to the action of the gust. The tail load on the horizontal surfaces can be best estimated as the tail load due to the gust alone multiplied by the factor $1-\frac{d\epsilon}{d\alpha}$. For the canard airplane, the downwash factor would be assumed to be zero.

Vertical tail loads.—The suggestion has been made that alleviating effects be neglected in the calculation of vertical tail loads due to the action of side gusts. On this basis, the effective gust velocity for the vertical tail would be related to the vertical velocity for the wing by the relation

$$U_{e_{vertical\ tail}}=\frac{U_{e_{wing}}}{\left(\frac{\Delta n}{\Delta n_s}\right)_{airplane}}$$

The experimental data in table XV show excellent agreement between the ratio of effective gust velocities and the reciprocal of the acceleration ratio. The relation given is equivalent to the calculation of the vertical tail load for a true gust velocity with no alleviation due to unsteady-lift effects or airplane motion. The suggestion appears satisfactory and it would presumably also apply to the vertical tail on the canard airplane.

Steady lift in contrast to unsteady lift.—Consideration of the equations of motion for steady and unsteady flow indicates that the use of steady-flow lift functions for generalized studies of gust-load problems is not warranted. The ratio of the "steady-flow" acceleration to the "unsteady-flow" acceleration in the same gust is

$$\frac{\Delta n_{steady}}{\Delta n_{unsteady}}=\frac{1-\frac{1}{\mu_g}\int_0^{s_1}\Delta n(s)\,ds}{C-\frac{1}{\mu_g}\int_0^{s_1}C_{L_\alpha}(s_1-s)\,\Delta n(s)\,ds}$$

where C is the unsteady lift coefficient for a gradient gust. For infinite mass parameter, the ratio of accelerations varies from infinity for zero gradient distance ($C=0$ at $H=0$) to 1.0 for infinite gradient distance (steady flow, $C=1.0$). The variation with mass parameter would not be so drastic because it affects only the alleviation term, but, since the integral in the denominator contains an unsteady-lift function, considerable deviation would be expected at small values of mass parameter. Therefore, the trends indicated by steady-flow calculations are not necessarily expected to be those for unsteady lift calculations.

The calculated results shown in figure 38 (b), in which the unsteady-lift functions for $A=6$ and ∞ were utilized, indicate the importance of unsteady-lift-curve shape at large gust-gradient distances. As indicated in the figure, for gradient distance of about 18 chords, the substitution of unsteady-lift functions of aspect ratio 6 for those of aspect ratio ∞ changed the calculated acceleration increment by 50 percent. It is apparent that, in the case in which the pitching motion of the airplance is significant and the detailed response of the airplane is to be calculated, minor changes in the unsteady-lift functions themselves can lead to serious discrepancies. The neglect of unsteady-lift relations should involve more radical deviations than the substitution of one unsteady-lift function for another and does not appear to be valid.

Gust shape.—Figure 40 shows that the sinusoidal gust can be substituted for the triangular gust with a small relative error. The curves indicate that the relative error is about 2 percent for a range of mass parameter from 5 to 80, with the absolute error varying from 5 to about 8 percent high. The results indicate, therefore, that the trends predicted for the one gust shape should apply equally well to the other gust shape.

Calculated and experimental results.—Inspection of figure 28 indicates that, for the case in which the pitch effects are negligible, the scatter in computing the acceleration ratio appears to be random and the experimental results fall on each side of the calculated curve. Some of the scatter noted is caused by pitching of the model and some is undoubtedly caused by difficulties in making the experimental measurements. On the whole, the calculated results appear to agree in a satisfactory manner with experiment. Similar agreement is indicated in figures 35, 38 (a), 38 (b), and 32 for $H=0$ where pitch is considered negligible. It is believed, therefore, on the basis of these results, that the unsteady-lift functions, the slope of the lift curve, and similar items involved in the calculations are known with an accuracy comparable to that for other elements of gust-load calculations.

For gradient distances other than zero or for those cases in which the pitch is a factor, the discrepancies between calculation and experiment become larger as the gradient distance increases until, as indicated by figure 35, the errors are serious for gradient distances of 16 to 20 chords. In the case of both the conventional airplanes (fig. 35) and the canard airplane (fig. 38(b)), the calculations for the longer gust-gradient distance are unconservative and lead to smaller predicted load factors. In the case of the tailless airplane (fig. 38(a)) the calculated values are in good agreement. Consideration of the data presented in figure 32, in which the effect of pitch has been neglected in the calculations, indicates that the neglect of pitch for the longer gust-gradient distances will be conservative. The good agreement for the tailless airplane (fig. 38(a)) at all gradient distances compared with the variation in agreement between calculation and experiment for the other cases indicates that the introduction of the tail surface and possibly the fuselage has much to do with the adequacy of the detailed calculations of airplane response to a gust. The errors indicated for the longer gust-gradient distances as compared with the sharper gust indicate that the pitch effect is probably the least accurately predicted quantity and, therefore, leads to the errors noted.

From the results obtained it appears that the wing load due to a gust can be calculated within 10 percent for gradient

distances up to 10 chords. The accuracy in any individual case or for large gradient distances cannot be estimated because of pitch and secondary effects that may be significant but are not recognized until test results are available. Minor changes in variables such as downwash can lead to serious variation of numerical results, and the estimation of loads by detailed or extensive calculations is not of sufficient accuracy to warrant much confidence in the results.

ELASTIC-AIRPLANE REACTIONS

Since the loads imposed when airplanes encounter gusts are applied suddenly, the dynamic response of the airplane structure has been of concern since the initiation of gust-load studies. A number of studies (references 2 and 35 to 40) have been made at various times to evaluate the importance of dynamic response and of the various parameters involved. In 1939, projected airplane designs indicated that dynamic response might be of concern and an analytical and experimental study was undertaken. The results of this investigation are presented in reference 38.

In this section the results obtained in reference 38 are summarized as well as some results from unpublished studies. The significance of dynamic response and the importance of the various parameters in producing dynamic responses in airplane structures are of chief concern.

METHODS

The analytical method developed in reference 38 was to reduce the airplane structure to an "equivalent" biplane whose upper wing had the same motion as the original wing tip and, by using an effective damping factor instead of unsteady-lift functions, to obtain two simultaneous linear differential equations. The equivalent biplane, in which the upper wing is connected by springs to the lower wing-fuselage combination, is adjusted so that the components have the same motions as the wing tip and fuselage of the airplane under study. The equivalent system must include the proper distribution of aerodynamic forces as well as inertia and elastic forces. The deflection of the upper wing of the biplane is taken as a measure of dynamic stress. The dynamic-stress ratio is defined as the ratio of dynamic to static wing-tip deflections. The static deflection is computed in the same manner as for normal design by including inertia effects but neglecting aerodynamic damping due to vibration of the upper wing.

The spring constant, equivalent masses, and aerodynamic damping for the equivalent system are calculated so that the static and vibration characteristics of the original wing are represented. In general, the following conditions are to be satisfied:

1. The total mass of and the total load on the equivalent biplane should be identical with those of the original airplane.
2. The upper wing should deflect under the equivalent static load the same amount as the original wing tip under its corresponding static-load distribution.
3. The natural frequency of the equivalent system should be the same as that of the original wing.
4. The kinetic energy of vibration of the upper wing should closely approximate that of the original wing for the same tip amplitude of vibration.
5. The damping coefficient of the upper wing should represent, at least up to peak load, the damping of the motion of the original wing.

The shape of the forcing function used in the calculations of reference 38 was obtained from accelerometer records of gust-tunnel tests of different models by subtracting the computed acceleration increment due to vertical motion. This procedure was followed since the prediction of airplane reactions as affected by stability and other factors is of doubtful accuracy, as previously noted. For representative gust sizes ($H=0$ to $H=20$ chords) it was found in reference 38 that a curve of the form Ate^{-bt} was a good representation. The forcing function for the complete airplane was then divided so that the upper wing of the equivalent biplane would have the same static deflection as the original wing tip.

In addition to and as a check on the method of calculation, tests were made in the Langley gust tunnel with a model having two wings of different frequencies. The wing deflection and fuselage acceleration were the primary quantities measured. The model used is shown diagrammatically in figure 42 and its characteristics together with the test conditions are given in table XVI.

For each of the two wing frequencies tests were made at one forward speed and three gust sizes. Time histories of pitch, acceleration increment of the fuselage, and wing deflection were obtained. Some results of the tests are shown in figure 43, in which the maximum wing-tip deflection per unit acceleration increment is plotted for one wing as a function of gradient distance.

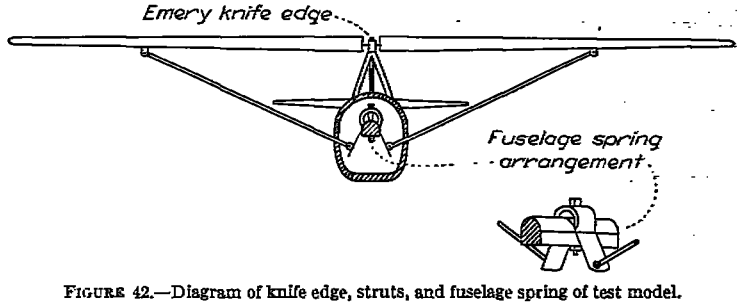

FIGURE 42.—Diagram of knife edge, struts, and fuselage spring of test model.

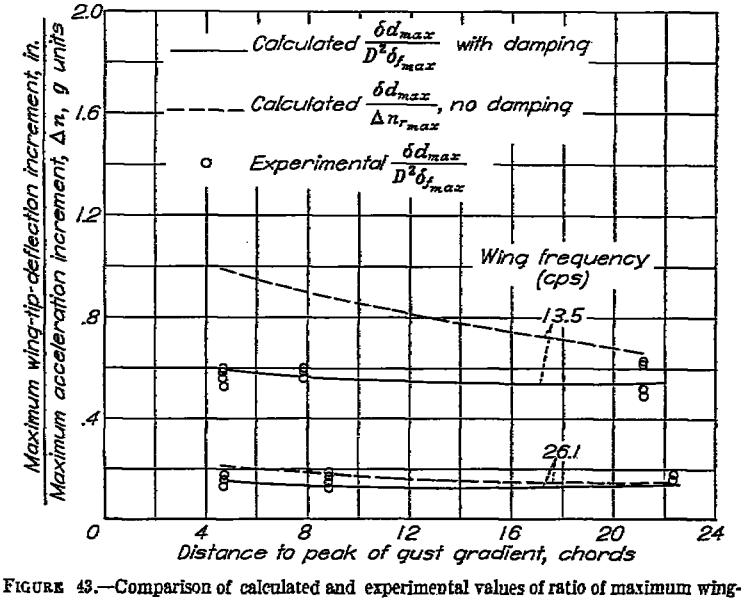

FIGURE 43.—Comparison of calculated and experimental values of ratio of maximum wing-tip-deflection increment to maximum acceleration increment for change in gradient distance.

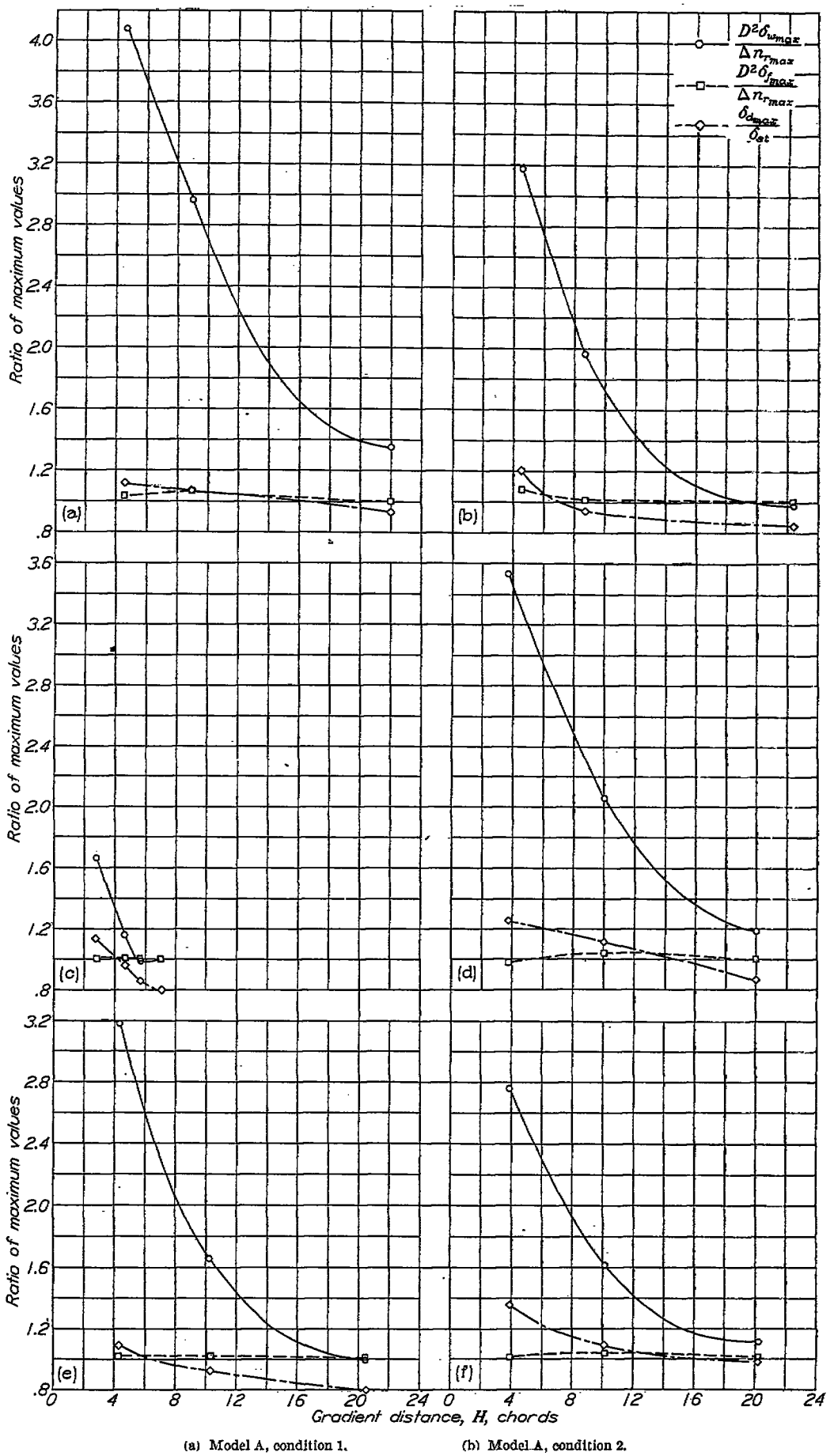

(a) Model A, condition 1.
(b) Model A, condition 2.
(c) Model B, condition 1.
(d) Model C, condition 1.
(e) Model D, condition 1.
(f) Model D, condition 2.

FIGURE 44.—Variation of ratio of maximum dynamic response to static response with gradient distance.

The analytical procedure described in reference 38 was utilized to compute the response of the system when damping of the motion is included and when aerodynamic damping is neglected. The results have been included in figure 43 for comparison with experiment.

ANALYTICAL STUDY

In order to determine the effect of the various parameters on dynamic response, a series of calculations was made at three gust-gradient distances for four airplanes. The characteristics of the airplanes, which were designated as A, B, C, and D, are given in table XVII. The parameters studied were the wing stiffness, airplane weight, and forward speed; and all damping was neglected. The gust velocity was not varied since ratios of dynamic to static conditions were utilized, and it was not a factor for linear equations. The conditions used in the calculations are given in table XVII.

The calculated results for each airplane of the maximum deflection ratio, wing-tip acceleration ratio, and fuselage acceleration ratio are shown in figure 44.

DISCUSSION

Inspection of the results of figure 43 indicates, in general, that dynamic response is overestimated when damping is neglected; whereas the inclusion of damping leads to fair agreement with the experimental results. The results obtained were not sufficiently accurate to provide an absolute check of the calculation. The results do indicate, however, that the calculations give a fair prediction of the ratio of maximum wing deflection to maximum fuselage acceleration.

Time histories given in reference 38 but not shown herein indicate that the method of calculation did not predict correctly the amplitude of the wing oscillations after passing the peak load. The result is due in part to the fact that the damping coefficient was adjusted to give a good estimate for the first wing motion and would be overestimated for the subsequent vibratory motion. Putnam (reference 39) attempted to resolve this difficulty when he extended the method of reference 38. Another possible factor is that the simplifications used are still too drastic. Other results (reference 38) indicate that the use of a constant damping factor is reasonable if its magnitude is adjusted for the average effect of unsteady lift.

Inspection of figure 44 indicates that the dynamic-stress ratios $\delta_{d_{max}}/\delta_{st}$ and wing-tip acceleration ratios $D^2\delta_{w_{max}}/\Delta n_{r_{max}}$ increase as the gradient distance decreases. Recent calculations for more modern aircraft bear out this result and indicate that elastic response is becoming increasingly important. The fuselage acceleration ratio $D^2\delta_{f_{max}}/\Delta n_{r_{max}}$ did not appear to differ greatly from 1.0 and does not appear to be seriously affected by gust size.

The calculations shown in figure 45 for the effect of wing stiffness on the dynamic-stress ratios indicate that, at the "critical" gradient distance of 10 chords, the high-frequency wing shows a dynamic-stress ratio of 14 percent below the low-frequency wing. Further analysis is needed before a definite conclusion can be reached that a reduction of wing frequency by changing wing stiffness tends to increase the dynamic-stress ratio at any gradient distance.

The results given in figure 46 illustrate the variations of the three ratios due to increasing the forward velocity of model C from 200 to 400 miles per hour. The increase in velocity together with the corresponding increase in the rate of application of the gust load would appear to result in an increase in the dynamic-stress ratio. Figure 46, however, shows that the dynamic-stress ratio does not vary much as the speed increases and this lack of variation is thought to be caused partly by the increase in aerodynamic damping with speed. Although the results for the fuselage acceleration ratio show little effect of speed, the wing-tip acceleration ratio increases from about 1.8 to 2.5 as the speed is doubled.

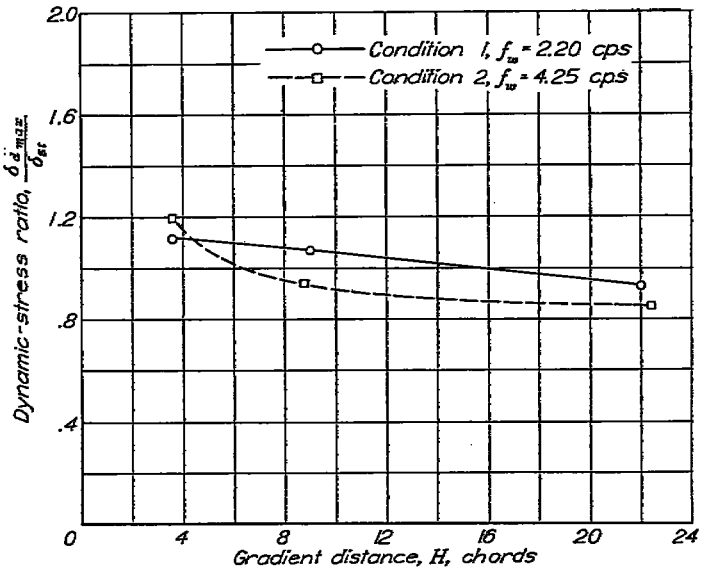

FIGURE 45.—Effect of change of wing frequency due to change of stiffness. Model A, conditions 1 and 2.

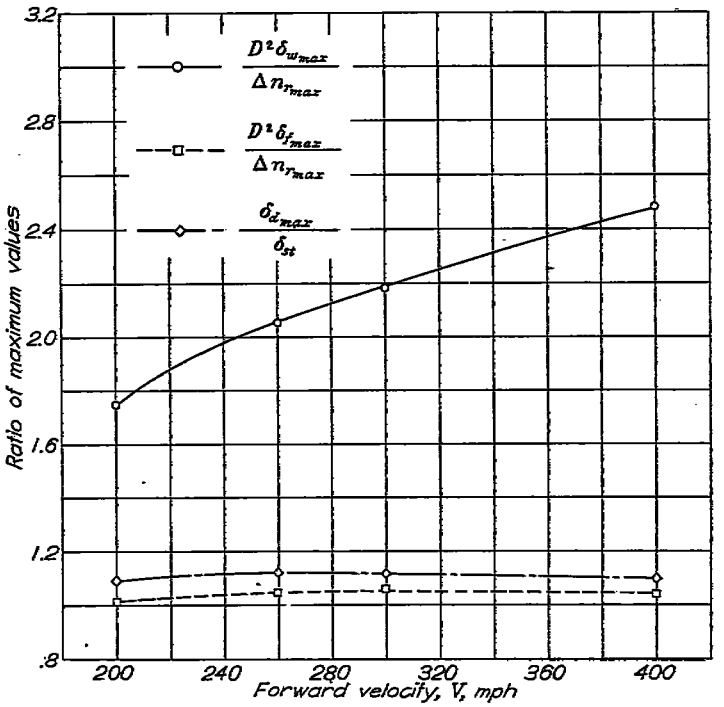

FIGURE 46.—Variations of ratios with change in forward velocity. Model C, conditions 1, 2, 3, and 4.

The calculations for model D were made to show the effect on the dynamic-stress ratio of a change in flight condition from normal gross weight to overload gross weight. Table XVII shows that the forward velocity is different in the two cases, but consideration of the foregoing discussion may justify the assumption that speed has a negligible effect on the findings. The results are given in figure 47 with dynamic-stress ratio plotted as a function of the gradient distance of the gust. A reduction in wing frequency brought about by the addition of mass is shown to result in an increase in the dynamic-stress ratio.

Available information on repeated gusts such as given in table IV has been used (reference 38) to determine the dynamic effects on wing deflection in repeated gusts. The following table (from reference 38) indicates the dynamic-deflection ratios for two gusts of given intensity spaced 25 chords apart. Also given in the table are the deflection ratios for the single gusts of greater intensity which have the same probability of occurrence as the sequence of two gusts used.

Model	Condition	"Design" repeated gusts $\left(\delta_{d\,max}/\delta_{s\,t}\right)$	"Design" single gusts $\left(\delta_{d\,max}/\delta_{s\,t}\right)$
C	1	0.96	1.07
D	1	1.08	.92
D	2	1.10	1.09

The variation in the results indicates that the dynamic-stress ratios for a repeated gust should be investigated. The results also indicate that these dynamic-stress ratios are probably not much greater than those determined for a single gust likely to be encountered in flight.

CONCLUDING REMARKS CONCERNING ELASTIC-AIRPLANE REACTIONS

Study of available results and unpublished data indicates that dynamic response is becoming of greater importance with modern advances in airplane design. As mass tends to be distributed along the wing, more exact solutions are needed and, until the various factors such as unsteady-lift functions, inertia terms, elastic constants, and the spanwise gust distribution are known more exactly, such calculations should be utilized on a relative basis. Although new and more elaborate methods of calculation are available, serious problems still remain as to the basic aerodynamic and elastic coefficients.

OPERATING STATISTICS

A knowledge of gust structure and methods for computing airplane reactions is insufficient for gust-load calculations without knowing the conditions for which load calculations are required. Thus, in order to solve the practical problem of load prediction, the gusts that airplanes encounter and the operating conditions (speed, weight, altitude, and, perhaps, center-of-gravity position) that are likely to exist at the time the gust is encountered must be known. The fact that the source of load, the atmospheric gust, is of a fairly random character and that the operating conditions vary widely make it impractical to predict the exact loads and the associated conditions that are experienced by a given airplane during its lifetime.

METHOD

The general method of obtaining the desired information has been to install instruments in aircraft and to record their experiences and operating conditions without interfering with routine practices. Three procedures have been used: The installation of simple instruments such as the NACA V-G recorder giving broad coverage as to route, airplane type, and time but no detailed information, the installation of special instrumentation for a very limited period of time to obtain information on a particular quantity in detail, and, finally, the installation of fairly elaborate instrumentation controlled by an observer to obtain as much detailed data as possible on several quantities during one or more flights.

The NACA V-G recorder (reference 4) records on a smoked glass plate the normal acceleration as a function of the airspeed at which it was imposed. In use, a record plate is left in the instrument during operations and the resulting clear areas on the glass represents an envelope of accelerations and airspeeds experienced by the airplane.

Standard NACA photographically recording instruments or motion pictures of indicating instruments are used for more detailed measurements.

SCOPE OF DATA

The characteristics and pertinent dimensions of transport airplanes for which gust statistics have been collected are given in table XVIII. The listed values of the limit load-factor increment due to gusts, the high speed in level flight, and the placard do-not-exceed speed were obtained when possible from official sources. For the older airplanes where the design conditions differed from modern requirements, the pertinent speeds and load factors were recomputed according to reference 1 in order to place all the characteristics on a comparable basis.

Table XIX is a summary of the conditions investigated and includes the routes, periods covered, and the amount of data obtained. The operations have been subdivided into prewar, wartime, and postwar periods. For the prewar and

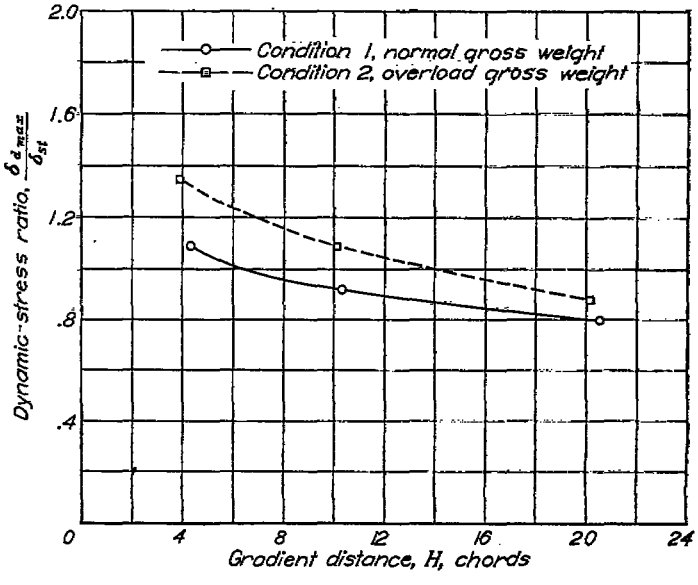

FIGURE 47.—Effect of change of wing frequency due to addition of mass. Model D, conditions 1 and 2.

wartime periods information was obtained with the V–G recorder, but for the postwar period sufficient V–G records are not available. Special studies of speed and Mach number variations are available and some of the results have been included. The material covered in table XIX does not include all the data obtained since scattered V–G data of insufficient scope for analysis have been disregarded.

STATISTICAL METHODS

The random character of gusts and the lack of control over flight conditions have resulted in the use of statistical methods of analysis to smooth data, to eliminate improper weighting, to extrapolate results, and to place data from different sources on a comparable basis. The basic data in most cases are a count of the values of a quantity according to magnitude. Since the application of statistical methods to gust loads is fairly recent, the mass of data collected earlier offers some difficulties because the requirements of statistical analysis were not considered in their collection.

Pearson type III probability distribution curves (see references 41 and 42) have been utilized in the analysis on the assumption that they adequately represent the data on operating statistics. The curve is determined by three parameters: the mean value, the standard deviation, and the coefficient of skewness. In general, the goodness of fit has been based on engineering judgment rather than any test procedure.

An important problem in the study of the frequency of exceeding the larger values of load or speed under operating conditions is the determination of whether observed or estimated differences in frequencies between samples are real or represent limitations of the data. No satisfactory test for this purpose has been found, but a 5:1 ratio of frequencies has been used in reference 43 as an engineering measure. If the differences are less than this criterion, real differences may exist but are considered too small to be determined from the available data.

A serious limitation in the analysis of operating statistics exists since the results are used to predict future operating experience. If no extraneous factor enters, such as changes in design rules, operating regulations, or the introduction of newer airplanes, then the prediction may be satisfactory. Such changes as, for example, the shift from prewar to postwar operations may lead to some uncertainty as to the applicability of a prediction. Predictions assume that the trend in the data has not been affected by new factors. (No method yet is available for evaluating or detecting the effect of changes in the data now used.)

Other questions that occur in statistical analyses arise in connection with the existence or inclusion of data from two different regions or populations as part of the same sample, the presence of absolute and physical boundaries that cannot be exceeded, the effect of extraneous variables, and the effect of gradual transitions from one region to another. The presence of such limitations can have serious results as far as the significance of the results is concerned and such effects cannot always be evaluated or separated. An example of the effect of different regions might be the combination of acceleration data involving flight below maximum lift coefficient and flight above maximum lift coefficient. The aerodynamic characteristics of the airplane and its behavior in the two regions are entirely different. Thus, a sample that combines such data does not offer an adequate means of predicting future expectations of a given acceleration except for the conditions of the original data, since any derived curves are a composite of two independent sets and therefore the prediction can only apply to the same combination.

RESULTS

V-G data.—From the individual V-G records that are summarized in table XIX, frequency distributions of the maximum acceleration increment Δn_{max}, the maximum speed V_{max}, and the speed V_0 at which maximum acceleration increment was experienced have been compiled for the wartime and prewar periods. The statistical parameters—the mean, the standard deviation, and the skewness—are given in table XX, which also includes the values of $V_{0_{max}}$, Δn_{max}, and V_{max} recorded during the period under consideration.

The parameters of the Pearson type III curves given in table XX have been used to obtain the flight miles to exceed the specified values of a selected quantity. The transformation from probability to flight miles was performed through use of a nominal cruising speed and the average flight hours per V-G record. Table XXI gives the flight miles to exceed: (1) the limit load-factor increment, (2) the placard speed of the airplane, and (3) an acceleration increment corresponding to encountering a gust with an effective gust velocity of $37.5K$ feet per second at the most probable value of V_0, V_p. The probable speed V_p has been included in table XXI as a fraction of the high speed in level flight V_L.

Time-history data.—Time histories from the special investigations of the postwar period have been evaluated to obtain the flight miles to exceed the placard speed, the probable speed of flight for each sample, and the distribution of airspeed. Because of the limited duration of the samples, each sample was read to obtain the maximum speed during a fixed interval of time (6 to 10 min) and the resulting frequency distributions were then used to obtain the flight miles to exceed the placard speed. The results are included in table XXI and in figure 48. Figure 48 presents the percent of total flight time spent at speeds equal to or greater than any selected fraction of the high speed V_L. The probable speed noted in table XXI for airplanes E and F is the probable speed of flight and is not, as in the case of other airplanes, the probable speed at which maximum acceleration will occur. A simple analysis in which the velocity-acceleration envelopes were synthesized from the speed-frequency-distribution data and the gust-frequency data of reference 9 indicated that the probable speed for maximum acceleration was about $0.03V_L$ greater than the probable speed of flight.

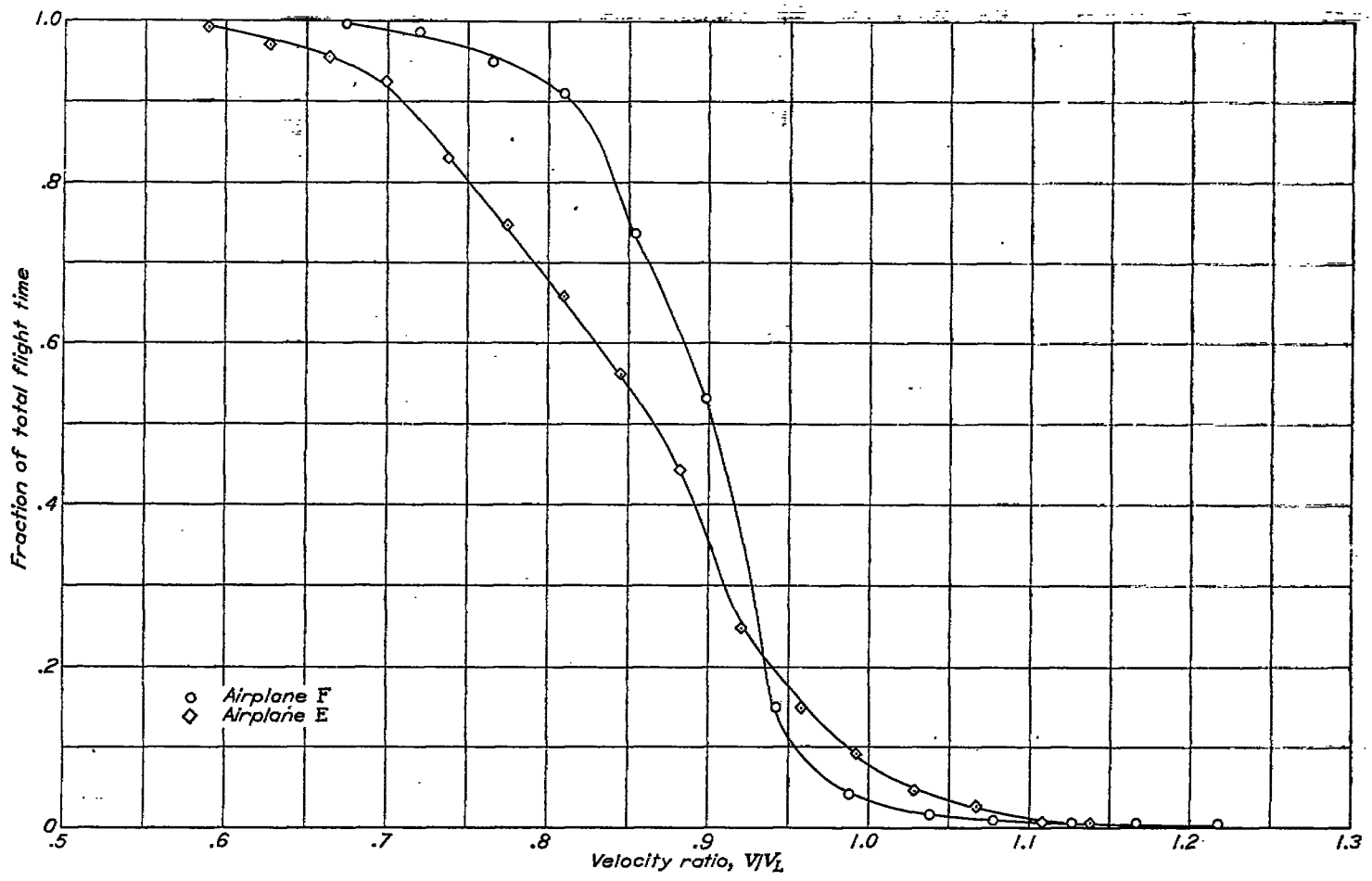

FIGURE 48.—Fraction of flight time spent at speeds equal to or greater than selected values during airline operations.

The data obtained have also been evaluated according to flight condition to obtain curves of the flight hours required in climb, cruise, and descent to exceed given values of speed. Figure 49 is typical of the results obtained for airplane E.

Disturbed motions.—From the data obtained in the special investigations a statistical study has been made of other quantities of interest in gust-load studies, such as the effects of disturbances on the relative frequency distribution and the fraction of the time spent in rough air.

Some question has arisen as to the effect of the selected datum on the frequency distributions obtained in continuous rough air. This question is partly answered by the tests reported in reference 9 on one of the roughest flights with the XC–35 airplane where the relative gust-frequency distribution was determined by using a disturbed datum and an arbitrary 1 g datum. The results of the study are given in figure 50.

Camera records of the pilot's instrument panel in the XC–35 airplane have been evaluated to obtain the relative frequency of occurrence of the maximum total variations in the angular displacements of the XC–35 airplane during separate traverses through clouds. The results are summarized in figure 51 as the relative frequency of exceeding selected values of yawing, rolling, and the pitching displacements and the rate of turn. It should be noted in considering this figure that the quantity plotted is the sum of the maximum positive and the maximum negative values recorded during each cloud traverse.

Path ratio.—The available data for prewar transport operation given in reference 9 indicate that the path ratio (the miles of rough air divided by the total miles flown) varied from 0.24 to 0.006 for different routes in the United States and abroad and had an average value of 0.1. Since, on the average, $500/\overline{c}$ gusts with an effective gust velocity greater than 0.3 foot per second are encountered per mile of rough air (reference 9), the number of gusts that will be encountered on the average during the lifetime of an airplane can be estimated. No path-ratio data are available for postwar operations. Attempts to obtain such data from the indirect evidence of V-G records lead to erroneous results.

DISCUSSION

Applied acceleration increments.—For the prewar period, table XXI shows a wide scatter in the flight miles to exceed the limit acceleration increment. The values vary by a factor of about 300. A variation by a factor of 42 occurs for the same type of airplane operated on different routes by different airlines. In four out of six samples, the flight miles to exceed the limit acceleration increment would be greater than 13 million, or, if a cruising speed of 200 miles per hour is assumed, it might be expected that the limit load factor would be exceeded about once on the average in every 60,000 hours of flight.

The data for the wartime period do not show as much variation of flight miles and the variations do not appear significant within that group. In comparison with the prewar

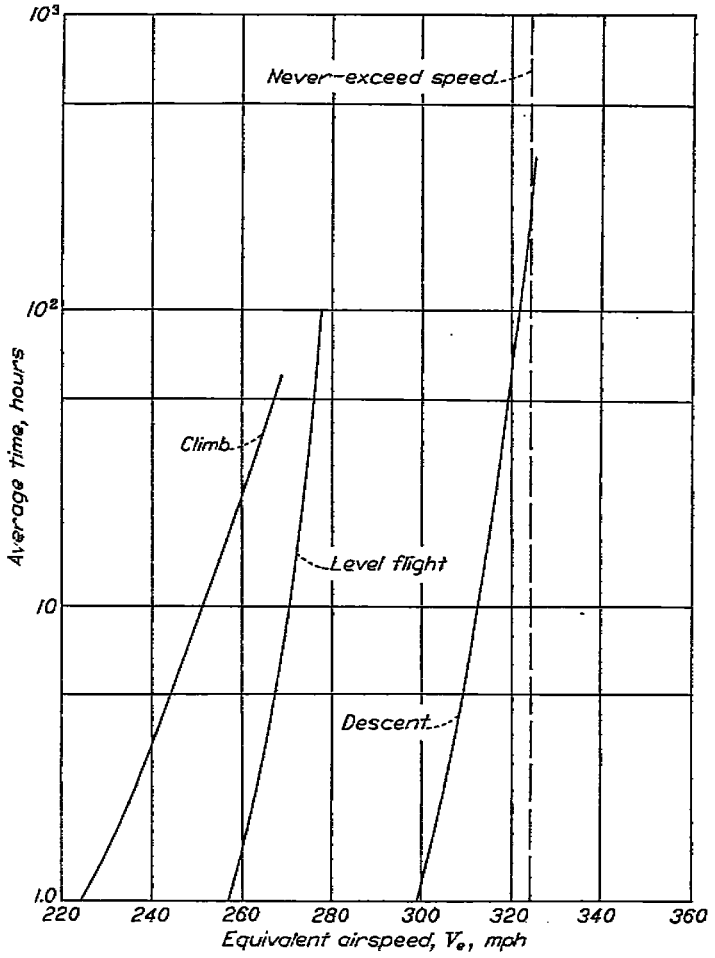

FIGURE 49.—Average time required to exceed a given value of airspeed. Airplane E.

operations, however, the flight miles to exceed limit acceleration have consistently decreased; this fact indicates that the pressure of the emergency on wartime commercial operations resulted in higher imposed loads on the airplane.

Atmospheric gustiness.—The flight miles to exceed the acceleration increment corresponding to an effective gust velocity of $37.5K$ feet per second at the probable speed (table XXI) indicate that the operational experience on the basis of a "gust intensity" shows much less scatter. The spread in flight miles was 15:1 for the prewar operations and about 7:1 for the wartime period. For prewar conditions, when the data for airplane D on route V are neglected, the scatter is within the arbitrary 5:1 criterion and, in comparison with the spread in flight miles for limit acceleration increment, indicates that the difference in the level of roughness encountered on various routes is not of engineering concern. A similar observation is indicated for the wartime period although the smaller average flight miles indicate that flights during that period were through more severe weather conditions than for the prewar period.

In connection with prewar data for airplane D on route V of table XXI, the low value of flight miles shown may be significant and indicates that early trans-Pacific flights encountered more severe weather than was experienced along other routes. When the distances involved in trans-Pacific operations and the lack of weather ships in this period are considered, more frequent accidental encounters with

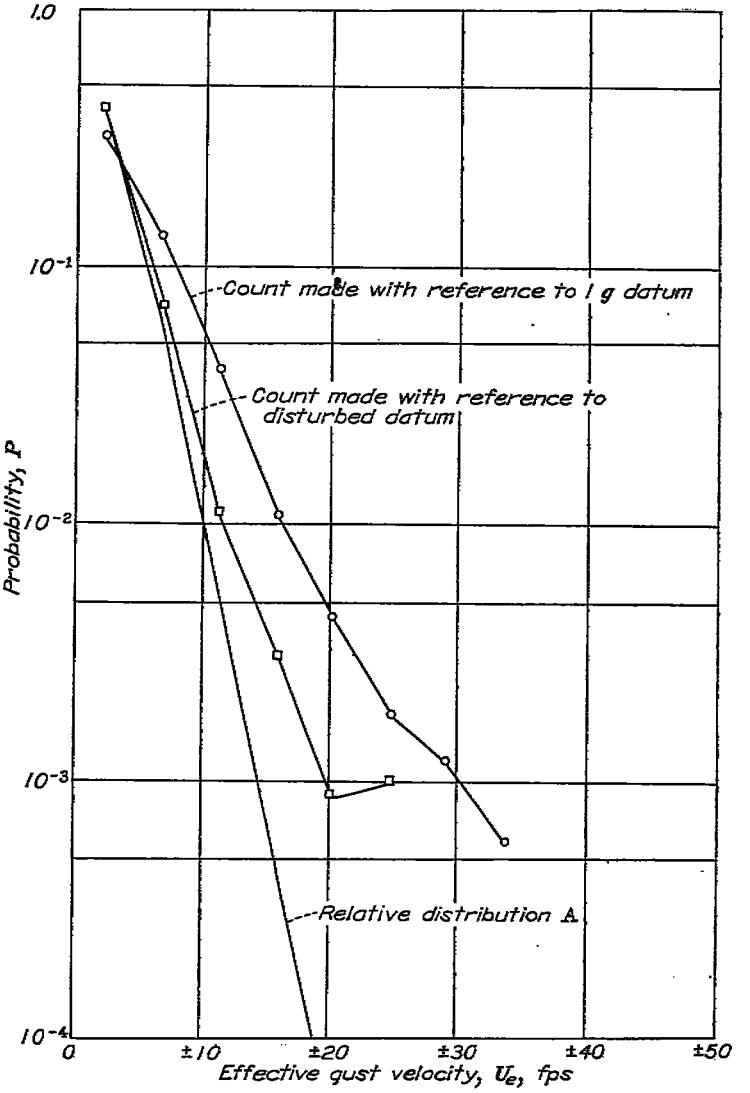

FIGURE 50.—Influence of disturbed motion of XC-35 airplane on apparent gust frequency distribution in very rough air.

severe weather might be expected than for the transcontinental routes or operations in more populated regions.

On the basis of the information concerning the flight miles to equal or exceed the acceleration increment corresponding to $37.5K$ feet per second at the probable speed, the level of route roughness is concluded to be largely independent of the route, airplane, or operator. It is not possible at this time to state whether the maintenance of a constant level of roughness is due to dispatching practices, meteorological forecasting abilities, or both.

Frequency of encountering gusts.—The available data on path ratio given in reference 9 indicate a wide spread in values obtained, and at this time an average value of 0.1 seems to be the best estimate available. Since the path ratio is the proportion of the total miles flow that are spent in rough air and the number of gusts per mile of rough air has been found to be essentially constant at $500/\bar{c}$, the path ratio can be defined as the actual number of gusts divided by the total number expected if the total flight path were rough. It should be noted that the path ratio defined by gust counts depends on the threshold (in this case, the threshold is 0.3 fps). When used with a gust count of $500/\bar{c}$ gusts per mile

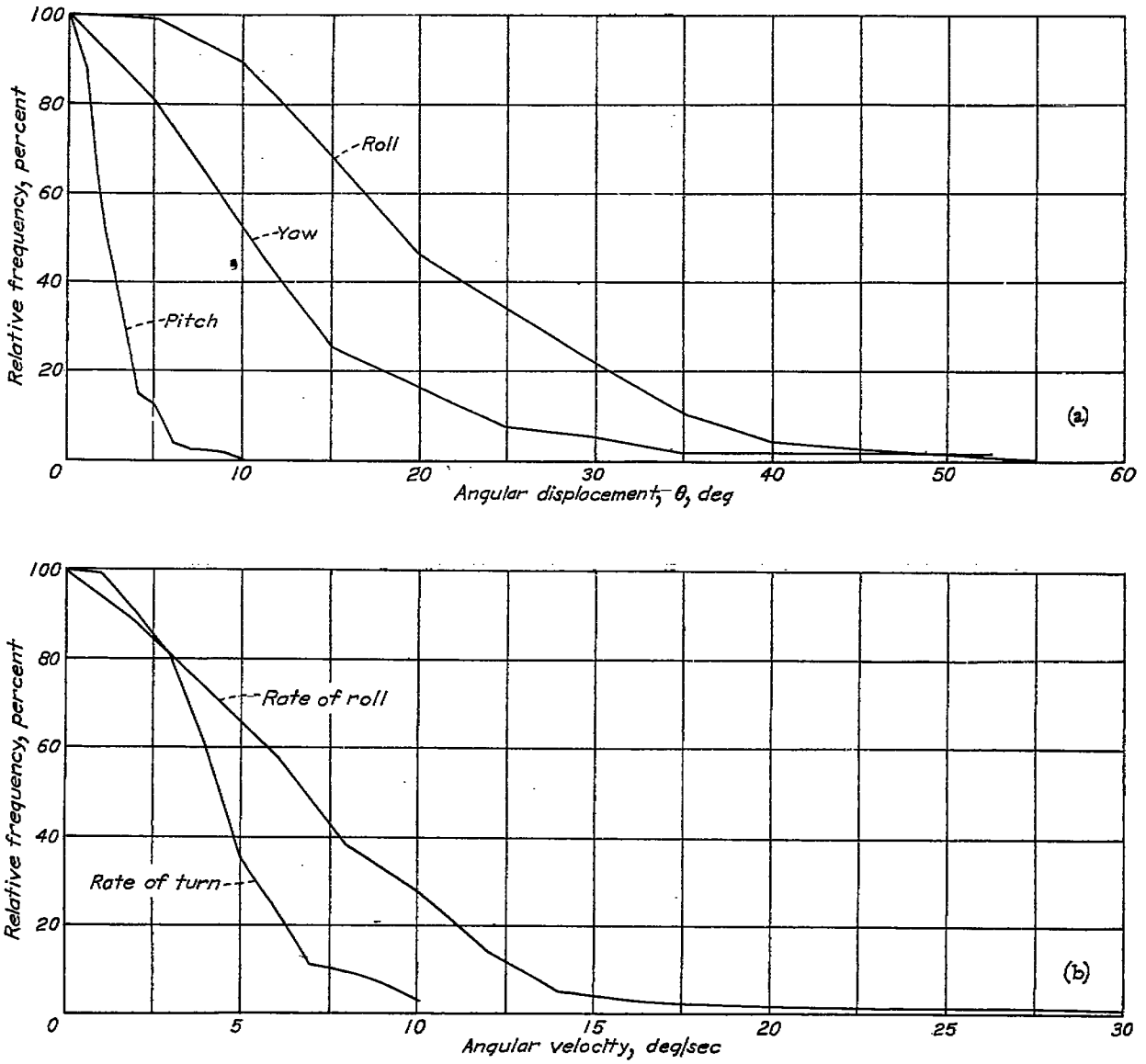

(a) Relative frequency of given values of angular displacement.
(b) Relative frequency of given values of angular velocity.

FIGURE 51.—Relative frequency with which selected values of angular motions will be exceeded in rough air.

of rough air and the gust frequency distributions of figure 8, the recommended average value of path ratio can be used to estimate the probability of an airplane encountering a gust of any specified intensity.

Although no information is available as to the variation of the number of gusts or path ratio with altitude, terrain, or weather, the path ratio would probably decrease with altitude.

Probable speed V_p.—The determination of the miles to exceed $37.5K$ feet per second at the probable speed showed the flight miles to be relatively constant and, therefore, the wide variations in the flight miles for limit load factor might be ascribed to variations in the probable speed. On this basis, the results indicate that the probable speed is important in determining flight miles to limit acceleration increment.

The data on the probable-speed ratio (table XXI) indicate a scatter in the speed ratios for any given period. The speed ratio for maximum acceleration increased from the prewar period to the postwar period for the same airplanes and routes from an average value of 0.75 to about 0.86. It appears that the speed ratio might be a function of the route, airline policy, and the airplane characteristics, but no conclusion can be drawn as to the significant parameters that determine the speed ratio.

Although no data have been analyzed with regard to the imposed gust loads for the postwar period, on the basis of the current design requirements and if the level of roughness is

assumed to remain the same as for the prewar period, the imposed gust acceleration increment for a given number of flight hours will be about 12 percent higher on the average for the postwar period than for the prewar period. Alternatively, the increased probable speed for the postwar period would result in an appreciable decrease in the flight miles to exceed a given acceleration increment.

Maximum speeds.—Inspection of figure 49 indicates that the probability of exceeding a given value of airspeed is a function of the flight condition. Figure 49 indicates that the descent is most important, and for one postwar airplane the placard speed might be exceeded on the average about once in 200 hours in descent. A simple sorting of the data with regard to the smooth air and rough air showed no apparent effect of rough air on the speed tendencies.

For complete flight operations, the data given in table XXI show that the flight miles to exceed the placard speed decreased from many millions of miles during the prewar period to about a quarter of million of miles during the postwar period. The reduction in the flight miles to exceed the placard speed for the postwar period is of considerable significance.

Speed-time distributions.—Figure 48 shows that a relatively higher percentage of time is spent above high speed in level flight than would be expected from estimates made by airline personnel, which estimates have indicated a value of less than 1 percent. The high percentage may be due in part to performance abilities of the airplanes in excess of that indicated by the regulated speeds or due to high-speed descents at the end of flights. Until further information is obtained, the results in figure 48 might be assumed to be representative of postwar operations.

Disturbed motions.—Tolefson (reference 44) showed that the maximum angular displacements of an airplane do not correlate with the maximum intensity of gusts encountered during a given run. The correlation coefficient between the angular motions and the maximum gust intensity was about 0.3. The disturbed motions may depend more on the sequence of the gusts encountered than on the intensity of any individual gust encountered. The data cannot be extended to other flight conditions except by assuming dynamically similar conditions.

Inspection of figure 51(a) indicates that the amplitude of the rolling motion is much greater than either pitch or yaw. Similar results are indicated in figure 51(b) for the angular velocities. The data of figure 51 can be utilized, if dynamically similar airplanes and a constant level of atmospheric turbulence are assumed, to estimate the fraction of the airplane life flown before displacements or angular velocities of the airplane in excess of selected values are experienced.

Relatively little data have been obtained on angular accelerations in rough air and the data for roll are discussed in the section about gust structure. Twenty-one values of angular acceleration in pitch were available from flights of the XB–15 airplane and show that the linear acceleration increments at the tail were 0 to 40 percent greater than the acceleration increment at the center of gravity. The average increase was about 25 percent. If dynamically similar airplanes are assumed, the results can be expressed as an average value of the angular acceleration in pitch for any airplane as

$$\frac{dq}{dt}=\frac{20\,\Delta n}{c^{3/2}}$$

At present, exact estimations of the angular acceleration in pitch are not possible.

The effect of disturbed motions on imposed loads is appreciable and may affect the frequency distribution by as much as 50 percent (fig. 50). A previously mentioned analysis of piloting effects that could be construed as disturbed motion indicated a variation of some 20 percent in the imposed loads. Although such variations cannot be predicted at this time, current methods of estimating loads consider this factor in that the measured flight load experience includes such effects.

RÉSUMÉ

A résumé of the more important findings under gust structure, airplane reactions, and operating statistics is included because of the variety of subjects covered.

GUST STRUCTURE

The gust-gradient distance and gust size are largely independent of weather, altitude, and airplane when expressed in terms of the mean geometric chord. The gradient distance for a vertical gust has a probable value of 10 to 14 chords for the higher gust intensities and is the same for both spanwise and flight directions.

The gust shapes vary widely but triangular or sinusoidal profiles in the direction of flight seem good approximations.

An approximation to the spanwise gust profile for unsymmetrical gusts would be a uniform distribution on which is superimposed a linear variation of gust velocity with equal and opposite gust intensities at each wing tip.

Gust spacing for use in estimating the number of gusts in rough air as a function of gust intensity is about 11 chords for velocities above a threshold of 0.3 foot per second. The spacing is independent of other factors.

Lateral, longitudinal, and vertical gusts have essentially the same characteristics.

The frequency distribution of gust intensities in rough air is independent of altitude and airplane when the gust intensity is expressed in terms of indicated velocity.

AIRPLANE REACTIONS

Aerodynamics.—Although the two-dimensional unsteady-lift functions yield the most satisfactory estimates of the load increments due to gusts for conventional airplanes with fuselages, finite-aspect-ratio unsteady-lift functions appear pertinent for flying wings. For unconventional configurations such as swept wings, strip theory with two-dimensional unsteady-lift functions appears adequate.

The slope of the lift curve for gust-load calculation can be best estimated for engineering purposes by using an arbitrary section value of 6 per radian and simple aspect-ratio corrections. For swept wings, the best estimate of lift-curve slope is obtained by correcting the value for the equivalent straight wing by the cosine of the sweep angle.

Available information on compressibility effects indicates that the unsteady-lift functions would be only slightly affected below the critical Mach number and would tend to disappear for supersonic speeds. At this time, the use of high-speed wind-tunnel data is suggested for estimating the slope of the lift curve.

Rigid-body reactions.—Analysis indicates that the mass parameter is a significant measure of airplane reactions and that the use of net wing area results in best agreement between calculation and experiment. Analyses neglecting unsteady-lift effects are not considered adequate.

No one significant parameter of airplane stability for flight in gusty air has been found. The center-of-gravity position is an important factor for a given airplane and arrangement and tail volume have somewhat less effect. Comparison of experiment and calculation shows that minor differences in the constants used in calculation can vary the agreement from good to poor. Detailed calculations of airplane reactions for estimating loads are not warranted at this time because the accuracy required is beyond the scope of present information.

Available data on horizontal and vertical tail loads indicate that detailed calculations of tail load are not warranted. The lift on either tail surface due to a gust can be estimated apparently by utilizing a true gust velocity and neglecting the alleviating effects of unsteady lift and airplane motion but considering the downwash.

Elastic-airplane reactions.—Analytical and experimental studies indicate that extensive simplifications lead to unrealistic answers and more exact solutions are required as the wing mass becomes a greater fraction of the total mass.

The effect of forward speed on elastic response was negligible, but the wing-tip accelerations increased with speed.

It does not appear feasible to obtain generalized solutions of dynamic response.

OPERATING STATISTICS

The average miles to exceed limit load factor varies widely according to operator and period. A most important factor in setting the level of load appears to be the probable speed—that is, the speed at which maximum acceleration is most likely to be experienced—since the gust experience on all routes was about the same. The probable-speed ratio (ratio of probable speed to the high speed in level flight) is increasing as new airplanes are introduced with a consequent reduction in the average number of flight miles required to exceed limit acceleration increment.

The flight miles to exceed the placard speed has decreased for the newer types of airplanes.

The total number of gusts encountered by an airplane during its life is a function of the amount of rough air flown. The amount of rough air is on the average about 10 percent of the total mileage. The number of gusts encountered in rough air depends on airplane size and an average figure would be $500/\bar{c}$ gusts per mile greater than 0.3 foot per second.

The disturbed motions of an airplane in gusty air do not correlate with the maximum gust intensities experienced. Results indicate that the disturbed motions may change the loads in gusty air by 20 to 50 percent.

CONCLUDING REMARKS

The available information on gust loads does not permit the determination of applied loads under actual operating conditions on an absolute basis. Lack of information on gust statistics, the behavior of airplanes in rough air, transient aerodynamics, and operating conditions make such an estimation of doubtful accuracy. Consequently, the procedure has been to transfer loads data from a reference airplane to new airplanes by using available knowledge of aircraft behavior. Statistical data on flight loads and gust experience under actual operating conditions are collected in order to set the level of loading, and "transfer" coefficients based on a knowledge of airplane reaction are then calculated and applied to new airplanes. No radical change in operating conditions or airplane characteristics are assumed to be introduced. In addition, it is implied that all airplanes are of the same general character (conventional) and that the relative loads for single isolated gusts are a measure of the relative loads in a sequence of gusts. The important features and implications in this procedure are that the same procedures must be used to evaluate loads data as are used in loads calculations. In addition, the procedure presupposes no drastic change in airplane configuration. The use of the same procedures of calculation tends to eliminate errors that are due to inability to predict airplane reactions on an absolute basis in that errors in the evaluation of loads data cancel those in the calculation of loads.

Extensive changes in configuration may be a serious limitation since the procedure assumes in its general application that the effect of pitch on gust loads is the same for all aircraft and that all aircraft respond to the same gusts (as function of airplane size) to experience significant loads. When

new configurations such as tailless airplanes or canard airplanes are considered, the load transfer must be based on the relative motions of the reference airplane and the new airplane and not on the motions of the new airplane alone. A second element—gust selection—has not yet been resolved but it would appear that tailless airplanes, because of small damping in pitch, canard airplanes, because of the adverse initial pitching moment in a gust, and swept-wing airplanes might select some other ranges of gust sizes than those selected by conventional aircraft. So far, no information is available on this problem and it can only be assumed that available gust-structure data are adequate.

In some generalized solutions of load prediction, a further restriction has been introduced by the substitution of wing loading for mass parameter as a significant variable. The use of an alleviation factor based on such a substitution is still further restricted by the assumption that all airplanes have the same relation between wing loading and mass parameter. Information presented on the load transfer coefficient indicates that the load transfer coefficient has appreciable spread when this substitution is made and the spread seems to be a function of airplane type and use since the data can be grouped according to land transports, flying boats, and personal airplanes. If wing loading is used, therefore, different relations should be considered according to airplane class and use.

In cases where the dynamic response may be a factor, it should be considered as an amplifying factor for the incremental loads whether for studies of large loads or repeated loads. Dynamic response should be considered on a relative basis since the uncertainties in calculations due to lack of knowledge and practical simplifications have not been resolved.

Of the many related problems, that of gust-alleviating systems is of great importance. Such systems are of particular interest in reducing loads and improving riding comfort for high-speed aircraft. The two problems may not have compatible solutions since load reduction implies the reduction of stresses in all critical members without impairing other qualities of the airplane, whereas the improvement in riding comfort implies the reduction of airplane motions and accelerations. Although the basic problem of reducing the load due to a single gust is amenable to analysis, the related problems of maintaining other airplane qualities and of determining alleviation in rough air introduce difficulties.

Three fundamental systems of gust alleviation are available and consist of changing airplane characteristics, aeroelastic systems, and aeromechanical systems. The first method consists of emphasizing the pertinent characteristics of the airplane, such as increasing the wing loading to reduce accelerations, decreasing the slope of the lift curve (by use of vents or sweep and by changing the aspect ratio), adjusting the stability characteristics to obtain favorable response in rough air, or using free-floating flaps. Aeroelastic systems generally involve torsional deflections of the wing due to imposed loads. Such systems can be designed by incorporating slant hinges or flaps operated by wing deflections or by the adjustment of the torsional and bending rigidity. Aeroelastic systems have the advantage of being inherent in the construction of the airplane and the disadvantage that they form an additional source of elastic phenomena such as flutter or dynamic response due to a series of gusts. Aeromechanical systems cover combinations of servomechanisms, detectors, and aerodynamic controls. Some detector systems considered are the use of an accelerometer or strain gage to measure accelerations or load and the use of a feeler vane or similar system to detect gust-velocity or angle-of-attack changes. The servo systems are assumed to operate the conventional controls of the airplane or to operate wing flaps or spoilers. The difficulties are those of possible failures of complicated mechanisms, the question of oscillation of the system, the response of repeated gusts, and, finally, the need as airplane speed increases of obtaining a servo system that has a high frequency response (imposed frequencies up to 10 cps). The advantages are flexibility and utilization of many of the available mechanisms.

LANGLEY AERONAUTICAL LABORATORY,
NATIONAL ADVISORY COMMITTEE FOR AERONAUTICS,
LANGLEY FIELD, VA., *August 5, 1949.*

APPENDIX

COOPERATING AIRLINES AND AGENCIES

The following airlines and agencies have cooperated extensively with the NACA in obtaining much of the data used in the preparation of this report:

American Airlines, Inc.
Eastern Air Lines, Inc.
Pan American World Airways System
Trans World Airline, Inc.
United Air Lines, Inc.
Department of Commerce
    U. S. Weather Bureau
    Civil Aeronautics Administration
U. S. Air Force
    Air Materiel Command
    Air Weather Service
U. S. Navy, Bureau of Aeronautics, Structures Unit

REFERENCES

1. Anon.: Airplane Airworthiness. Civil Aero. Manual 04, CAA, U. S. Dept. Commerce, Feb. 1, 1941.
2. Küssner, Hans Georg: Stresses Produced in Airplane Wings by Gusts. NACA TM 654, 1932.
3. Rhode, Richard V., and Lundquist, Eugene E.: Preliminary Study of Applied Load Factors in Bumpy Air. NACA TN 374, 1931.
4. Rhode, Richard V.: Gust Loads on Airplanes. SAE Trans., vol. 32, 1937, pp. 81–88.
5. Küssner, H. G.: The Two-Dimensional Problem of an Aerofoil in Arbitrary Motion Taking into Account the Partial Motions of the Fluid. R.T.P. Translation No. 1541, British Ministry of Aircraft Production. (From Luftfahrtforschung, vol. 17, no. 11/12, Dec. 10, 1940, pp. 355–362.)
6. Lovitt, William Vernon: Linear Integral Equations. First ed., McGraw-Hill Book Co., Inc., 1924, pp. 23–72.
7. Donely, Philip: Effective Gust Structure at Low Altitudes as Determined from the Reactions of an Airplane. NACA Rep. 692, 1940.
8. Donely, Philip, and Shufflebarger, C. C.: Tests in the Gust Tunnel of a Model of the XBM–1 Airplane. NACA TN 731, 1939.
9. Rhode, Richard V., and Donely, Philip: Frequency of Occurrence of Atmospheric Gusts and of Related Loads on Airplane Structures. NACA ARR L4I21, 1944.
10. Tolefson, H. B.: An Analysis of the Variation with Altitude of Effective Gust Velocity in Convective-Type Clouds. NACA TN 1628, 1948.
11. Moskovitz, A. I., and Peiser, A. M.: Statistical Analysis of the Characteristics of Repeated Gusts in Turbulent Air. NACA ARR L5H30, 1945.
12. Moskovitz, A. I.: XC–35 Gust Research Project—Preliminary Analysis of the Lateral Distribution of Gust Velocity along the Span of an Airplane. NACA RB, March 1943.
13. Rhode, Richard V., and Pearson, Henry A.: A Semi-Rational Criterion for Unsymmetrical Gust Loads. NACA ARR, Aug. 1941.
14. Jones, Robert T.: The Unsteady Lift of a Finite Wing. NACA TN 682, 1939.
15. Donely, Philip, Pierce, Harold B., and Pepoon, Philip W.: Measurements and Analysis of the Motion of a Canard Airplane Model in Gusts. NACA TN 758, 1940.
16. Berg, Ernst Julius: Heaviside's Operational Calculus. Second ed., McGraw-Hill Book Co., Inc., 1936.
17. Kuethe, Arnold M.: Circulation Measurements about the Tip of an Airfoil during Flight through a Gust. NACA TN 685, 1939.
18. Donely, Philip, and Shufflebarger, C. C.: Tests of a Gust-Alleviating Flap in the Gust Tunnel. NACA TN 745, 1940.
19. Donely, Philip: An Experimental Investigation of the Normal Acceleration of an Airplane Model in a Gust. NACA TN 706, 1939.
20. Wagner, Herbert: Über die Entstehung des dynamischen Auftriebes von Tragflügeln. Z.f.a.M.M., Bd. 5, Heft 1, Feb. 1925, pp. 17–35.
21. Walker, P. B.: Experiments on the Growth of Circulation about a Wing with a Description of an Apparatus for Measuring Fluid Motion. R. & M. No. 1402, British A.R.C., 1932.
22. Küssner, H. G.: Zusammenfassender Bericht über den instationären Auftrieb von Flügeln. Luftfahrtforschung, Bd. 13, Nr. 12, Dec. 20, 1936, pp. 410–424.
23. Garrick, I. E.: On Some Fourier Transforms in the Theory of Non-Stationary Flows. Proc. Fifth Int. Cong. Appl. Mech. (Cambridge, Mass., 1936), John Wiley & Sons, Inc., 1939, pp. 590–593.
24. Jones, Robert T.: The Unsteady Lift of a Wing of Finite Aspect Ratio. NACA Rep. 681, 1940.
25. Von Kármán, Th., and Sears, W. R.: Airfoil Theory for Non-Uniform Motion. Jour. Aero. Sci., vol. 5, no. 10, Aug. 1938, pp. 379–390.
26. Sears, W. R., and Kuethe, A. M.: The Growth of the Circulation of an Airfoil Flying through a Gust. Jour. Aero. Sci., vol. 6, no. 9, July 1939, pp. 376–378.
27. Jones, Robert T.: Correction of the Lifting-Line Theory for the Effect of the Chord. NACA TN 817, 1941.
28. Quinn, John H., Jr.: Effects of Reynolds Number and Leading-Edge Roughness on Lift and Drag Characteristics of the NACA 65_3–418, $a=1.0$ Airfoil Section. NACA CB L5J04, 1945.
29. Theodorsen, T., and Garrick, I. E.: General Potential Theory of Arbitrary Wing Sections. NACA Rep. 452, 1933.
30. Pierce, Harold B.: Tests of a 45° Sweptback-Wing Model in the Langley Gust Tunnel. NACA TN 1528, 1948.
31. Jones, Robert T., and Fehlner, Leo F.: Transient Effects of the Wing Wake on the Horizontal Tail. NACA TN 771, 1940.
32. Cowley, W. L., and Glauert, H.: The Effect of the Lag of the Downwash on the Longitudinal Stability of an Aeroplane and on the Rotary Derivative M_q. R. & M. No. 718, British A.R.C., 1921.
33. Farren, W. S.: The Reaction of a Wing Whose Angle of Incidence Is Changing Rapidly. Wind Tunnel Experiments with a Short Period Recording Balance. R. & M. No. 1648, British A.R.C., 1935.
34. Pearson, H. A.: Pressure-Distribution Measurements on an O–2H Airplane in Flight. NACA Rep. 590, 1937.
35. Bryant, L. W., and Jones, I. M. W.: Stressing of Aeroplane Wings Due to Symmetrical Gusts. R. & M. No. 1690, British A.R.C., 1936.
36. Williams, D., and Hanson, J.: Gusts Loads on Tails and Wings. R. & M. No. 1823, British A.R.C., 1937.
37. Sears, William R., and Sparks, Brian O.: On the Reaction of an Elastic Wing to Vertical Gusts. Jour. Aero. Sci., vol. 9, no. 2, Dec. 1941, pp. 64–67.
38. Pierce, Harold B.: Investigation of the Dynamic Response of Airplane Wings to Gusts. NACA TN 1320, 1947.
39. Putnam, Abbott A.: An Improved Method for Calculating the Dynamic Response of Flexible Airplanes to Gusts. NACA TN 1321, 1947.
40. Pierce, Harold B.: Dynamic Stress Calculations for Two Airplanes in Various Gusts. NACA ARR, Sept. 1941.
41. Peiser, A. M., and Wilkerson, M.: A Method of Analysis of V–G Records from Transport Operations. NACA Rep. 807, 1945.
42. Kenney, John F.: Mathematics of Statistics. D. Van Nostrand Co., Inc., 1939, Pt. I, pp. 60–75, and Pt. II, pp. 49–51.
43. Peiser, A. M.: An Analysis of the Airspeeds and Normal Accelerations of Douglas DC–3 Airplanes in Commercial Transport Operation. NACA TN 1142, 1946.
44. Tolefson, H. B.: Airspeed Fluctuations as a Measure of Atmospheric Turbulence. NACA ARR L5F27, 1945.

TABLE I.—CHARACTERISTICS OF AIRPLANES USED IN GUST RESEARCH

Airplane	Type	Weight, W (lb)	Wing area, S (sq ft)	W/S (lb/sq ft)	$\frac{dC_L}{d\alpha}$ (per radian)	Mean wing chord, $\bar{c}$ (ft)	Span, b (ft)	Mass parameter (sea level), μ_g
XC-35	Monoplane	10,500	458.30	24.30	3.95	9.23	55.0	17.41
XBM-1	Biplane	5,200	412.00	12.60	4.16	5.66	41.0	14.00
Aeronca C-2	Monoplane	782	144.00	5.44	4.73	4.00	36.0	7.50
XB-15	Monoplane	55,000	2,780.00	19.80	4.76	18.65	149.0	5.33
F-61C	Monoplane	29,500	662.40	44.50	4.83	10.50	66.0	22.92

TABLE II.—SCOPE OF GUST-STRUCTURE INVESTIGATION

Airplane	Weather	Flight hours in rough air	Altitude range (ft)	Locality	Purpose	Auxiliary measurements	Items investigated			
							U	H	U_e	H (*)
XBM-1	Cumulus clouds, air mass thunderstorms.	10 (estimated)	0 to 18,000	Langley Air Force Base, Va.	Special cloud flight investigation.	Airplane observation	X	X	X	
Aeronca C-2	Clear air	6 (estimated)	0 to 3,500	Langley Air Force Base, Va.	Low-altitude investigation.	Temperature and wind gradients.	X	X		
XC-35	Thunderstorm, line squalls.	7.10	0 to 35,000	Langley Air Force Base, Va.	Thunderstorm and meteorology investigation.	Radio observation, airplane observation, and weather maps.	X	X	X	X
XB-15	Clear air	4.84	0 to 15,000	Transcontinental	Routine flight	Wing strain and wing deflection.	X	X	X	
F-61C	Air mass thunderstorms.	20	6,000 to 25,000	Orlando, Fla.	Thunderstorm and meteorology investigation.	Radio observation, radar, temperature, altitude variations, and weather maps.	X	X	X	X

* Measured from spanwise gust distribution.

TABLE III.—FREQUENCY DISTRIBUTION OF EFFECTIVE GUST VELOCITY FOR DIFFERENT RANGES OF ALTITUDES

[Data obtained during 1941 and 1942; total record time, 7.1 hr]

U_e (fps) \ Altitude range (ft)	Frequency of gusts						
	0 to 5,000	5,000 to 10,000	10,000 to 15,000	15,000 to 20,000	20,000 to 25,000	25,000 to 30,000	30,000 to 35,000
4 to 8	340	1,322	571	760	354	449	215
8 to 12	75	351	233	335	198	274	161
12 to 16	10	70	89	129	109	75	51
16 to 20	0	15	29	48	41	34	17
20 to 24	0	2	8	15	14	15	7
24 to 28	1	2	2	5	6	6	4
28 to 32	0	0	4	4	1	3	1
32 to 36	0	0	0	1	1	0	0
36 to 40	0	0	0	1	0	0	0
Total	426	1,762	936	1,298	724	856	456
Record time (percent total time)	6.7	29.3	12.3	17.3	11.6	14.0	8.8
Miles per gust	0.164	0.140	0.139	0.139	0.158	0.210	0.257

TABLE IV.—COMPARISON OF THE CHARACTERISTICS OF SINGLE GUSTS AND SETS OF TWO AND THREE REPEATED GUSTS OCCURRING WITH EQUAL FREQUENCY

[From reference 11]

Single gust	Set of two repeated gusts				Set of three repeated gusts			
Effective gust velocity, U_e (fps)	Effective gust velocity, U_e (fps)		Spacing, λ (chords)		Effective gust velocity, U_e (fps)		Spacing, λ (chords)	
	$U_{e_{av}}$	Range	λ_{av}	Range	$U_{e_{av}}$	Range	λ_{av}	Range
20	17	5 to 29	28	5 to 64	15.5	7 to 31.5	26	8 to 43
25	21	9 to 33	28	12 to 54	19.5	8 to 33.5	24	8 to 41
30	25	15 to 35	22	15 to 32	23.5	9.5 to 36.0	20	12 to 32
35	29.5	21.5 to 37.5	22	15 to 30	27.5	10.5 to 38.5	20	15 to 25

TABLE V.—FREQUENCY OF OCCURENCE OF GIVEN VALUES OF ANGULAR ACCELERATION IN ROLL WITH ASSOCIATED VALUES OF NORMAL ACCELERATION INCREMENT

[Data for XC-35 airplane]

$\frac{dp}{dt}$ (radians/sec²) \ Δn (g units)	0 to 0.1	0.1 to 0.2	0.2 to 0.3	0.3 to 0.4	0.4 to 0.5	0.5 to 0.6	0.6 to 0.7	0.7 to 0.8	0.8 to 0.9	0.9 to 1.0	1.0 to 1.1	1.1 to 1.2	1.2 to 1.3	1.3 to 1.4	1.4 to 1.5	1.5 to 1.6	1.6 to 1.7	1.7 to 1.8	1.8 to 1.9	1.9 to 2.0	2.0 to 2.1	2.1 to 2.2	2.2 to 2.3	2.3 to 2.4	Total
1.9 to 2.0																1									1
1.8 to 1.9																									
1.7 to 1.8																									
1.6 to 1.7							1	1			1														3
1.5 to 1.6					1				1																2
1.4 to 1.5																									
1.3 to 1.4																									
1.2 to 1.3					1																				1
1.1 to 1.2						2		1						1											4
1.0 to 1.1						3		3	2		1			1											10
0.9 to 1.0					3		4	1					2	1	1										12
0.8 to 0.9					1	5	3	6	3		1			1					1						21
0.7 to 0.8					4	4		7	3		1	2	2	2			1								26
0.6 to 0.7			1			9	8	16	2		1		2		1										40
0.5 to 0.6				1	2	15	7	30	17	1	2	1	2	2		1	1								82
0.4 to 0.5				1	1	8	21	45	24		1	3	1	5	1	1	4	1			1				118
0.3 to 0.4		1	1	1	3	11	32	77	66	2	6	13	7	17	6	1	2	1							247
0.2 to 0.3			1	3	2	13	14	107	129	8	12	6	11	30	11	4	2								353
0.1 to 0.2			1	4	4	20	36	136	153	5	13	20	21	27	13	1	13		1						468
0 to 0.1				2	1	9	27	101	147	12	16	23	40	42	15	11	6	1	1	1					455
0 to −0.1				2	6	13	23	80	178	17	19	85	99	79	9	7	1							1	519
−0.1 to −0.2			1	3	3	10	9	62	69	15	15	51	152	78	17	10	13	2	4	1					545
−0.2 to −0.3					1	10	9	54	58	5	20	161	116	120	30	15	13	3	1		1				617
−0.3 to −0.4			1	1	1	4	8	29	42	5	22	148	264	128	28	17	8	5			1				712
−0.4 to −0.5						8	10	20	31	1	11	111	116	124	19	16	8	1	1						477
−0.5 to −0.6					1	1	7	9	15	2	10	35	83	100	26	7	10	2							308
−0.6 to −0.7						1	8	1	5		3	24	52	50	20	3	5	2			1				175
−0.7 to −0.8	1					2	3	1	3			12	24	36	24	8	5	3							122
−0.8 to −0.9							1	3	2			11	19	31	9	8		1		1					86
−0.9 to −1.0						1	3	2		1		6	14	11	6	2	6	3							55
−1.0 to −1.1									2			1	8	13	2	0	1	1			1				38
−1.1 to −1.2											1	2	3	1	3	2	1	2							15
−1.2 to −1.3												2	1	1	3		1					1			9
−1.3 to −1.4							1						3	5						1					10
−1.4 to −1.5												2		2			2				1				7
−1.5 to −1.6																	1	1	1						3
−1.6 to −1.7														4											4
−1.7 to −1.8														1		1									2
−1.8 to −1.9														1			1								2
−1.9 to −2.0															1										1
−2.0 to −2.1																									
−2.1 to −2.2																									
−2.2 to −2.3																		1							1
Total	1	1	6	18	35	149	235	792	952	74	156	749	1,042	914	245	125	105	30	9	5	6	1		1	5,651

TABLE VI.—EFFECT OF FUSELAGE INTERFERENCE ON GUST ACCELERATION

Aspect ratio, A	Fuselage intercept (percent wing area)	Gross area		Experimental Δn, g units (reference 19)	Net area + $\frac{1}{2}$ fuselage intercept	
		Δn, g units (reference 14) (a)	Δn, g units (reference 4) (b)		Δn, g units (reference 14) (a)	Δn, g units (reference 4) (b)
6.73	9.7	1.65	1.44	1.40	1.57	1.37
2.06	18.1	.82	.68	.60	.74	.62
2.18	22.0	.80	.67	.60	.71	.59

(a) Finite-aspect-ratio functions used.
(b) Infinite-aspect-ratio functions used.

TABLE VII.—CHARACTERISTICS OF AIRPLANE MODEL

[Laminar-flow wing]

Weight, lb	11.84
Wing area, sq ft	5.44
Wing loading, lb/sq ft	2.18
Span, ft	7
Mean aerodynamic chord, ft	0.829
Aspect ratio	9
Taper ratio	0.382
Center of gravity, percent M. A. C.	30.5
Wing section	65_3-418, $a=1.0$
Lift-curve slope, per radian:	
Smooth wing (steady flow)	5.01
Roughened wing (steady flow)	4.18
Theoretical	5.41

TABLE VIII.—COMPARISON OF EXPERIMENTAL AND CALCULATED ACCELERATION INCREMENTS

Experiment		Calculation	
Average maximum acceleration increment, "smooth-condition" flights.	$1.69g \pm 0.02g$	Acceleration increment, "smooth condition," based on section data of reference 28.	$1.73g \pm 0.08g$
Average maximum acceleration increment, "rough-condition" flights.	$1.67g \pm 0.02g$	Acceleration increment "rough condition," based on section data of reference 28.	$1.47g \pm 0.08g$
Difference between average maximum acceleration increments for the two conditions ("smooth" minus "rough").	$0.02g \pm 0.02g$	Difference between acceleration increments for the two conditions ("smooth" minus "rough").	$0.26g \pm 0.08g$
		Acceleration increment for both conditions, based on theoretical lift-curve slope.	$1.84g$

TABLE IX.—EXPERIMENTAL AND CALCULATED ACCELERATION INCREMENTS FOR A STRAIGHT AND A SWEPT WING

[From reference 30]

Gradient distance (chords)	Experimental maximum acceleration increment, Δn (g units)		Calculated maximum acceleration increment, Δn (g units)	
	$\Delta\theta \neq 0$	$\Delta\theta = 0$	Cosine law	Experimental wind tunnel
Equivalent straight-wing model				
0	2.11	2.03	1.96	1.96
9	1.73	1.67	1.65	1.65
45° sweptback-wing model				
0	1.48	1.34	1.35	1.12
9	1.13	1.03	1.05	.87

TABLE X.—CHARACTERISTICS OF BOEING B-247 AIRPLANE AND MODELS

Item	Full-scale	$\frac{1}{12}$-scale	$\frac{1}{24}$-scale
Weight, lb	13,650	9.79	1.27
Wing area, sq ft	836	5.80	1.435
Wing loading, lb/sq ft	16.32	1.69	0.885
Span, ft	74	6.17	3.08
Mean wing chord, ft	12	1.0	0.50
Center of gravity, percent M. A. C.	28.5	28.5	28.5
Natural wing period, sec	----	0.0125	0.0125
Moment of inertia, slug-ft^2	796,000	3.94	0.124
Slope of lift curve, per radian	4.47	4.47	4.47
Gust velocity, fps	39.2	11.32	8.0
Forward velocity, mph	200	57.5	40.8

TABLE XI.—CHARACTERISTICS OF GUST-TUNNEL MODELS

Item	Conventional			Canard	Tailless
Fixed quantities					
Wing area (net), sq ft	1.373			1.302	1.25
Mean wing chord, ft	0.50			0.422	0.463
Slope of lift curve, per radian	4.30			4.5	3.73
Parameters					
Weight, lb	----	1.27	----	1.30	2.2
Center-of-gravity position, percent M. A. C.	15.0	25.0	35.0	−41.0	20.0
Tail length, ft	0.91	1.37	1.825	1.11	----
Tail area, sq ft	0.199	0.283	0.364	0.257	----
Moment of inertia, slug-ft^2	----	0.0103	----	0.00790	0.001805
Stabilizer chord, ft	0.318	0.382	0.436	0.242	----
Derived quantities					
Mass parameter	10.25 to 30.75			12.65	26.9
Neutral point, percent M. A. C.	35.0 to 65.0			−23.0	24.0
Static margin, $dC_{m_{cg}}/dC_L$	−0.503 to 0.009			−0.18	−0.04 to −0.08
Tail volume, cu ft	0.181 to 0.665			0.235	----

TABLE XII.—MAXIMUM TOTAL ACCELERATION INCREMENTS ON CONVENTIONAL AIRPLANE

[All increments given in g units]

(a) Center of gravity, 15 percent M.A.C.

Tail length (ft)	Tail area (sq ft)	Δn_{0_w}	Δn_{m_w}	Δn_{θ_w}	Δn_{q_w}	Δn_{T_w}	Δn_{0_z}	Δn_{m_z}	Δn_{ϵ_0}	Δn_{ϵ_m}	Δn_{θ_z}	Δn_{q_z}	Δn_{T_z}	Δn_T
						$H=0$								
0.91	0.199	1.86	−0.21	−0.05	0	1.60	0.23	−0.03	−0.07	0	−0.01	−0.01	0.11	1.71
	.283	------	------	------	------	------	------	------	------	------	------	------	------	1.72
	.364	1.88	−.24	−.07	0	1.57	.40	−.05	−.14	0	−.01	−.03	.17	1.74
1.37	.199	------	------	------	------	------	------	------	------	------	------	------	------	1.68
	.283	------	------	------	------	------	------	------	------	------	------	------	------	1.70
	.364	------	------	------	------	------	------	------	------	------	------	------	------	1.72
1.825	.199	1.92	−.28	−.06	0	1.58	.19	−.04	−.08	0	−.01	−.02	.06	1.64
	.283	------	------	------	------	------	------	------	------	------	------	------	------	1.66
	.364	1.92	−.28	−.05	0	1.59	.32	−.07	−.11	0	−.01	−.03	.10	1.69
						$H=8$								
0.91	0.199	1.90	−0.45	−0.27	−0.01	1.17	0.21	−0.06	−0.08	0.02	−0.03	−0.02	0.04	1.21
	.283	------	------	------	------	------	------	------	------	------	------	------	------	1.20
	.364	1.90	−.45	−.30	−.01	1.14	.38	−.10	−.15	.02	−.07	−.04	.04	1.18
1.37	.199	------	------	------	------	------	------	------	------	------	------	------	------	1.24
	.283	------	------	------	------	------	------	------	------	------	------	------	------	1.22
	.364	------	------	------	------	------	------	------	------	------	------	------	------	1.21
1.825	.199	1.90	−.48	−.15	−.01	1.26	.16	−.06	−.06	.01	−.02	−.03	0	1.26
	.283	------	------	------	------	------	------	------	------	------	------	------	------	1.25
	.364	1.91	−.49	−.17	−.01	1.24	.30	−.11	−.11	.02	−.04	−.05	.01	1.25
						$H=16$								
0.91	0.199	1.93	−0.47	−0.75	−0.01	0.70	0.22	−0.06	−0.08	0.02	−0.09	−0.03	−0.02	0.68
	.283	------	------	------	------	------	------	------	------	------	------	------	------	.02
	.364	1.93	−.39	−.90	−.01	.63	.39	−.09	−.15	.03	−.20	−.05	−.07	.56
1.37	.199	------	------	------	------	------	------	------	------	------	------	------	------	.76
	.283	------	------	------	------	------	------	------	------	------	------	------	------	.73
	.364	------	------	------	------	------	------	------	------	------	------	------	------	.70
1.825	.199	1.93	−.58	−.48	−.01	.86	.19	−.07	−.07	.02	−.06	−.03	−.02	.84
	.283	------	------	------	------	------	------	------	------	------	------	------	------	.84
	.364	1.93	−.60	−.44	−.01	.88	.34	−.14	−.13	.03	−.10	−.04	−.04	.84

(b) Center of gravity, 25 percent M.A.C.

						$H=0$								
0.91	0.199	1.86	−0.22	−0.01	0	1.63	0.23	−0.03	−0.07	0	0	0	0.13	1.76
	.283	1.87	−.23	−.02	0	1.62	.32	−.04	−.11	0	0	−.01	.16	1.78
	.364	1.88	−.25	−.03	0	1.60	.40	−.06	−.14	0	0	−.02	.18	1.78
1.37	.199	------	------	------	------	------	------	------	------	------	------	------	------	1.74
	.283	------	------	------	------	------	------	------	------	------	------	------	------	1.76
	.364	------	------	------	------	------	------	------	------	------	------	------	------	1.79
1.825	.199	1.92	−.29	.01	0	1.64	.19	−.04	−.06	0	0	0	.09	1.73
	.283	------	------	------	------	------	------	------	------	------	------	------	------	1.76
	.364	1.92	−.30	.02	0	1.64	.32	−.07	−.11	0	0	0	.14	1.78
						$H=8$								
0.91	0.199	1.90	−0.51	−0.11	0	1.28	0.21	−0.07	−0.08	0.02	−0.01	−0.01	0.06	1.34
	.283	------	------	------	------	------	------	------	------	------	------	------	------	1.33
	.364	1.90	−.50	−.16	0	1.24	.38	−.12	−.15	.03	−.03	−.03	.08	1.32
1.37	.199	------	------	------	------	------	------	------	------	------	------	------	------	1.37
	.283	1.90	−.51	−.10	0	1.29	.26	−.09	−.10	.02	−.02	−.02	.05	1.34
	.364	------	------	------	------	------	------	------	------	------	------	------	------	1.34
1.825	.199	1.90	−.53	−.02	0	1.35	.16	−.07	−.06	.01	0	−.01	.03	1.38
	.283	------	------	------	------	------	------	------	------	------	------	------	------	1.37
	.364	1.91	−.54	−.05	0	1.32	.30	−.12	−.11	.02	−.01	−.03	.05	1.37
						$H=16$								
0.91	0.199	1.93	−0.66	−0.35	0	0.92	0.22	−0.08	−0.08	0.02	−0.04	−0.01	0.03	0.95
	.283	------	------	------	------	------	------	------	------	------	------	------	------	.88
	.364	1.93	−.58	−.53	0	.82	.39	−.13	−.15	.04	−.12	−.03	0	.82
1.37	.199	------	------	------	------	------	------	------	------	------	------	------	------	.96
	.283	------	------	------	------	------	------	------	------	------	------	------	------	.92
	.364	------	------	------	------	------	------	------	------	------	------	------	------	.88
1.825	.199	1.93	−.68	−.28	0	.97	.19	−.08	−.07	.02	−.04	−.02	0	.97
	.283	------	------	------	------	------	------	------	------	------	------	------	------	.95
	.364	1.93	−.66	−.32	0	.95	.34	−.15	−.13	.03	−.07	−.03	−.01	.94

TABLE XII.—MAXIMUM TOTAL ACCELERATION INCREMENTS ON CONVENTIONAL AIRPLANE—Concluded

[All increments given in g units]

(c) Center of gravity, 35 percent M.A.C.

Tail length (ft)	Tail area (sq ft)	Δn_{0_w}	Δn_{m_w}	Δn_{θ_w}	Δn_{q_w}	Δn_{T_w}	Δn_{0_z}	Δn_{m_z}	Δn_{ϵ_0}	Δn_{ϵ_m}	Δn_{θ_z}	Δn_{q_z}	Δn_{T_z}	Δn_T
						$H=0$								
0.91	0.199	1.86	−0.22	0.03	0	1.67	0.23	−0.03	−0.07	0	0.01	0	0.14	1.81
	.283													1.84
	.364	1.88	−.25	.03	0	1.66	.40	−.06	−.14	0	.01	0	.21	1.87
1.37	.199													1.82
	.283													1.84
	.364													1.86
1.825	.199	1.92	−.30	.08	0	1.70	.19	−.04	−.06	0	.01	.02	.12	1.82
	.283													1.84
	.364	1.92	−.32	.08	0	1.68	.32	−.07	−.11	0	.02	.02	.18	1.86
						$H=8$								
0.91	0.199	1.90	−0.54	0.04	0	1.40	0.21	−0.07*	−0.08	0.02	0.01	0	0.09	1.49
	.283													1.48
	.364	1.90	−.56	.01	0	1.35	.38	−.13	−.15	.03	0	−.01	.12	1.47
1.37	.199													1.50
	.283													1.50
	.364													1.50
1.825	.199	1.90	−.58	.12	0	1.44	.16	−.07	−.05	.01	.02	.01	.07	1.51
	.283													1.52
	.364	1.91	−.60	.12	0	1.43	.30	−.14	−.11	.02	.03	−.01	.09	1.52
						$H=16$								
0.91	0.199	1.93	−0.85	0.06	0	1.14	0.22	−0.11	−0.08	0.03	0.01	0	0.07	1.21
	.283	1.93	−.79	−.07	0	1.07	.31	−.14	−.12	.04	−.01	−.01	.07	1.14
	.364	1.93	−.75	−.18	0	1.00	.39	−.17	−.15	.05	−.04	−.01	.07	1.07
1.37	.199													1.19
	.283													1.14
	.364													1.08
1.825	.199	1.93	−.82	.01	0	1.12	.19	−.10	−.07	.02	0	0	.04	1.16
	.283													1.13
	.364	1.93	−.77	−.10	0	1.06	.34	−.18	−.13	.04	−.02	−.02	.03	1.09

TABLE XIII.—MAXIMUM TOTAL ACCELERATION INCREMENTS ON TAILLESS AIRPLANE

[All increments are given in g units; data from reference 14]

Method	Center of gravity (percent M. A. C.)	Δn_0	Δn_m	Δn_θ	Δn_q	Δn_T
			$H=0$			
Calculation	20	2.90	−0.375	--------	--------	2.525
	28	2.90	−.375	--------	--------	2.525
Experiment	20					2.64±0.06
			$H=8$			
Calculation	20	2.30	−0.28	0.48	--------	2.50
	28	2.30	−.28	.82	--------	2.84
Experiment	20					2.60±0.09
			$H=17.5$			
Calculation	20	2.88	−1.00	0.20	--------	2.08
	28	--------	--------	--------	--------	--------
Experiment	20					2.36±0.15

TABLE XIV.—MAXIMUM TOTAL ACCELERATION INCREMENTS ON CANARD AIRPLANE

[All increments are given in g units; data from reference 15]

Method	Aspect ratio, A	Δn_{0_w}	Δn_{m_w}	Δn_{δ_w}	Δn_{q_w}	Δn_{T_w}	Δn_{0_s}	Δn_{m_s}	Δn_{δ_s}	Δn_{q_s}	Δn_{T_s}	Δn_T
					$H=0$							
Calculation	∞	1.85	−0.24	--------	--------	1.61	0.35	−0.05	--------	--------	0.30	1.91
	6	1.92	−.20	--------	--------	1.72	.37	−.04	--------	--------	.33	2.05
Experiment	6.55											2.03
					$H=7.88$							
Calculation	∞	1.88	−0.55	0.25	−0.03	1.55	0.35	−0.10	0.04	0.02	0.31	1.86
	6	1.87	−.51	.23	−.02	1.57	.36	−.09	.04	.01	.32	1.89
Experiment	6.55											2.11
					$H=17.5$							
Calculation	∞	1.58	−0.61	−0.04	−0.04	0.89	0.33	−0.11	−0.01	0.02	0.23	1.12
	6	1.65	−.67	−.42	−.09	.47	.31	−.12	−.08	.05	.16	.63
Experiment	6.55											1.35

TABLE XV.—EFFECTIVE GUST VELOCITY AT HORIZONTAL AND VERTICAL TAILS AS DETERMINED FROM LOAD MEASUREMENTS IN FLIGHT

Airplane	Wing	Vertical tail surface		Horizontal tail surface	
	$U_{e_{max}}$ (fps)	U_d/U_{e_w}	$\frac{1}{\Delta n/\Delta n_z}$ [a]	U_d/U_{e_w}	$1-\frac{d\epsilon}{d\alpha}$
XB-15	8.0	1.9 ±0.3	1.89	0.53±0.4	0.5 (Estimate)
0-2H	13.5	1.72	1.59	.64	.5 (Estimate)

[a] Value of $\frac{U_e}{U_{e_w}}=\frac{1}{\Delta n/\Delta n_z}$ on assumptions of infinite effective wing loading of vertical tail and probable gust gradient at wing and tail of 10 chords.

TABLE XVI.—TEST MODEL CHARACTERISTICS

[Nonrigid airplane]

Weight, lb	1.832
Wing area, sq ft	1.183
Mean geometric chord, ft	0.394
Span, ft	3.0
Slope of lift curve, per radian	4.73
Forward velocity, fps	61.0
Gust velocity, fps	6.0
Pitching moment of inertia, slug-ft^2	0.00782
Radius of gyration of wing, ft	0.663
Weight of wing, lb	0.293

TABLE XVII.—CHARACTERISTICS OF AIRPLANES CHOSEN FOR CALCULATIONS

Airplane	Condition	Weight, W (lb)	Wing area, S (sq ft)	Wing loading, W/S (lb/sq ft)	Span, b (ft)	Mean wing chord, $\bar{c}$ (ft)	Natural wing frequency, f_w (cps)	Slope of lift curve, $dC_L/d\alpha$ (per radian)	Number of engines	Forward velocity, V (mph)	Remarks
A	1	100,000	1,700	58.8	113.8	14.93	2.20	4.73	4	256	Hypothetical airplane scaled from flexible-wing model.
	2	100,000	1,700	58.8	113.8	14.93	4.25	4.73	4	256	
B	1	44,860	2,780	16.1	150.0	18.53	3.89	4.76	4	200	
C	1	100,000	1,710	58.5	140.0	12.21	2.45	5.04	4	260	Speeds assumed for calculation.
	2	100,000	1,710	58.5	140.0	12.21	2.45	5.04	4	200	
	3	100,000	1,710	58.5	140.0	12.21	2.45	5.04	4	300	
	4	100,000	1,710	58.5	140.0	12.21	2.45	5.04	4	400	
D	1	62,500	1,826	34.2	140.0	13.04	2.50	4.93	2	190	Normal gross weight.
	2	102,000	1,826	56.0	140.0	13.04	1.43	4.93	2	160	Overload gross weight.

TABLE XVIII.—AIRPLANE CHARACTERISTICS

Airplane	Gross weight, W (lb)	Wing area, S (sq ft)	Span, b (ft)	Mean wing chord, $\bar{c}$ (ft)	$dC_L/d\alpha$ (per radian)	n_{limit} (g units)	V_L (mph)	V_{max} (mph)	K
A	25,200	987	95	11.5	4.53	3.14	211	257	1.090
B	45,000	1,486	107.25	13.9	4.42	2.96	230	270	1.120
C	41,000	1,340	118.17	12.33	4.54	2.58	181	226	1.125
D	50,000	2,145	130	17.46	4.45	2.80	168	214	1.075
E	90,000	1,650	123	14.67	4.67	2.45	271	324	1.200
F	62,000	1,460	117.5	13.6	4.70	2.50	222	262	1.173

TABLE XIX.—SCOPE OF DATA

Airplane	Route Number	Route	Year	Records obtained		Records analyzed			Remarks
				Number of records	Flight hours	Number of records	Hours per record	Range of hours	
Prewar (V–G)									
A	I	Transcontinental	1937–1941	35	17,675	15	645	575 to 800	Operating conditions and flight load experience.
A	II	Transcontinental	1937–1941	52	12,048	37	275	200 to 400	
A	III	Transcontinental	1937–1941	13	4,455	11	295	150 to 450	
B	IV	Caribbean, northern part of South America	1940–1941	109	5,000	83	29.0	3 to 268	
C	IV	Caribbean, transcontinental, trans-Pacific	1936–1939	193	15,902	117	95.1	70 to 130	
D	V	Trans-Pacific	1936–1941	142	18,001	100	128.1	120 to 140	
Wartime (V–G)									
A	I	Transcontinental	1942–1944	33	20,002	20	695	600 to 800	Operating conditions and flight load experience.
B	IV	Caribbean, northern part of South America	1942–1944	305	18,178	193	53	3 to 268	
D	VI	Trans-Pacific	1942–1945	50	4,373	30	36	30 to 90	
Postwar (airspeed-altitude)									
E	VII	Trans-Atlantic	1946		130				Speed tendency.
E	III	Transcontinental	1946		197				
F	VIII	Seattle-Anchorage-Fairbanks	1947		57.6				

TABLE XX.—STATISTICAL PARAMETERS OF V–G DATA

Airplane	Route	Δn_{max} (g units)			V_{max} (mph)			V_0 (mph)			Maximum values recorded		
		Average value	Standard deviation	Skewness	Average value	Standard deviation	Skewness	Average value	Standard deviation	Skewness	$V_{0_{max}}$ (mph)	Δn_{max} (g units)	V_{max} (mph)
Prewar													
A	I	1.23	0.30	0.46	229.8	8.3	1.04	172.0	21.2	−0.57	210	2.00	250
A	II	1.21	.34	.74	215.7	9.9	1.48	158.9	24.2	−.22	210	2.20	260
A	III	.89	.32	.25	206.6	8.7	.79	149.5	16.4	.73	200	1.50	230
B	IV	.63	.19	.79	205.7	10.00	.44	149.6	22.24	.07	210	1.30	235
C	IV	.73	.20	.58	167.1	9.60	.58	139.2	13.00	.40	200	1.50	200
D	V	.71	.27	1.77	169.45	11.85	1.41	133.20	14.15	.22	185	2.40	230
Wartime													
A	I	1.45	0.39	0.48	227.8	12.7	0.77	168.5	30.9	−0.75	210	2.50	265
B	IV	.91	.29	1.14	223.0	10.06	.31	163.8	21.60	.09	240	2.40	255
D	VI	.77	.20	1.36	170.84	9.52	.19	132.17	14.30	.08	170	1.70	195

TABLE XXI.—AIRPLANE LIFE AND PROBABLE-SPEED RATIO FOR SCHEDULED AIRLINE OPERATIONS

Airplane	Route	Flight miles to exceed			V_p/V_L
		Δn_{limit}	V_{new}	V_e (37.5K at V_p)	
Prewar					
A	I	13 $\times 10^6$	15 $\times 10^6$	23 $\times 10^6$	0.83
A	II	2	12	6	.80
A	III	85	1,200	8	.69
B	IV	460	7,400	7	.63
C	IV	15	1,600	6	.76
D	V	1.6	3.3	1.5	.79
Wartime					
A	I	1.2×10^6	5×10^6	1.7×10^6	0.83
B	IV	1.1	220	.35	.72
D	VI	2.9	300	2.6	.79
Postwar					
E	III	----------	0.077×10^6	----------	*0.79
E	VII	----------	.46	----------	*.89
F	VIII	----------	.12	----------	*.90

* V_p denotes probable speed of flight.